

**Role of Bile Acids and Compensatory Hepatic Transport Proteins in  
Troglitazone-Mediated Hepatotoxicity**

Tracy L. Marion

A dissertation submitted to the faculty of the University of North Carolina at Chapel Hill in partial fulfillment of the requirements for the degree of Doctor of Philosophy in the Curriculum in Toxicology

Chapel Hill  
2010

Approved By	Kim L. R. Brouwer, Pharm.D., Ph.D.
	William B. Coleman, Ph.D.
	Jasminder Sahi, Ph.D.
	Robert L. St. Claire, III, Ph.D.
	Paul B. Watkins, M.D.

© 2010  
Tracy L. Marion  
ALL RIGHTS RESERVED

## **Abstract**

Tracy L. Marion

### **Role of Bile Acids and Compensatory Hepatic Transport Proteins in Troglitazone-Mediated Hepatotoxicity**

(Under the direction of Kim L. R. Brouwer, Pharm.D., Ph.D.)

Drug-induced hepatotoxicity is the most common reason pharmaceuticals are removed from clinical use. Understanding mechanisms of hepatotoxicity, and in vitro models to predict hepatotoxicity in humans, are essential for drug development and patient safety. The drug troglitazone (TRO) was removed from the market because of hepatotoxicity, but preclinical testing failed to predict toxicity in humans. One hypothesized mechanism for TRO's hepatotoxicity is impairment of bile acid (BA) transport, causing cholestasis and subsequent hepatocellular apoptosis or necrosis. The goal of this research was to demonstrate that inhibition of BA transport and compensatory transport proteins contribute to the hepatotoxicity of TRO by causing intracellular accumulation of BAs and altering the BA pool composition.

In human sandwich-cultured hepatocytes (SCH) and suspended hepatocytes, TRO inhibited uptake and biliary efflux of [<sup>3</sup>H] taurocholic acid ([<sup>3</sup>H]TCA), consistent with published reports in rat SCH; however, intracellular accumulation of [<sup>3</sup>H]TCA was not observed in either species. Because BAs differ in affinity for transport proteins, it was hypothesized that TRO causes intracellular accumulation of more cytotoxic BAs, such as chenodeoxycholic acid (CDCA). Indeed, TRO caused significant intracellular accumulation of [<sup>14</sup>C]CDCA species in rat SCH. In suspended

rat hepatocytes, TRO inhibited [<sup>3</sup>H]TCA uptake more potently than [<sup>14</sup>C]CDCA uptake. This differential effect on individual BA disposition was hypothesized to shift the intracellular BA pool toward more toxic species. However, 24-h exposure of rat and human SCH to TRO had no significant effect on the concentration or composition of BAs in medium, cell, or bile, although the SCH model reflected reasonably well the in vivo BA pool composition in rats and humans. TRO-sulfate (TS), the major TRO metabolite, inhibited TCA transport in plasma membrane vesicles overexpressing the efflux protein multidrug resistance-associated protein 4 (MRP4). Accumulation of TS may inhibit BA efflux and increase intrahepatic accumulation of cytotoxic BAs in susceptible patients. This may explain, in part, the idiosyncratic nature of TRO hepatotoxicity. This research indicates that preclinical drug testing should include in vitro screens for drug-induced transport inhibition of multiple BAs, not just TCA, to fully characterize the effects of a compound on BA homeostasis.

This work is dedicated with love to my parents.

## ACKNOWLEDGEMENTS

There are numerous people without whose guidance, support, knowledge, and wisdom, this dissertation would not be possible. First, I would like to thank my advisor, Dr. Kim L. R. Brouwer, for the investment she has made in me. She and all the members of my committee, Dr. William Coleman, Dr. Jasminder Sahi, Dr. Robert St. Claire, III, and Dr. Paul Watkins, have humbled me with their dedication to my growth and development as a scientist. Had it not been for the early encouragement of Dr. James Knopp, I would not have even considered pursuing graduate studies. Likewise, Dr. Krishna Fisher was a wonderful and encouraging mentor who was never too busy to answer my questions. Dr. Stephanie Padilla's guidance, sound advice, and willingness to listen will always be remembered and greatly appreciated. All the members of the Brouwer lab past and present also deserve thanks for their help. In particular, Dr. Kristina Wolf has my sincerest gratitude for her scientific knowledge and advice, moral support, and steadfast friendship. Dr. Jin Kyung Lee also deserves my thanks for being a patient teacher and a dear friend. Drs. Elaine Leslie and Wei Yue are also gratefully acknowledged for their kind and generous assistance. Elaine Kimple was the glue that held the Brouwer Lab together for many years until her retirement; I couldn't have done it without her. And thankfully, Arlo

Brown filled Elaine's shoes capably and admirably. Julie Cannefax's patience with me is truly commendable.

Most importantly, my family and friends, both near and far, deserve my deepest and most heartfelt appreciation for their continuing love and encouragement. Last but certainly not least, I owe the greatest thanks to my fiancé, Dr. Erin Whalen, for his unwavering love and support throughout this experience. I happily look forward to our bright future together.

## TABLE OF CONTENTS

LIST OF TABLES.....ix

LIST OF FIGURES.....x

LIST OF ABBREVIATIONS.....xiii

### CHAPTERS

1	Introduction.....	1
2	Differential Disposition of Cheodeoxycholic Acid versus Taurocholic Acid in Response to Acute Troglitazone Exposure in Rat Sandwich-Cultured Hepatocytes.....	40
3	Endogenous Bile Acid Disposition in Rat and Human Sandwich-Cultured Hepatocytes: Effect of Troglitazone.....	77
4	Inhibition of MRP4-Mediated Taurocholic Acid Transport by Troglitazone Sulfate.....	119
5	Conclusions and Future Directions.....	148

### APPENDICES

A	Troglitazone-Mediated Inhibition of Taurocholic Acid Transport in Human and Rat Suspended and Sandwich-Cultured Hepatocytes.....	168
B	Data Summary.....	195

## LIST OF TABLES

<b>Table 2.1:</b> Transitions monitored at unit resolution for LC-MS/MS analysis of parent CDCA and taurine- and glycine-conjugated CDCA metabolites in cell lysates from WT rat SCH following a 10-min incubation with 1 $\mu$ M CDCA.....	63
<b>Table 2.2:</b> Accumulation (% total) of CDCA, TCDCA, GCDCA, TMCA, and GMCA in cells and bile in rat SCH following a 10-min incubation with vehicle (0.1% DMSO; CTL) or with 1 $\mu$ M CDCA.....	64
<b>Table 3.1:</b> Demographic data for human liver donors.....	101
<b>Table 3.2:</b> Transitions monitored at unit resolution for LC-MS/MS analysis.....	102
<b>Table 3.3:</b> BEI (%) and concentrations ( $\mu$ M) of BAs in cells + bile, cells, and medium in rat SCH.....	103
<b>Table 3.4:</b> BEI (%) and concentrations ( $\mu$ M) of BAs in cells + bile, cells, and medium in human SCH.....	104
<b>Table 3.5:</b> Concentration ( $\mu$ M) of total CA species (TCA + GCA) and total CDCA species (TCDCA + GCDCA) in cells + bile, cells, and medium of CTL rat and human SCH.....	105
<b>Table A.1.</b> $Cl_{bile}$ (ml/min/kg) of TCA in sandwich-cultured rat and human hepatocytes with increasing concentrations of TRO.....	185

## LIST OF FIGURES

<b>Figure 1.1:</b> Troglitazone ((+/-)-5-[4-(6-hydroxy-2, 5, 7, 8-tetramethyl-chroman-2-yl-methoxy)benzyl]-2,4-thiazolidinedione).....	25
<b>Figure 1.2:</b> Common structure of bile acids, and relative hydrophilicity or hydrophobicity.....	26
<b>Figure 1.3:</b> Human hepatic bile acid transport proteins.....	27
<b>Figure 2.1:</b> Accumulation of [ <sup>14</sup> C]CDCA species in cells + bile (black bars) or cells (white bars) in WT rat SCH following a 10-min incubation with 1 μM [ <sup>14</sup> C]CDCA and vehicle control (0.1% DMSO; CTL), 1, 10, or 100 μM TRO, or 50 μM MK571.....	65
<b>Figure 2.2:</b> Accumulation of (A) [ <sup>14</sup> C]CDCA species and (B) [ <sup>3</sup> H]TCA in cells + bile (black bars) or cells (white bars) in TR <sup>-</sup> rat SCH following a 10-min incubation with 1.2 μM [ <sup>14</sup> C]CDCA or 1 μM [ <sup>3</sup> H]TCA and vehicle control (0.1% DMSO; CTL), 1, 10, or 100 μM TRO, or 50 μM MK571.....	66
<b>Figure 2.3:</b> Accumulation of [ <sup>3</sup> H]TCA in cells + bile (black bars) or cells (white bars) in WT rat SCH following a 10-min incubation with 1 μM [ <sup>3</sup> H]TCA and vehicle control (0.1% DMSO; CTL), or 10, 20, or 50 μM MK571.....	68
<b>Figure 2.4:</b> Parent CDCA and formed CDCA species (taurine- and glycine-conjugated CDCA); TMCA, and GMCA in cells + bile (solid bars) and cells (white bars) in WT rat SCH following a 10-min incubation with vehicle CTL (0.1% DMSO; CTL) or 1 μM unlabeled CDCA.....	69
<b>Figure 2.5:</b> Accumulation of [ <sup>14</sup> C]CDCA (A, B, C) or [ <sup>3</sup> H]TCA (D, E, F) in suspended rat hepatocytes in the presence of 1 μM [ <sup>14</sup> C]CDCA or 1 μM [ <sup>3</sup> H]TCA, and vehicle (● 0.3% DMSO; CTL), 10 μM TRO (■), or 50 μM MK571 (▲).....	70
<b>Figure 3.1:</b> Total accumulation (pmol/mg protein) of total BAs in cells + bile (solid bars), cells (open bars), and medium (hatched bars) in rat SCH over days 1 through 4 of culture.....	106
<b>Figure 3.2:</b> Accumulation (pmol/mg protein) of TCA in cells + bile (solid bars), cells (open bars), and medium (hatched bars) in rat and human SCH following 24-h treatment with vehicle (0.1% DMSO) or 10 μM TRO.....	107
<b>Figure 3.3:</b> Accumulation (pmol/mg protein) of GCA in cells + bile (solid bars), cells (open bars), and medium (hatched bars) in rat and human SCH following 24-h treatment with vehicle (0.1% DMSO) or 10 μM TRO.....	108

<b>Figure 3.4:</b> Accumulation (pmol/mg protein) of TCDCA in cells + bile (solid bars), cells (open bars), and medium (hatched bars) in rat and human SCH following 24-h treatment with vehicle (0.1% DMSO) or 10 $\mu$ M TRO.....	109
<b>Figure 3.5:</b> Accumulation (pmol/mg protein) of GCDCA in cells + bile (solid bars), cells (open bars), and medium (hatched bars) in rat and human SCH following 24-h treatment with vehicle (0.1% DMSO) or 10 $\mu$ M TRO.....	110
<b>Figure 3.6:</b> Accumulation (pmol/mg protein) of total BAs measured in cells + bile (solid bars), cells (open bars), and medium (hatched bars) in rat and human SCH following 24-h treatment with vehicle (0.1% DMSO) or 10 $\mu$ M TRO.....	111
<b>Figure 3.7:</b> Accumulation of individual BA species as percent of total in cells + bile, cells, bile, and medium in rat and human SCH following 24-h treatment with vehicle (0.1% DMSO) or 10 $\mu$ M TRO.....	112
<b>Figure 4.1:</b> ATP-dependent uptake (nM) at 1 and 5 min of TS into MRP4-expressing membrane vesicles incubated with 10 $\mu$ M TS.....	137
<b>Figure 4.2:</b> Uptake of [ <sup>3</sup> H]MTX (pmol/mg protein/90 s) into MRP4-expressing membrane vesicles in the presence of vehicle (0.1% DMSO; CTL), 1 or 10 $\mu$ M TS, or 18 $\mu$ M MK571.....	138
<b>Figure 4.3:</b> Uptake clearance ( $\mu$ l/min/mg protein) of [ <sup>3</sup> H]DHEAS into MRP4-expressing membrane vesicles in the presence of vehicle (0.1% DMSO; CTL), 50 $\mu$ M TS, or 50 $\mu$ M MK571.....	139
<b>Figure 4.4:</b> Time-dependent uptake (pmol/mg protein) of [ <sup>3</sup> H]TCA in CTL (solid circles) and MRP4-expressing (open squares) membrane vesicles.....	140
<b>Figure 4.5:</b> ATP-dependent uptake rate (pmol/mg protein/min) of [ <sup>3</sup> H]TCA in CTL membrane vesicles (solid circles) and MRP4-expressing membrane vesicles (open squares) in the presence of increasing concentrations of TS (0-100 $\mu$ M).....	141
<b>Figure 4.6:</b> MRP4 protein expression in membrane vesicles from CTL (untransfected) HEK293 cells (lanes 1 and 2, 2 $\mu$ g protein/lane; lanes 5 and 6, 10 $\mu$ g protein/lane) and in membrane vesicles from MRP4-transfected HEK293 cells (lanes 3 and 4, 2 $\mu$ g protein/lane; lanes 7 and 8, 10 $\mu$ g protein/lane).....	142
<b>Figure A.1:</b> TCA uptake and excretion by sandwich-cultured rat (A) and human (B) hepatocytes in the presence and absence of TRO.....	186

**Figure A.2:** TCA uptake by rat and human primary suspended hepatocytes in the presence and absence of TRO.....188

**Figure A.3:** Potential implications of NTCP and BSEP inhibition in plasma, hepatocyte, and bile compartments.....190

## LIST OF ABBREVIATIONS

ABC	ATP binding cassette
AdNT	non-targeting adenoviral vector
AdMrp4	multidrug resistance-associated protein 4-targeting adenoviral vector
ALP	alkaline phosphatase
ALT	alanine aminotransferase
APAP	acetaminophen
ATP	adenosine triphosphate
BA	bile acid
BAAT	bile acid–coenzyme A:amino acid N-acyltransferase
BCRP	breast cancer resistance protein
BEI	biliary excretion index
BSEP	bile salt export pump
BSO	buthionine sulfoximine
<sup>14</sup> C	carbon 14
CA	cholic acid
Ca <sup>2+</sup>	calcium ion
CDCA	chenodeoxycholic acid
CDF	5 (and 6)-carboxy-2',7'-dichlorofluorescein
Cl <sub>bile</sub>	biliary clearance
CT	computed tomography
CTL	control
CYP	cytochrome P450

d	deuterium
DCA	deoxycholic acid
DEX	dexamethasone
DHEAS	dehydroepiandrosterone sulfate
DILI	drug-induced liver injury
DMEM	Dulbecco's modified Eagle's medium
DPDPE	[D-Pen2, D-Pen5]-enkephalin
E <sub>2</sub> -17βG	estradiol-17-β-D glucuronide
EHBR	eisai hyperbilirubinemic rats
FBS	fetal bovine serum
GCA	glycocholic acid
GCDCA	glycochenodeoxycholic acid
GGT	gamma-glutamyl transpeptidase
GSH	reduced glutathione
GST	glutathione-S-transferase
h	hour
<sup>3</sup> H	tritium
HBSS	Hanks' balanced salt solution
IC <sub>50</sub>	half-maximal inhibitory concentration
K <sup>+</sup>	potassium ion
K <sub>m</sub>	Michaelis constant
LCA	lithocholic acid
LC-MS/MS	liquid chromatography-tandem mass spectrometry

LDH	lactate dehydrogenase
LPS	lipopolysaccharide
MATE	multidrug and toxic compound extrusion
MCA	muricholic acid
Mg <sup>2+</sup>	magnesium ion
min	minute
MRI	magnetic resonance imaging
MRP	multidrug resistance-associated protein
MTT	(3-(4,5-Dimethylthiazol-2-yl)-2,5-diphenyltetrazolium bromide
MTX	methotrexate
Na <sup>+</sup>	sodium ion
NF	nitrofurantoin
NTCP	sodium/taurocholate cotransporting polypeptide
OAT	organic anion transporter
OATP	organic anion transporting polypeptide
OST $\alpha/\beta$	organic solute transporter alpha/beta
PFIC	progressive familial intrahepatic cholestasis
P-gp	P-glycoprotein
RNAi	ribonucleic acid interference
s	second
SCH	sandwich-cultured hepatocytes
SD	standard deviation
SEM	standard error of the mean

shRNA	short hairpin ribonucleic acid
siRNA	short interfering ribonucleic acid
SULT	sulfotransferase
TCA	taurocholic acid
TCDCA	taurochenodeoxycholic acid
TR <sup>-</sup>	transport (Mrp2) deficient
TRO	troglitazone
TG	troglitazone glucuronide
TQ	troglitazone quinone
TS	troglitazone sulfate
TUDCA	tauroursodeoxycholic acid
UGT	uridine diphosphoglucuronosyl transferase
V <sub>max</sub>	maximal velocity

## **CHAPTER 1**

### **Introduction**

Portions of this chapter are reproduced with permission from: Use of Sandwich-Cultured Hepatocytes To Evaluate Impaired Bile Acid Transport as a Mechanism of Drug-Induced Hepatotoxicity. Tracy L. Marion, Elaine M. Leslie, Kim L. R. Brouwer. *Molecular Pharmaceutics* 2007 4 (6), 911-918. Copyright 2007 American Chemical Society.

**Overview.** Drug-induced hepatotoxicity is a significant problem in drug development and patient care. One manifestation of drug-induced hepatotoxicity is the development of cholestasis, or the inhibition of bile flow. One of the major functions of the liver is the synthesis from cholesterol of bile acids (BAs), which are the primary constituents of bile. BAs are remarkably conserved across species and are very similar between humans and other mammals, including the rat. The hepatobiliary architecture allows for continuous BA recirculation; BAs are transported from hepatocytes into bile canaliculi, are concentrated within the gall bladder, transit through the intestines, are taken back up into the portal venous circulation, and finally are extracted from the blood back into the liver. Because of this enterohepatic circulation, approximately 95% of the BA pool is conserved in humans. While BAs perform important functions in the body, they can be toxic to the liver if they accumulate to high concentrations, and some BAs are more cytotoxic than others. Although some differences exist, hepatic transport proteins that are responsible for the transport of BAs into and out of the liver also are conserved between species. Thus, the study of BA homeostasis in rats is highly relevant to humans. It is well established that inhibition of BA transport proteins by some drugs is a contributing factor to the development of cholestasis and liver injury in some patients. The diabetes drug troglitazone (TRO) (**Figure 1.1**) was removed from clinical use because it caused severe, idiosyncratic hepatotoxicity, requiring liver transplant or even causing death in some patients. In vitro and animal models have established that TRO inhibits BA transport, which is one proposed mechanism of TRO hepatotoxicity. This dissertation research examined the effects of TRO on the

hepatobiliary transport of individual BAs, the effect of TRO on BA composition, and the contribution of the basolateral efflux protein MRP4 in the hepatocellular response to accumulated BAs, parent TRO, and TRO metabolites. A number of model systems were employed to carry out this work, including primary human and rat SCH, suspended rat and human hepatocytes, and inside-out plasma membrane vesicles prepared from MRP4-overexpressing HEK293 cells.

**Drug-induced Hepatotoxicity.** Drug-induced hepatotoxicity can lead to acute liver failure and even death, and is the most common adverse event responsible for the removal of pharmaceuticals from clinical use (Kaplowitz 2001). In Western countries, >65% of acute liver failure cases may be attributed to drugs and toxins, with acetaminophen (APAP) toxicity accounting for the majority of cases (Polson and Lee 2007). Drug-induced hepatotoxicity falls into two categories: intrinsic and idiosyncratic. Intrinsic hepatotoxicity is generally dose-dependent, somewhat predictable, and characteristic for a particular drug, such as the hepatotoxicity associated with APAP. In contrast, idiosyncratic toxicity is a rare hepatotoxic reaction of unknown etiology occurring in a small subset of patients; it is unpredictable, not dose-dependent, and displays no clear underlying mechanism. In most instances, there is no specific treatment for drug-induced liver injury except to remove the causative agent. Symptoms may resolve over time or progress to serious, and even life-threatening, disease. Clearly, drug-induced hepatotoxicity represents a critical problem for pharmaceutical companies, clinicians, and patients alike. Accordingly, an understanding of the possible mechanisms of drug-induced

hepatotoxicity is crucial to limit injury to patients and wasted resources in drug development. Much research into causes of drug-induced hepatotoxicity has focused on well-established mechanisms, including metabolism of compounds to reactive species, adduct formation and subsequent cellular damage, or perturbation of cellular energetics. However, recent research has led to the hypothesis that inhibition of BA transport is an important mechanism of drug-induced hepatotoxicity (Byrne *et al.* 2002; Fattinger *et al.* 2001; Stieger *et al.* 2000).

**Cholestasis.** While drug-induced hepatotoxicity can resemble all forms of liver injury (Kaplowitz 2003), it most often displays characteristics of hepatocellular, cholestatic, or mixed injury, depending on serum biochemical markers (Abboud and Kaplowitz 2007; Benichou 1990; FDA 2009; Pauli-Magnus and Meier 2006). Hepatocellular injury is marked by an initial elevation of alanine aminotransferase (ALT) levels, cholestatic injury is characterized by an increase in serum alkaline phosphatase (ALP) levels, and mixed injury displays features of both types of injury (Navarro and Senior 2006). Cholestasis is defined as the impairment of bile flow, and can be caused by intrahepatic or extrahepatic mechanisms. Intrahepatic cholestasis occurs at the cellular level and is caused by the perturbation of bile formation, while extrahepatic cholestasis occurs at the bile duct level as a result of mechanical obstruction or impairment of bile secretion and flow (Zollner and Trauner 2008). Drugs or hormones can cause a type of noninflammatory cholestasis through the inhibition of BA transporters or the retrieval of transporters from the plasma membrane, whereas “cholestatic hepatitis” or inflammatory cholestasis, occurs as a

result of repression of transporter expression or function due to pro-inflammatory cytokine release in response to sepsis, viral hepatitis, alcohol, or drugs (Zollner and Trauner 2008). Clinically, symptoms of cholestasis include fatigue, nausea, jaundice, dark urine, pale stools, and pruritus. Cholestasis is diagnosed based on plasma concentrations of alkaline phosphatase (ALP), gamma-glutamyl transpeptidase (GGT), total serum BAs, and plasma conjugated bilirubin; ultrasound, computed tomography (CT) scans, and/or magnetic resonance imaging (MRI) also are used to diagnose extrahepatic cholestasis; liver biopsy also can aid in diagnosis (Pauli-Magnus and Meier 2006). Acute cholestasis can progress to chronic vanishing bile duct syndrome (Altraif *et al.* 1994), and lead to chronic intrahepatic cholestasis. In adults, acute cholestasis is most commonly caused by prescription drugs, over-the-counter drugs, and herbal remedies (Heathcote 2007).

**Bile Constituents and Function.** One of the many functions of the liver is the synthesis and secretion of bile, which plays an essential role in the digestion of lipids from the diet. Bile is a mixture of BAs, cholesterol, and phospholipids. Bile is formed in the liver and transported through the biliary tract to the gall bladder, where it is stored and concentrated up to ten-fold (Nathanson and Boyer 1991). The uptake of BAs from the blood, and BA efflux into the bile is the major driving force for BA-*dependent* flow, which occurs as a result of electrical and ionic gradients generated by the  $\text{Na}^+/\text{K}^+$  ATPase and diffusion of  $\text{K}^+$  ions through potassium channels (Bohan and Boyer 2002). Additionally, the canalicular secretion of bicarbonate and reduced glutathione contributes to BA-*independent* bile flow. Bile is secreted postprandially

from the gall bladder into the small intestine where it forms mixed micelles with lipids and cholesterol to aid in the digestion of dietary fats. Approximately 95-98% of the BAs secreted into the intestine are reabsorbed in the distal ileum, returned to the liver via the portal venous circulation, and re-extracted by hepatocytes in a process known as enterohepatic circulation (Wolkoff and Cohen 2003); because of this highly efficient process, the BA pool is constantly recycled (Hofmann 2007a). The small proportion of BAs that are not reabsorbed in each cycle are excreted in the feces and must be replaced through *de novo* synthesis (Hofmann 1999b). The size of the BA pool in humans is ~50-60  $\mu\text{mol/kg}$  body weight, and totals ~3-4 g (Koopman *et al.* 1999; Trauner and Boyer 2003). In addition to the important function of bile in the digestive process, bile also acts as an excretory fluid and is a major route of excretion for some endogenous products and xenobiotics that are not eliminated in the urine by the kidneys. Major constituents of bile in addition to BAs are conjugated bilirubin and/or biliverdin, phospholipids, organic molecules such as plant sterols and drug metabolites, and heavy metal cations (Hofmann 2007a).

**Bile Acids: Synthesis, Structure, and Relative Cytotoxicity.** BAs are the major products of cholesterol catabolism; ~500 mg cholesterol are converted to BAs per day in the adult human liver (reviewed in Thomas *et al.* 2008). BAs are amphipathic detergent-like molecules consisting of a rigid steroidal nucleus of three six-membered rings and one five-membered ring, with a short aliphatic side chain of variable length (**Figure 1.2**). There are two major classes of BAs, depending on the length of the aliphatic side chain (either 24 carbons [ $\text{C}_{24}$ ] or 27 carbons [ $\text{C}_{27}$ ]);  $\text{C}_{24}$

BAs are the major form in the bile of higher vertebrates (Mukhopadhyay and Maitra 2004). BAs are synthesized in the hepatocyte through a number of enzymatic modifications of cholesterol, which begins with the hydroxylation of the cholesterol moiety at the 7 $\alpha$  position by cholesterol 7 $\alpha$ -hydroxylase (CYP7A1) (Bertolotti *et al.* 2001; Higuchi and Gores 2003). The resulting 7 $\alpha$ -hydroxycholesterol is again hydroxylated at the 12 $\beta$  position by CYP8B1, and ultimately, the aliphatic side chain is hydroxylated by mitochondrial CYP27A (reviewed in Thomas *et al.* 2008).

BAs share a common structure because they are all synthesized from cholesterol. The number and location of hydroxyl groups on the steroid nucleus determine the individual BA species and its physicochemical properties.

Hepatocytes of humans and most other mammals synthesize two primary BAs—cholic acid (CA) and chenodeoxycholic acid (CDCA). CA has two hydroxyl groups, whereas CDCA has a single hydroxyl group. In rodents, but not humans, CDCA can be further hydroxylated to form  $\alpha$ -,  $\beta$ -, or  $\omega$ -muricholic acid (MCA) (Botham and Boyd 1983). During enterohepatic circulation, a small percentage of the primary BAs undergo 7 $\alpha$ -dehydroxylation by bacterial enzymes in the intestines to form two major secondary BAs: deoxycholic acid (DCA), which has a single hydroxyl group, and lithocholic acid (LCA), which has no hydroxyl groups (reviewed in Thomas *et al.* 2008).

In humans, virtually all BAs within the hepatocyte are conjugated to glycine (~75%) or taurine (~25%) at the terminal carboxyl group of the aliphatic side chain by the enzyme bile acid–coenzyme A:amino acid N-acyltransferase (BAAT) (Byrne *et al.* 2002; Falany *et al.* 1994; Solaas *et al.* 2000); in rats, ~95-98% of BAs are

conjugated to taurine, also by the rat homologue of BAAT (Alvaro *et al.* 1986; Mizuta *et al.* 1999; Pellicoro *et al.* 2007). This conjugation of BAs to glycine or taurine confers a negative charge, lowers the  $pK_a$ , and increases aqueous solubility, facilitating excretion into bile (Kullak-Ublick *et al.* 2004). Conjugation of BAs with glycine or taurine is highly efficient, and only a tiny fraction of BAs (<1%) remains unconjugated in the bile in humans (Fracchia *et al.* 1996). However, BAs can be conjugated, deconjugated, hydroxylated, and dehydroxylated multiple times by bacterial enzymes as they circulate through the intestines during enterohepatic circulation. Analysis of plasma from healthy human subjects revealed that about 30% of the BAs in the blood returning from the intestines are not conjugated to taurine or glycine (Tagliacozzi *et al.* 2003). Sulfation or glucuronidation of BAs also occurs, but these are generally considered minor pathways of BA conjugation in humans (Hofmann 1990, 2007b). BA concentrations in plasma vary over time and reflect the fed or fasted state (Angelin and Bjorkhem 1977). BA concentrations in hepatocytes can range from 1-2  $\mu\text{M}$  (Hofmann 1999a) up to  $\sim 200 \mu\text{M}$  (Blitzer and Boyer 1982), and up to 1 mM in bile (Hofmann 1999a).

BAs perform important physiological roles, but they are cytotoxic when they accumulate to high intracellular concentrations, and cause mitochondrial dysfunction and trigger apoptosis or necrosis (Roberts *et al.* 1997). Each BA has different physicochemical properties and can have distinct biological activities. The hydrophobicity of BAs, which is predictive of their toxicity, is inversely proportional to the number of hydroxyl groups on the steroid nucleus and their orientation, as well as the conjugation state of the BA (**Figure 1.2**). The order of toxicity of BAs, from

most toxic to least toxic, is: LCA > DCA > CDCA > CA; taurine conjugates are less toxic than glycine conjugates (Thomas *et al.* 2008). BAs have different affinities for BA transporters (Byrne *et al.* 2002; Gerloff *et al.* 1998; Noe *et al.* 2001); therefore, perturbation of BA transport that causes an increase in intracellular BAs may cause the accumulation of some BAs that are more cytotoxic than others through competition for efflux.

**Hepatic Bile Acid Transport Proteins.** BA uptake into hepatocytes from sinusoidal blood, and excretion of BAs from hepatocytes into the bile canaliculi, is dependent on a number of transport proteins (**Figure 1.3**). The Na<sup>+</sup>-taurocholate co-transporting polypeptide NTCP (SLC10A1) is the only Na<sup>+</sup>-dependent basolateral (sinusoidal) BA transport protein in the human hepatocyte; NTCP transports conjugated and unconjugated BAs from the blood into the hepatocyte (Geyer *et al.* 2006; Mita *et al.* 2006; Pauli-Magnus and Meier 2006). The basolateral organic anion transporting polypeptides (OATPs/SLCOs) are generally considered hepatic uptake transporters, and translocate BAs and a variety of organic anions and select organic cations in a Na<sup>+</sup>-independent manner into the hepatocyte (Pauli-Magnus and Meier 2006). The multidrug resistance-associated proteins MRP3 (ABCC3) and MRP4 (ABCC4) are involved in the basolateral excretion of BAs from the hepatocyte back into the blood (Rius *et al.* 2006; Rius *et al.* 2003; Zelcer *et al.* 2003a; Zelcer *et al.* 2003b). Apical (canalicular) BA transport proteins include the bile salt export pump BSEP (ABCB11), which transports conjugated and unconjugated BAs into the bile canaliculi (Gerloff *et al.* 1998; Suchy and Ananthanarayanan 2006) and MRP2

(ABCC2), which transports glucuronidated and sulfated BAs, tauroursodeoxycholic acid (TUDCA), and reduced glutathione (GSH) (Gerk *et al.* 2006; Jedlitschky *et al.* 2006; Nies and Keppler 2006; Pauli-Magnus and Meier 2006). The heteromeric organic solute transporter OST $\alpha/\beta$  is a more recently identified facilitative transporter that transports substrates bidirectionally based on the concentration gradient; it may play a role in the basolateral efflux of bile acids during conditions of impaired canalicular bile acid efflux (reviewed in Soroka *et al.* 2010).

**Sandwich-Cultured Hepatocyte Model.** Sandwich-cultured hepatocytes (SCH) are a promising tool for elucidating the mechanisms of drug-induced toxicity. Unlike hepatocytes cultured using conventional techniques which lose polarity and metabolic function (Jauregui *et al.* 1986; Niemann *et al.* 1991), hepatocytes cultured between two layers of gelled collagen or extracellular matrix such as Matrigel<sup>®</sup> in a sandwich configuration maintain polarity, morphology, and liver-specific metabolic activity (Liu *et al.* 1998; Liu *et al.* 1999a; Liu *et al.* 1999b; Liu *et al.* 1999c). Over time in sandwich culture, hepatocytes develop functional bile canalicular networks sealed by tight junctions, and hepatic transport proteins are expressed and localized to the correct membrane domains allowing for assessment of transport function (LeCluyse *et al.* 1994; Liu *et al.* 1998; Liu *et al.* 1999a; Liu *et al.* 1999b; Liu *et al.* 1999c). In contrast to *in vivo* studies in which the bile canaliculi are inaccessible, the hepatocytes and canalicular networks of cells in a sandwich-cultured configuration are directly accessible, making it possible to measure substrates excreted into bile. Cryopreserved sandwich-cultured human hepatocytes also form bile canalicular

networks, and the function of multiple uptake and excretory transport proteins is similar to that of fresh hepatocytes (Bi *et al.* 2006). This technology is applicable to hepatocytes from species commonly used in toxicological testing including rats, dogs, and monkeys (Rose *et al.* 2006), as well as from humans, and therefore represents an effective *in vitro* approach to study drug-induced hepatotoxicity.

Transport studies in rat SCH reported by Liu *et al.* (Liu *et al.* 1999a; Liu *et al.* 1999b; Liu *et al.* 1999c) first utilized these polarized cells to measure both the uptake of substrate across the basolateral membrane of the hepatocyte and excretion of substrate into the canalicular space. In  $\text{Ca}^{2+}$ -containing standard buffer (Hanks' balanced salts solution), the tight junctions that serve as a barrier between the canalicular lumen (intercellular junctions) and the extracellular space are maintained, and substrates are excreted into and contained within the bile canaliculi. The cumulative uptake of substrate across the basolateral surface of the hepatocyte is represented by the sum of substrate transported into the cytosol and that excreted into the bile canalicular networks. Depletion of  $\text{Ca}^{2+}$  results in disruption of the tight junctions and opens the canalicular spaces; thus, incubation of cells in  $\text{Ca}^{2+}$ -free buffer (Hanks' balanced salts solution without calcium chloride and magnesium sulfate, containing 1 mM EGTA) (Liu *et al.* 1999c) releases the contents of the bile canaliculi into the incubation medium within minutes. The amount of substrate excreted into the canalicular networks is calculated by subtracting the amount of substrate in cells preincubated in  $\text{Ca}^{2+}$ -free buffer (cellular accumulation) from the accumulated amount of substrate in cells preincubated in  $\text{Ca}^{2+}$ -containing buffer (cellular plus biliary accumulation). The biliary excretion of substrates can be

expressed as a biliary excretion index (BEI), which is the percentage of accumulated substrate residing within the bile canaliculi. The BEI is calculated from the following equation:  $BEI = [(Accumulation_{standard\ buffer} - Accumulation_{Ca^{2+}\text{-free}\ buffer}) / Accumulation_{standard\ buffer}] * 100\%$  (Liu *et al.* 1999a). The in vitro biliary clearance ( $Cl_{bile}$ ) is calculated using the following equation:  $Cl_{bile} = (Accumulation_{standard\ buffer} - Accumulation_{Ca^{2+}\text{-free}\ buffer}) / (AUC_{medium})$ , where AUC represents the area under the substrate concentration-time profile in the incubation buffer.

A comparison of the  $Cl_{bile}$  of the model substrates inulin, salicylate, methotrexate, [D-pen2,5]enkephalin, and TCA measured in rat SCH revealed an excellent correlation ( $r^2 = 0.99$ ) with the  $Cl_{bile}$  of these substrates measured in vivo in rats (Liu *et al.* 1999a). More recently, Ghibellini *et al.* (2007) reported a good relationship between the human in vivo  $Cl_{bile}$  of three different compounds (piperacillin,  $^{99m}Tc$ -sestamibi and  $^{99m}Tc$ -mebrofenin, which exhibit low, intermediate, and high  $Cl_{bile}$ , respectively) with that predicted from in vitro studies with human SCH (Ghibellini *et al.* 2007). This study established the relevance of SCH for prediction of human in vivo  $Cl_{bile}$ . When the effects on BEI and in vitro  $Cl_{bile}$  of the P-gp inhibitors verapamil and progesterone, the P-gp activator quercetin, and the P-gp inducers dexamethasone and rifampin were assessed (Annaert and Brouwer 2005), comparisons of BEI and  $Cl_{bile}$  values in the absence and presence of the modulators were used to localize transport interactions to the basolateral or canalicular membrane, thus elucidating potential mechanisms of drug interactions in hepatic transport. For example, a change in BEI implies that canalicular transport is altered,

while an alteration in  $Cl_{bile}$ , with no change in BEI, suggests that the interaction is localized to the basolateral membrane.

### **Additional In Vitro Models to Identify Inhibitors of Bile Acid Transport.**

Freshly-isolated hepatocytes in suspension are a useful tool for the characterization of the mechanisms of hepatic uptake of substrates. During the isolation process, hepatocytes maintain proper localization and function of uptake transport proteins. In contrast, canalicular transporters are internalized from the membrane (Bow *et al.* 2008); thus, suspended hepatocytes are not a suitable model system for studying hepatocyte efflux processes. By substituting choline for  $Na^+$  in the uptake buffer,  $Na^+$ -dependent substrate uptake can be determined by subtracting total uptake in  $Na^+$  conditions from uptake in  $Na^+$ -free conditions. A disadvantage of suspended hepatocytes is that metabolic capacity and transport protein function decrease rapidly, so cells should be used within 6-8 h of isolation.

The uptake of substrates into purified hepatic basolateral or canalicular plasma membrane vesicles is an established tool to determine the kinetics of substrate transport by membrane-bound proteins (Wolters *et al.* 1991). Although the preparation of highly enriched basolateral or canalicular membranes for vesicle transport studies is technically challenging, data from these vesicles can reveal information about transport mechanisms across a specific membrane that is not confounded by the presence of competing metabolic pathways or transport proteins on the opposite membrane. However, these vesicles theoretically include all transporters that reside together on the membrane, and thus may only differentiate

canalicular versus basolateral transport. The use of recombinant expression systems that overexpress a single transport protein in an immortalized parent cell (*i.e.*, HEK293 cells) allows for the preparation of membrane vesicles that can be used to determine whether a compound is an inhibitor and/or substrate for that specific transport protein. These membrane vesicles can be used to directly measure the transport of a specific compound into the vesicles, or to measure the ability of a compound to inhibit the transport of a known substrate of the transporter (El-Sheikh *et al.* 2006; Leslie *et al.* 2003).

**Inhibition of BA Transport is a Potential Mechanism of Hepatotoxicity for Numerous Drugs.** Inhibition of BSEP, leading to the intracellular accumulation of cytotoxic BAs, has been hypothesized as one mechanism of drug-induced hepatotoxicity (Byrne *et al.* 2002; Fattinger *et al.* 2001; Stieger *et al.* 2000). Evidence for the importance of proper BSEP function is clear in progressive familial intrahepatic cholestasis type 2 (PFIC2), which is a rare genetic disease caused by mutations in BSEP; PFIC2 results in severe cholestasis from birth, with rapid progression to cirrhosis, and liver failure (Suchy and Ananthanarayanan 2006). In addition to BSEP, compounds that inhibit one or more of the proteins responsible for BA excretion also may cause the intracellular accumulation of BAs in hepatocytes, and subsequent toxicity due to detergent effects on cellular membranes, mitochondrial dysfunction, and cellular necrosis (Delzenne *et al.* 1992; Desmet 1995; Gores *et al.* 1998; Pauli-Magnus *et al.* 2005). A number of drugs, including cyclosporin A, glibenclamide, rifampin, bosentan, and TRO, have been shown to

inhibit rat and human Bsep-mediated TCA biliary excretion in vitro (Fattinger *et al.* 2001; Funk *et al.* 2001a; Kemp *et al.* 2005; Mano *et al.* 2007; Marion *et al.* 2007; Pauli-Magnus and Meier 2006; Stieger *et al.* 2000). Ritonavir, saquinavir, and efavirenz, three antiretroviral drugs associated frequently with hepatotoxicity in patients infected with human immunodeficiency virus, also inhibit hepatic BA transport (McRae *et al.* 2006).

Kostrubsky *et al.* studied the hepatotoxic potential of a group of compounds that are eliminated preferentially by biliary excretion, but were not predicted to show clinical hepatotoxicity based on results of testing in preclinical species (Kostrubsky *et al.* 2003). The effects of these compounds on TCA transport in hepatocytes cultured in conventional and collagen-sandwich configuration were evaluated. Cyclosporin A, bosentan, CI-1034, glyburide, erythromycin estolate, and troleandomycin inhibited BA excretion in a concentration-dependent manner in human SCH, and to a lesser extent in human hepatocytes cultured in conventional configuration, while the macrolide antibiotics were much less potent inhibitors of TCA excretion. Cyclosporin A, CI-1034, glyburide, and bosentan also inhibited uptake of TCA in a concentration-dependent manner. As a result of these findings, Kostrubsky and coworkers suggested a strategy for using transport assays to rank compounds according to their hepatotoxic potential. Kostrubsky *et al.* also used data generated in SCH, in membrane vesicles isolated from Sf9 cells transfected with BSEP, and from in vivo studies in intact rats to compare the effects of the antidepressant nefazodone and the structural analogs buspirone and trazodone on hepatobiliary transport of TCA (Kostrubsky *et al.* 2006). Nefazodone potently inhibited BSEP in membrane vesicles

and inhibited TCA excretion in human SCH; in intact rats, nefazodone administration caused a transient increase in serum BAs. Buspirone and trazodone, in contrast, did not affect biliary transport in any of the models tested. These findings are consistent with clinical observations of hepatotoxicity and liver failure associated with nefazodone administration, and suggest that in vitro inhibition of BA transport may be predictive of hepatotoxicity in vivo.

**Troglitazone (TRO).** The peroxisome proliferator-activated receptor gamma (PPAR $\gamma$ ) agonist TRO ((+/-)-5-[4-(6-hydroxy-2, 5, 7, 8-tetramethyl-chroman-2-yl-methoxy)benzyl]-2,4-thiazolidinedione) was the first in a new class of thiazolidinedione antidiabetic agents. TRO was approved by the Food and Drug Administration in 1997 for the treatment of non-insulin-dependent diabetes mellitus (type II diabetes), but was subsequently withdrawn from the market in 2000 after numerous reports of hepatotoxicity and liver failure. For most patients who experienced hepatotoxicity, progression to acute liver failure was rapid and irreversible, occurred within a time period of less than one month, and occurred at any point during treatment (Graham *et al.* 2003b). Of the 94 cases of TRO-induced liver failure reported to the FDA, liver pathology data were available for 31 of these; hepatic necrosis was present in 71% of the cases, hepatitis was reported in 13%, and cholestasis with both acute and chronic inflammatory infiltrates was reported in 7% (Graham *et al.* 2003b). Taking into account underreporting to the FDA of adverse events associated with TRO, the likely number of cases of liver failure among patients treated with TRO for 26 months was 1 to 2 per 1000 (Graham *et al.*

2003a; Graham and Green 2000). Unfortunately, preclinical toxicological testing of TRO in animals failed to predict this hepatotoxicity, and subsequent research efforts have focused on elucidating the mechanism(s) of TRO-associated hepatotoxicity. While the precise mechanism(s) remain(s) unclear, several hypotheses have been suggested, including metabolism of TRO to electrophilic reactive intermediates, mitochondrial injury and induction of mitochondrial permeability transition, induction of apoptosis, PPAR $\gamma$ -mediated steatosis, and inhibition of BA transport (Masubuchi 2006; Smith 2003).

In humans, TRO is metabolized extensively in the liver primarily by sulfotransferase (SULT) 1A3 to a sulfate conjugate (TS) (Honma *et al.* 2002; Kawai *et al.* 1997), and via UDP-glucuronosyltransferase (UGT) 1A1 to a glucuronide conjugate (TG) (Watanabe *et al.* 2002; Yoshigae *et al.* 2000); TRO also is oxidized by cytochrome P450 isozymes CYP3A4 and CYP2C8 to a quinone (TQ) (Yamazaki *et al.* 1999). The sulfate and quinone metabolites of TRO accounted for 70% and 10%, respectively, of the metabolites detected in human plasma at steady-state after multiple oral dosing of TRO for 7 days (Loi *et al.* 1999a; Loi *et al.* 1997), while the glucuronide conjugate was a minor metabolite in plasma (Loi *et al.* 1999b; Parke-Davis 1998). At a dose of 400 mg, the majority of [ $^{14}\text{C}$ ]TRO administered orally to humans (about 85%) was recovered in feces, with only 3% recovered in urine; the absolute bioavailability was 40-50% (Parke-Davis 1998). Metabolism of TRO in rats is similar to humans; TRO is primarily metabolized to TS and to a lesser extent to TG, while the formation of TQ is minor. In both plasma and bile of rats, TS is the predominant metabolite, and biliary excretion of TS is about 6-fold higher than of TG

(Izumi *et al.* 1997). Metabolism of TRO is extensive, and very little parent compound is excreted unchanged into urine or bile; TS and TG (68.0% and 11.6%, respectively, of a 5 mg/kg oral dose of TRO) were excreted into the bile in rats, indicating that the total body clearance of TRO is governed by its metabolic clearance (Izumi *et al.* 1996; Izumi *et al.* 1997; Kawai *et al.* 1997). Experiments by Lee *et al.* determined that the metabolism of TRO in rat and human SCH mimicked that in vivo in rats and humans; TRO was metabolized primarily to TS, and to a lesser extent to TG and TQ (Lee *et al.* 2009). Additionally, following a 2-h incubation with TRO, the accumulation of TS was extensive, with intracellular concentrations reaching an estimated 132-222  $\mu\text{M}$  in rat SCH and 136-160  $\mu\text{M}$  in human SCH, based on the reported volume of  $6.2 \times 10^{-6}$   $\mu\text{l}$ /hepatocyte (Uhal and Roehrig 1982) and the accumulated mass of TS.

In vivo and in vitro experiments have demonstrated that TRO, and particularly TS, inhibit bile acid transport, which may lead to cholestasis and subsequent hepatocellular apoptosis or necrosis caused by the intracellular accumulation of BAs (Funk *et al.* 2001a; Funk *et al.* 2001b; Kemp *et al.* 2005; Preininger *et al.* 1999). Intravenous administration of TRO to rats increased plasma BA concentrations in a dose-dependent manner (Funk *et al.* 2001a). BA concentrations were greater in male rats than in females, and this effect was accompanied by accumulation of TS in liver tissue that was 5-fold greater in males than females (Funk *et al.* 2001a). In isolated perfused rat livers, TRO decreased bile secretion rates (Preininger *et al.* 1999). In vitro, both TRO and TS competitively inhibited TCA transport in rat canalicular liver plasma membrane vesicles, and TS was 10-fold more potent a Bsep

inhibitor than TRO (Funk *et al.* 2001a; Funk *et al.* 2001b). Although TS is a more potent Bsep/BSEP inhibitor, Kostrubsky *et al.* reported that when treating human hepatocytes with TRO, increased cytotoxicity correlated with the amount of unsulfated TRO, suggesting that TRO is more directly cytotoxic than TS (Kostrubsky *et al.* 2000). Experiments also indicate that TRO inhibits basolateral uptake of BAs, in addition to inhibiting canalicular efflux. Acute, 10-min treatment with 10  $\mu$ M TRO decreased both the cellular accumulation and biliary excretion of TCA in rat SCH, and decreased the initial uptake of TCA in rat suspended hepatocytes (Kemp *et al.* 2005). In rat basolateral plasma membrane vesicles, 100  $\mu$ M TRO also significantly inhibited Na<sup>+</sup>-dependent TCA uptake (Snow and Moseley 2006).

Like TRO, bosentan also has been shown to inhibit BA transport using multiple model systems. Inhibition of BSEP resulting in BA accumulation in the hepatocyte has been proposed as a mechanism of bosentan-induced hepatotoxicity. This mechanism is challenged by the observation that bosentan, like TRO, does not induce hepatotoxicity in rats. However, inhibition of both human and rat BSEP/Bsep by bosentan has been demonstrated in vitro using rat and human SCH and BSEP/Bsep enriched membrane vesicles (Fattinger *et al.* 2001; Kemp *et al.* 2005; Kostrubsky *et al.* 2003; Leslie *et al.* 2007; Mano *et al.* 2007). In both rat and human SCH, bosentan inhibited uptake, in addition to excretion, of TCA (Kemp *et al.* 2005; Leslie *et al.* 2007). These findings led to the hypothesis that the balance between inhibition of BA uptake and excretion processes could be very important for initiation of hepatotoxic events. Further analysis using rat and human suspended hepatocytes revealed that bosentan inhibited Na<sup>+</sup>-dependent TCA uptake, suggesting that

NTCP/Ntcp was inhibited (Kemp *et al.* 2005; Leslie *et al.* 2007). This observation was confirmed by examining the effect of bosentan on TCA uptake by HEK293 cells over-expressing rat Ntcp or human NTCP (Leslie *et al.* 2007). Interestingly, suspended hepatocytes and the HEK293 model system revealed that rat Ntcp was inhibited more potently by bosentan than human NTCP, suggesting that bosentan may cause toxicity in humans due to the combination of inhibition of BSEP and less potent inhibition of NTCP, resulting in accumulation of BAs in human hepatocytes; in rats, BAs may not accumulate in hepatocytes because both the uptake and excretion of BAs are inhibited, thus protecting the hepatocyte from toxicity.

With this observation regarding bosentan in mind, initial experiments in support of this dissertation research project were performed in order to determine the effect of TRO on TCA uptake and accumulation in human SCH compared to rat SCH (Appendix A). Results indicated that 10  $\mu\text{M}$  TRO decreased cellular accumulation and biliary excretion of [ $^3\text{H}$ ]TCA in a concentration-dependent manner in both human and rat SCH similarly, although the BEI was decreased more in human than in rat (54.3% vs 71.0%, respectively) (Marion *et al.* 2007). Unlike the situation with bosentan, TRO was a *more* potent inhibitor of  $\text{Na}^+$ -dependent [ $^3\text{H}$ ]TCA uptake in human suspended hepatocytes ( $\text{IC}_{50} = 0.33 \mu\text{M}$ ) than in rat suspended hepatocytes ( $\text{IC}_{50} = 1.9 \mu\text{M}$ ). This observation led to the following question: If TRO inhibits both basolateral uptake and canalicular efflux of TCA, then how could TRO cause the intracellular accumulation of BAs?

**Compensatory BA Transport.** This question was addressed by considering the potential role of individual BA species and compensatory BA transport proteins in the hepatotoxicity of TRO. Because there is evidence that individual BAs have different affinities for BA transporters (Byrne *et al.* 2002; Gerloff *et al.* 1998; Noe *et al.* 2001), perturbations in BA transport may increase the intracellular accumulation of some BAs that are more cytotoxic than others through competition for efflux. The basolateral efflux transport protein MRP4 normally is expressed at low levels in hepatocytes, but is induced in cholestasis in humans (Gradhand *et al.* 2008), presumably as an adaptive response mechanism to compensate for increased intracellular concentrations of BAs; MRP4 induction may explain the increased excretion of BAs in the urine of patients with cholestasis (Assem *et al.* 2004; Schuetz *et al.* 2001; Zollner *et al.* 2003). Also, patients with PFIC2 have significantly increased liver expression of MRP4 mRNA and protein (Keitel *et al.* 2005).

The substrate specificity of MRP4 is broad, and includes the cyclic nucleotides cAMP and cGMP, prostaglandins, and BAs as well as sulfate-conjugated BAs (Sampath *et al.* 2002; Zelcer *et al.* 2003a). If treatment with TRO causes an increase in intracellular BAs, MRP4/Mrp4 protein expression and/or membrane localization may increase in order to compensate, especially if TS accumulates within hepatocytes and continues to inhibit BSEP/Bsep function. Interestingly, Lee *et al.* found that pretreatment of rat SCH with buthionine sulfoximine (BSO), an inhibitor of glutathione synthesis, increased Mrp4 protein expression (Lee *et al.* 2008). This upregulation of Mrp4 may have been a direct effect of BSO, or a response to oxidative stress induced by GSH depletion. It has

been established that the canalicular transport proteins P-gp, BSEP, and MRP2 reside inside intracellular compartments and traffic to the canalicular membrane under increased physiological demand for BA and organic anion efflux; this membrane trafficking can occur within minutes, and allows for more rapid upregulation of transport capability than would be possible through increased protein synthesis (reviewed in Kipp and Arias 2002). Similarly, Hoque and Cole reported that downregulation of the protein Na<sup>+</sup>/H<sup>+</sup> exchanger regulatory factor 1 (NHERF1) by siRNA in MRP4-expressing HeLa cells increased MRP4 protein membrane localization, which was attributed to decreased internalization of this transport protein (Hoque and Cole 2008). Therefore, while basal MRP4 expression is considered low in liver, it is possible that increased mRNA and protein expression, as well as membrane trafficking, may play important roles in increasing MRP4 in cholestasis.

**Goals and Specific Aims.** The goal of this dissertation work was to examine the effect of TRO on the hepatobiliary disposition of individual BAs, to determine the effect of TRO on intracellular BA composition, and to elucidate the contribution of the basolateral efflux protein MRP4/Mrp4 to the hepatocellular response to accumulated BAs, parent TRO, and TRO metabolites. A number of model systems were employed to carry out this work, including primary rat and human SCH, suspended rat and human hepatocytes, and inside-out plasma membrane vesicles from MRP4 overexpressing HEK293 cells.

**SPECIFIC AIM 1:** Demonstrate that TRO differentially affects the intracellular accumulation of BAs, leading to the accumulation of more cytotoxic BA species.

**Hypothesis 1:** In contrast to TCA, acute TRO exposure causes the intracellular accumulation of more toxic BAs.

**Strategy:**

- Measure effect of TRO on acute (10-min) accumulation of [<sup>14</sup>C]CDCA species in medium, cells + bile, and cells in WT and TR<sup>-</sup> rat SCH
- Compare accumulation of [<sup>14</sup>C]CDCA species to effects on acute [<sup>3</sup>H]TCA accumulation
- Examine the effect of the pan-MRP/Mrp inhibitor MK571 to probe the effect of Mrp inhibition on disposition of both [<sup>14</sup>C]CDCA and [<sup>3</sup>H]TCA
- Measure parent and metabolites of unlabeled CDCA following a 10-min incubation in rat SCH

**Hypothesis 2:** TRO inhibits the accumulation of [<sup>14</sup>C]CDCA in WT and TR<sup>-</sup> rat SCH less than [<sup>3</sup>H]TCA because [<sup>14</sup>C]CDCA uptake is primarily Na<sup>+</sup>-independent, while TRO has a greater inhibitory effect on Na<sup>+</sup>-dependent Ntcp function.

**Strategy:**

- Measure the effect of TRO on initial uptake of [<sup>14</sup>C]CDCA and compare to effects on 1 μM [<sup>3</sup>H]TCA uptake in suspended rat hepatocytes
- Examine the effect of MK571 on the inhibition of TCA uptake

**SPECIFIC AIM 2:** Characterize the effects of TRO treatment on the endogenous BA pool, including composition and size, in medium, cells, and bile of rat and human

SCH. **Hypothesis:** TRO exerts differential effects on *endogenous* BAs, causing the intracellular accumulation of more toxic BAs, and shifts the intracellular BA pool composition toward more toxic species.

**Strategy:** Compare longer-term (24-h) effects of TRO on endogenous BA disposition in cells + bile, cells, and medium in rat and human SCH

- Measure and compare endogenous BAs common to both rat and human (TCA, GCA, TCDCA, GCDCA) in control SCH. Because of lack of enterohepatic cycling, secondary BAs and unconjugated BAs (LCA, DCA, CA, CDCA) were not included in the analysis.
- Examine the effect of 24-h treatment with TRO on endogenous BA disposition in cells + bile, cells, and medium of rat and human SCH

**SPECIFIC AIM 3:** Demonstrate that TS inhibits MRP4-mediated bile acid transport.

**Hypothesis:** Intracellular accumulation of TS can inhibit compensatory MRP4-mediated BA efflux.

**Strategy:** Measure uptake of [<sup>3</sup>H]TCA by MRP4-expressing membrane vesicles from HEK293 cells in the presence of TS.

- Measure uptake of TS in MRP4-expressing membrane vesicles
- Measure MRP4-mediated uptake of the known MRP4 substrates methotrexate (MTX) and dehydroepiandrosterone (DHEAS)
- Measure uptake of [<sup>3</sup>H]TCA in the presence of increasing concentrations of TS

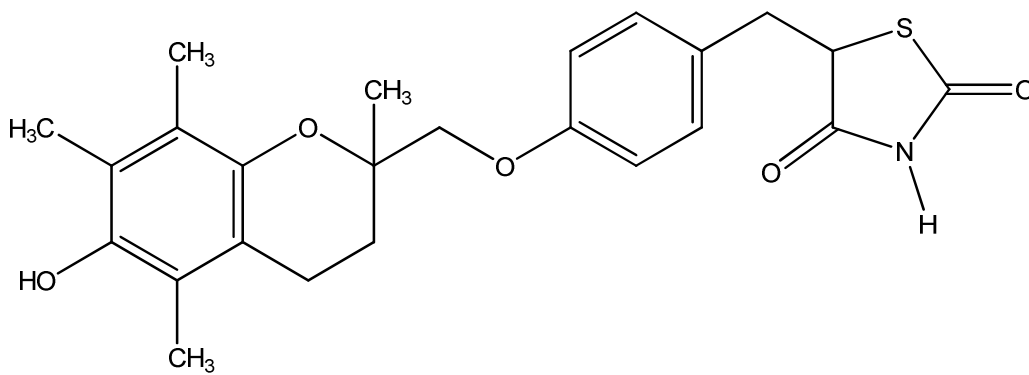


**Figure 1.1:** Troglitazone ((+/-)-5-[4-(6-hydroxy-2, 5, 7, 8-tetramethyl-chroman-2-yl-methoxy)benzyl]-2,4-thiazolidinedione).

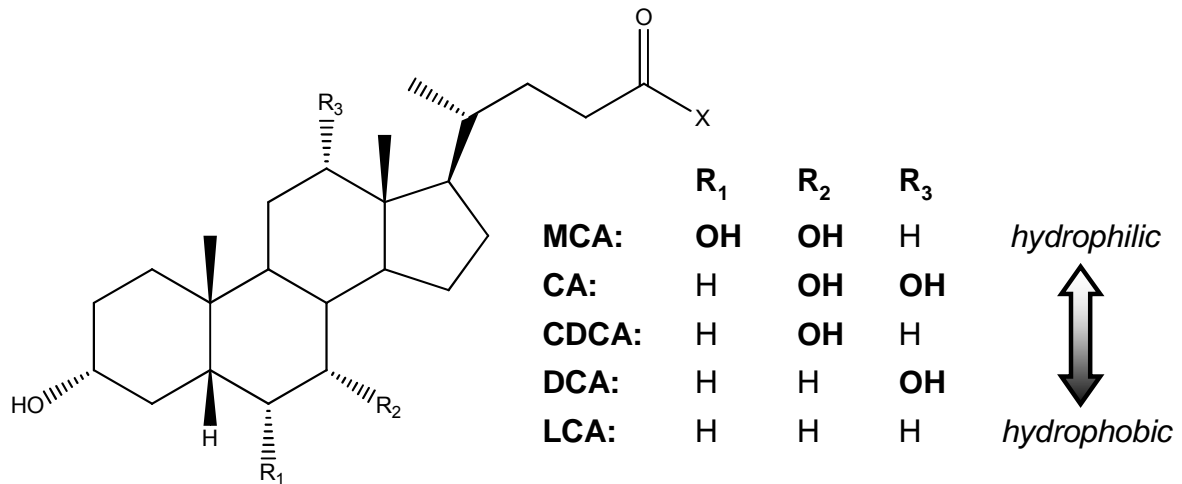


**Figure 1.2:** Common structure of bile acids, and relative hydrophilicity or hydrophobicity. R<sub>1</sub>, R<sub>2</sub>, and R<sub>3</sub> denote location of potential hydroxyl groups, X denotes location of taurine or glycine conjugation.

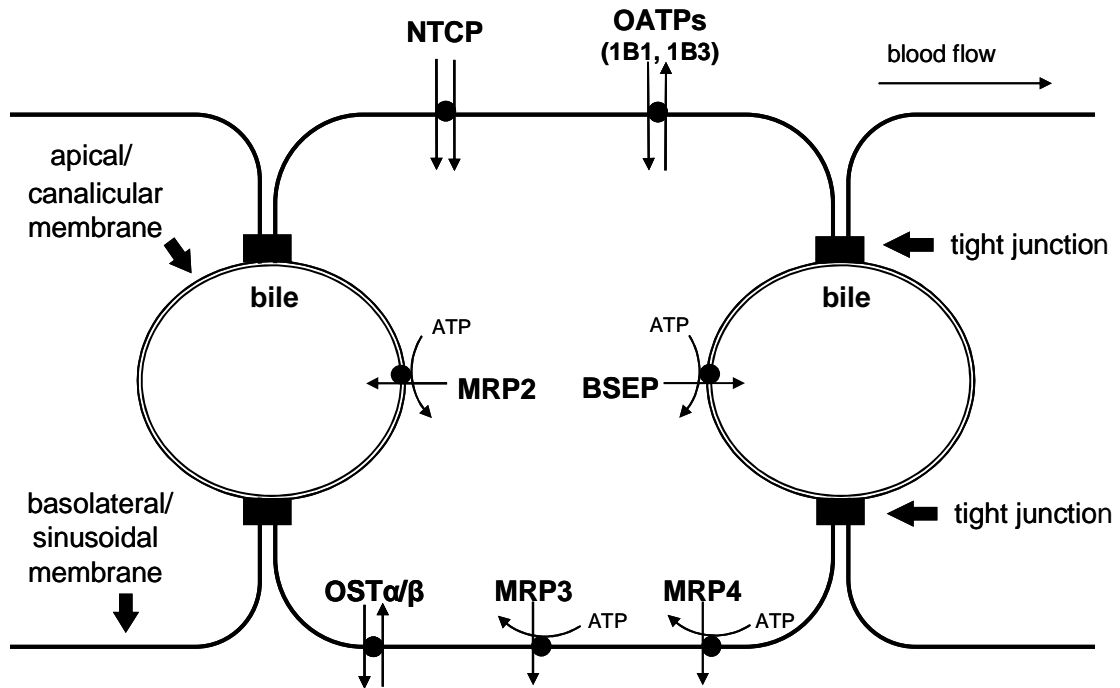


**Figure 1.3:** Human hepatic bile acid transport proteins.

## REFERENCES

- Abboud, G., and Kaplowitz, N. (2007). Drug-induced liver injury. *Drug Saf* **30**, 277-94.
- Altraif, I., Lilly, L., Wanless, I. R., and Heathcote, J. (1994). Cholestatic liver disease with ductopenia (vanishing bile duct syndrome) after administration of clindamycin and trimethoprim-sulfamethoxazole. *Am J Gastroenterol* **89**, 1230-4.
- Alvaro, D., Cantafora, A., Attili, A. F., Ginanni Corradini, S., De Luca, C., Minervini, G., Di Biase, A., and Angelico, M. (1986). Relationships between bile salts hydrophilicity and phospholipid composition in bile of various animal species. *Comp Biochem Physiol B* **83**, 551-4.
- Angelin, B., and Bjorkhem, I. (1977). Postprandial serum bile acids in healthy man. Evidence for differences in absorptive pattern between individual bile acids. *Gut* **18**, 606-9.
- Annaert, P. P., and Brouwer, K. L. (2005). Assessment of drug interactions in hepatobiliary transport using rhodamine 123 in sandwich-cultured rat hepatocytes. *Drug Metab Dispos* **33**, 388-94.
- Assem, M., Schuetz, E. G., Leggas, M., Sun, D., Yasuda, K., Reid, G., Zelcer, N., Adachi, M., Strom, S., Evans, R. M., Moore, D. D., Borst, P., and Schuetz, J. D. (2004). Interactions between hepatic Mrp4 and Sult2a as revealed by the constitutive androstane receptor and Mrp4 knockout mice. *J Biol Chem* **279**, 22250-7.
- Benichou, C. (1990). Criteria of drug-induced liver disorders. Report of an international consensus meeting. *J Hepatol* **11**, 272-6.
- Bertolotti, M., Carulli, L., Concari, M., Martella, P., Loria, P., Tagliafico, E., Ferrari, S., Del Puppo, M., Amati, B., De Fabiani, E., Crestani, M., Amorotti, C., Manenti, A., Carubbi, F., Pinetti, A., and Carulli, N. (2001). Suppression of bile acid synthesis, but not of hepatic cholesterol 7 $\alpha$ -hydroxylase expression, by obstructive cholestasis in humans. *Hepatology* **34**, 234-42.
- Bi, Y. A., Kazolias, D., and Duignan, D. B. (2006). Use of cryopreserved human hepatocytes in sandwich culture to measure hepatobiliary transport. *Drug Metab Dispos* **34**, 1658-65.

Blitzer, B. L., and Boyer, J. L. (1982). Cellular mechanisms of bile formation. *Gastroenterology* **82**, 346-57.

Bohan, A., and Boyer, J. L. (2002). Mechanisms of hepatic transport of drugs: implications for cholestatic drug reactions. *Semin Liver Dis* **22**, 123-36.

Botham, K. M., and Boyd, G. S. (1983). The metabolism of chenodeoxycholic acid to beta-muricholic acid in rat liver. *Eur J Biochem* **134**, 191-6.

Bow, D. A., Perry, J. L., Miller, D. S., Pritchard, J. B., and Brouwer, K. L. (2008). Localization of P-gp (Abcb1) and Mrp2 (Abcc2) in freshly isolated rat hepatocytes. *Drug Metab Dispos* **36**, 198-202.

Byrne, J. A., Strautnieks, S. S., Mieli-Vergani, G., Higgins, C. F., Linton, K. J., and Thompson, R. J. (2002). The human bile salt export pump: characterization of substrate specificity and identification of inhibitors. *Gastroenterology* **123**, 1649-58.

Delzenne, N. M., Calderon, P. B., Taper, H. S., and Roberfroid, M. B. (1992). Comparative hepatotoxicity of cholic acid, deoxycholic acid and lithocholic acid in the rat: in vivo and in vitro studies. *Toxicol Lett* **61**, 291-304.

Desmet, V. J. (1995). Histopathology of cholestasis. *Verh Dtsch Ges Pathol* **79**, 233-40.

El-Sheikh, A. A., van den Heuvel, J. J., Koenderink, J. B., and Russel, F. G. (2006). Interaction of non-steroidal anti-inflammatory drugs with MRP2/ABCC2- and MRP4/ABCC4-mediated methotrexate transport. *J Pharmacol Exp Ther.* **30**, 229-35.

Falany, C. N., Johnson, M. R., Barnes, S., and Diasio, R. B. (1994). Glycine and taurine conjugation of bile acids by a single enzyme. Molecular cloning and expression of human liver bile acid CoA:amino acid N-acyltransferase. *J Biol Chem* **269**, 19375-9.

Fattinger, K., Funk, C., Pantze, M., Weber, C., Reichen, J., Stieger, B., and Meier, P. J. (2001). The endothelin antagonist bosentan inhibits the canalicular bile salt export pump: a potential mechanism for hepatic adverse reactions. *Clin Pharmacol Ther* **69**, 223-31.

FDA (2009). Guidance for Industry Drug-Induced Liver Injury: Premarketing Clinical Evaluation Vol. 2010. U.S. Department of Health and Human Services Food and Drug Administration Center for Drug Evaluation and Research (CDER) Center for Biologics Evaluation and Research (CBER).

Fracchia, M., Setchell, K. D., Crosignani, A., Podda, M., O'Connell, N., Ferraris, R., Hofmann, A. F., and Galatola, G. (1996). Bile acid conjugation in early stage cholestatic liver disease before and during treatment with ursodeoxycholic acid. *Clin Chim Acta* **248**, 175-85.

Funk, C., Pantze, M., Jehle, L., Ponelle, C., Scheuermann, G., Lazendic, M., and Gasser, R. (2001a). Troglitazone-induced intrahepatic cholestasis by an interference with the hepatobiliary export of bile acids in male and female rats. Correlation with the gender difference in troglitazone sulfate formation and the inhibition of the canalicular bile salt export pump (Bsep) by troglitazone and troglitazone sulfate. *Toxicology* **167**, 83-98.

Funk, C., Ponelle, C., Scheuermann, G., and Pantze, M. (2001b). Cholestatic potential of troglitazone as a possible factor contributing to troglitazone-induced hepatotoxicity: in vivo and in vitro interaction at the canalicular bile salt export pump (Bsep) in the rat. *Mol Pharmacol* **59**, 627-35.

Gerk, P. M., Li, W., Megaraj, V., and Vore, M. (2006). Human multidrug resistance protein 2 (MRP2/ABCC2) transports the therapeutic bile salt tauroursodeoxycholate. *J Pharmacol Exp Ther* **320**, 893-9.

Gerloff, T., Stieger, B., Hagenbuch, B., Madon, J., Landmann, L., Roth, J., Hofmann, A. F., and Meier, P. J. (1998). The sister of P-glycoprotein represents the canalicular bile salt export pump of mammalian liver. *J Biol Chem* **273**, 10046-50.

Geyer, J., Wilke, T., and Petzinger, E. (2006). The solute carrier family SLC10: more than a family of bile acid transporters regarding function and phylogenetic relationships. *Naunyn Schmiedebergs Arch Pharmacol* **372**, 413-31.

Ghibellini, G., Vasist, L. S., Leslie, E. M., Heizer, W. D., Kowalsky, R. J., Calvo, B. F., and Brouwer, K. L. R. (2007). In Vitro-In Vivo Correlation of Hepatobiliary Drug Clearance in Humans. *Clin Pharmacol Ther* **81**, 406-13.

Gores, G. J., Miyoshi, H., Botla, R., Aguilar, H. I., and Bronk, S. F. (1998). Induction of the mitochondrial permeability transition as a mechanism of liver injury during

cholestasis: a potential role for mitochondrial proteases. *Biochim Biophys Acta* **1366**, 167-75.

Gradhand, U., Lang, T., Schaeffeler, E., Glaeser, H., Tegude, H., Klein, K., Fritz, P., Jedlitschky, G., Kroemer, H. K., Bachmakov, I., Anwald, B., Kerb, R., Zanger, U. M., Eichelbaum, M., Schwab, M., and Fromm, M. F. (2008). Variability in human hepatic MRP4 expression: influence of cholestasis and genotype. *Pharmacogenomics J* **8**, 42-52.

Graham, D. J., Drinkard, C. R., and Shatin, D. (2003a). Incidence of idiopathic acute liver failure and hospitalized liver injury in patients treated with troglitazone. *Am J Gastroenterol* **98**, 175-9.

Graham, D. J., and Green, L. (2000). Final Report: Liver Failure Risk with Troglitazone. Office of Postmarketing Drug Risk Assessment, Center for Drug Evaluation and Research, Food and Drug Administration, Rockville, MD.

Graham, D. J., Green, L., Senior, J. R., and Nourjah, P. (2003b). Troglitazone-induced liver failure: a case study. *Am J Med* **114**, 299-306.

Heathcote, E. J. (2007). Diagnosis and management of cholestatic liver disease. *Clin Gastroenterol Hepatol* **5**, 776-82.

Higuchi, H., and Gores, G. J. (2003). Bile acid regulation of hepatic physiology: IV. Bile acids and death receptors. *Am J Physiol Gastrointest Liver Physiol* **284**, G734-8.

Hofmann, A. F. (1990). Bile acid secretion, bile flow and biliary lipid secretion in humans. *Hepatology* **12**, 17S-22S; discussion 22S-25S.

Hofmann, A. F. (1999a). Bile Acids: The Good, the Bad, and the Ugly. *News Physiol Sci* **14**, 24-29.

Hofmann, A. F. (1999b). The continuing importance of bile acids in liver and intestinal disease. *Arch Intern Med* **159**, 2647-58.

Hofmann, A. F. (2007a). Biliary secretion and excretion in health and disease: current concepts. *Ann Hepatol* **6**, 15-27.

- Hofmann, A. F. (2007b). Why bile acid glucuronidation is a minor pathway for conjugation of endogenous bile acids in man. *Hepatology* **45**, 1083-4.
- Honma, W., Shimada, M., Sasano, H., Ozawa, S., Miyata, M., Nagata, K., Ikeda, T., and Yamazoe, Y. (2002). Phenol sulfotransferase, ST1A3, as the main enzyme catalyzing sulfation of troglitazone in human liver. *Drug Metab Dispos* **30**, 944-9.
- Hoque, M. T., and Cole, S. P. (2008). Down-regulation of Na<sup>+</sup>/H<sup>+</sup> exchanger regulatory factor 1 increases expression and function of multidrug resistance protein 4. *Cancer Res* **68**, 4802-9.
- Izumi, T., Enomoto, S., Hosiyama, K., Sasahara, K., Shibukawa, A., Nakagawa, T., and Sugiyama, Y. (1996). Prediction of the human pharmacokinetics of troglitazone, a new and extensively metabolized antidiabetic agent, after oral administration, with an animal scale-up approach. *J Pharmacol Exp Ther* **277**, 1630-41.
- Izumi, T., Hosiyama, K., Enomoto, S., Sasahara, K., and Sugiyama, Y. (1997). Pharmacokinetics of troglitazone, an antidiabetic agent: prediction of in vivo stereoselective sulfation and glucuronidation from in vitro data. *J Pharmacol Exp Ther* **280**, 1392-400.
- Jauregui, H. O., McMillan, P. N., Driscoll, J., and Naik, S. (1986). Attachment and long term survival of adult rat hepatocytes in primary monolayer cultures: comparison of different substrata and tissue culture media formulations. *In Vitro Cell Dev Biol* **22**, 13-22.
- Jedlitschky, G., Hoffmann, U., and Kroemer, H. K. (2006). Structure and function of the MRP2 (ABCC2) protein and its role in drug disposition. *Expert Opin Drug Metab Toxicol* **2**, 351-66.
- Kaplowitz, N. (2001). Drug-induced liver disorders: implications for drug development and regulation. *Drug Saf* **24**, 483-90.
- Kaplowitz, N., DeLeve, L.D. (2003). *Drug-Induced Liver Disease*. Marcel Dekker, New York.
- Kawai, K., Kawasaki-Tokui, Y., Odaka, T., Tsuruta, F., Kazui, M., Iwabuchi, H., Nakamura, T., Kinoshita, T., Ikeda, T., Yoshioka, T., Komai, T., and Nakamura, K. (1997). Disposition and metabolism of the new oral antidiabetic drug troglitazone in rats, mice and dogs. *Arzneimittelforschung* **47**, 356-68.

Keitel, V., Burdelski, M., Warskulat, U., Kuhlkamp, T., Keppler, D., Haussinger, D., and Kubitz, R. (2005). Expression and localization of hepatobiliary transport proteins in progressive familial intrahepatic cholestasis. *Hepatology* **41**, 1160-72.

Kemp, D. C., Zamek-Gliszczynski, M. J., and Brouwer, K. L. (2005). Xenobiotics inhibit hepatic uptake and biliary excretion of taurocholate in rat hepatocytes. *Toxicol Sci* **83**, 207-14.

Kipp, H., and Arias, I. M. (2002). Trafficking of canalicular ABC transporters in hepatocytes. *Annu Rev Physiol* **64**, 595-608.

Koopen, N. R., Post, S. M., Wolters, H., Havinga, R., Stellaard, F., Boverhof, R., Kuipers, F., and Princen, H. M. (1999). Differential effects of 17alpha-ethinylestradiol on the neutral and acidic pathways of bile salt synthesis in the rat. *J Lipid Res* **40**, 100-8.

Kostrubsky, S. E., Strom, S. C., Kalgutkar, A. S., Kulkarni, S., Atherton, J., Mireles, R., Feng, B., Kubik, R., Hanson, J., Urda, E., and Mutlib, A. E. (2006). Inhibition of hepatobiliary transport as a predictive method for clinical hepatotoxicity of nefazodone. *Toxicol Sci* **90**, 451-9.

Kostrubsky, V. E., Sinclair, J. F., Ramachandran, V., Venkataramanan, R., Wen, Y. H., Kindt, E., Galchev, V., Rose, K., Sinz, M., and Strom, S. C. (2000). The role of conjugation in hepatotoxicity of troglitazone in human and porcine hepatocyte cultures. *Drug Metab Dispos* **28**, 1192-7.

Kostrubsky, V. E., Strom, S. C., Hanson, J., Urda, E., Rose, K., Burliegh, J., Zocharski, P., Cai, H., Sinclair, J. F., and Sahi, J. (2003). Evaluation of hepatotoxic potential of drugs by inhibition of bile-acid transport in cultured primary human hepatocytes and intact rats. *Toxicol Sci* **76**, 220-8.

Kullak-Ublick, G. A., Stieger, B., and Meier, P. J. (2004). Enterohepatic bile salt transporters in normal physiology and liver disease. *Gastroenterology* **126**, 322-42.

LeCluyse, E. L., Audus, K. L., and Hochman, J. H. (1994). Formation of extensive canalicular networks by rat hepatocytes cultured in collagen-sandwich configuration. *Am J Physiol* **266**, C1764-74.

Lee, J. K., Leslie, E. M., Zamek-Gliszczynski, M. J., and Brouwer, K. L. (2008). Modulation of trabectedin (ET-743) hepatobiliary disposition by multidrug resistance-

associated proteins (Mrps) may prevent hepatotoxicity. *Toxicol Appl Pharmacol* **228**, 17-23.

Lee, J. K., Marion, T., Abe, K., Lim, C., Pollack, G. M., and Brouwer, K. L. (2009). Hepatobiliary Disposition of Troglitazone and Metabolites in Rat and Human Sandwich-Cultured Hepatocytes: Use of Monte Carlo Simulations to Assess the Impact of Changes in Biliary Excretion on Troglitazone Sulfate Accumulation. *J Pharmacol Exp Ther*.

Leslie, E. M., Bowers, R. J., Deeley, R. G., and Cole, S. P. (2003). Structural requirements for functional interaction of glutathione tripeptide analogs with the human multidrug resistance protein 1 (MRP1). *J Pharmacol Exp Ther* **304**, 643-53.

Leslie, E. M., Watkins, P. B., Kim, R. B., and Brouwer, K. L. (2007). Differential Inhibition of Rat and Human Na<sup>+</sup>-dependent Taurocholate Co-transporting Polypeptide (NTCP/SLC10A1) by Bosentan: A Mechanism for Species Differences in Hepatotoxicity. *J Pharmacol Exp Ther*.

Liu, X., Brouwer, K. L., Gan, L. S., Brouwer, K. R., Stieger, B., Meier, P. J., Audus, K. L., and LeCluyse, E. L. (1998). Partial maintenance of taurocholate uptake by adult rat hepatocytes cultured in a collagen sandwich configuration. *Pharm Res* **15**, 1533-9.

Liu, X., Chism, J. P., LeCluyse, E. L., Brouwer, K. R., and Brouwer, K. L. R. (1999a). Correlation of biliary excretion in sandwich-cultured rat hepatocytes and in vivo in rats. *Drug Metab Dispos* **27**, 637-44.

Liu, X., LeCluyse, E. L., Brouwer, K. R., Gan, L. S., Lemasters, J. J., Stieger, B., Meier, P. J., and Brouwer, K. L. R. (1999b). Biliary excretion in primary rat hepatocytes cultured in a collagen-sandwich configuration. *Am J Physiol* **277**, G12-21.

Liu, X., LeCluyse, E. L., Brouwer, K. R., Lightfoot, R. M., Lee, J. I., and Brouwer, K. L. (1999c). Use of Ca<sup>2+</sup> modulation to evaluate biliary excretion in sandwich-cultured rat hepatocytes. *J Pharmacol Exp Ther* **289**, 1592-9.

Loi, C. M., Alvey, C. W., Vassos, A. B., Randinitis, E. J., Sedman, A. J., and Koup, J. R. (1999a). Steady-state pharmacokinetics and dose proportionality of troglitazone and its metabolites. *J Clin Pharmacol* **39**, 920-6.

Loi, C. M., Randinitis, E. J., Vassos, A. B., Kazierad, D. J., Koup, J. R., and Sedman, A. J. (1997). Lack of effect of type II diabetes on the pharmacokinetics of troglitazone in a multiple-dose study. *J Clin Pharmacol* **37**, 1114-20.

Loi, C. M., Young, M., Randinitis, E., Vassos, A., and Koup, J. R. (1999b). Clinical pharmacokinetics of troglitazone. *Clin Pharmacokinet* **37**, 91-104.

Mano, Y., Usui, T., and Kamimura, H. (2007). Effects of bosentan, an endothelin receptor antagonist, on bile salt export pump and multidrug resistance-associated protein 2. *Biopharm Drug Dispos* **28**, 13-8.

Marion, T. L., Leslie, E. M., and Brouwer, K. L. (2007). Use of sandwich-cultured hepatocytes to evaluate impaired bile acid transport as a mechanism of drug-induced hepatotoxicity. *Mol Pharm* **4**, 911-8.

Masubuchi, Y. (2006). Metabolic and non-metabolic factors determining troglitazone hepatotoxicity: a review. *Drug Metab Pharmacokinet* **21**, 347-56.

McRae, M. P., Lowe, C. M., Tian, X., Bourdet, D. L., Ho, R. H., Leake, B. F., Kim, R. B., Brouwer, K. L. R., and Kashuba, A. D. (2006). Ritonavir, saquinavir, and efavirenz, but not nevirapine, inhibit bile acid transport in human and rat hepatocytes. *J Pharmacol Exp Ther* **318**, 1068-75.

Mita, S., Suzuki, H., Akita, H., Hayashi, H., Onuki, R., Hofmann, A. F., and Sugiyama, Y. (2006). Vectorial transport of unconjugated and conjugated bile salts by monolayers of LLC-PK1 cells doubly transfected with human NTCP and BSEP or with rat Ntcp and Bsep. *Am J Physiol Gastrointest Liver Physiol* **290**, G550-6.

Mizuta, K., Kobayashi, E., Uchida, H., Ogino, Y., Fujimura, A., Kawarasaki, H., and Hashizume, K. (1999). Cyclosporine inhibits transport of bile acid in rats: comparison of bile acid composition between liver and bile. *Transplant Proc* **31**, 2755-6.

Mukhopadhyay, S., and Maitra, U. (2004). Facile synthesis, aggregation behavior, and cholesterol solubilization ability of avicholic acid. *Org Lett* **6**, 31-4.

Nathanson, M. H., and Boyer, J. L. (1991). Mechanisms and regulation of bile secretion. *Hepatology* **14**, 551-66.

Navarro, V. J., and Senior, J. R. (2006). Drug-related hepatotoxicity. *N Engl J Med* **354**, 731-9.

Niemann, C., Gauthier, J. C., Richert, L., Ivanov, M. A., Melcion, C., and Cordier, A. (1991). Rat adult hepatocytes in primary pure and mixed monolayer culture. Comparison of the maintenance of mixed function oxidase and conjugation pathways of drug metabolism. *Biochem Pharmacol* **42**, 373-9.

Nies, A. T., and Keppler, D. (2006). The apical conjugate efflux pump ABCC2 (MRP2). *Pflugers Arch* **453**, 643-59.

Noe, J., Hagenbuch, B., Meier, P. J., and St-Pierre, M. V. (2001). Characterization of the mouse bile salt export pump overexpressed in the baculovirus system. *Hepatology* **33**, 1223-31.

Parke-Davis (1998). *Rezulin (troglitazone) package insert*, Morris Plains, NJ.

Pauli-Magnus, C., and Meier, P. J. (2006). Hepatobiliary transporters and drug-induced cholestasis. *Hepatology* **44**, 778-87.

Pauli-Magnus, C., Stieger, B., Meier, Y., Kullak-Ublick, G. A., and Meier, P. J. (2005). Enterohepatic transport of bile salts and genetics of cholestasis. *J Hepatol* **43**, 342-57.

Pellicoro, A., van den Heuvel, F. A., Geuken, M., Moshage, H., Jansen, P. L., and Faber, K. N. (2007). Human and rat bile acid-CoA:amino acid N-acyltransferase are liver-specific peroxisomal enzymes: implications for intracellular bile salt transport. *Hepatology* **45**, 340-8.

Polson, J., and Lee, W. M. (2007). Etiologies of acute liver failure: location, location, location! *Liver Transpl* **13**, 1362-3.

Preininger, K., Stingl, H., Englisch, R., Furnsinn, C., Graf, J., Waldhausl, W., and Roden, M. (1999). Acute troglitazone action in isolated perfused rat liver. *Br J Pharmacol* **126**, 372-8.

Rius, M., Hummel-Eisenbeiss, J., Hofmann, A. F., and Keppler, D. (2006). Substrate specificity of human ABCC4 (MRP4)-mediated cotransport of bile acids and reduced glutathione. *Am J Physiol Gastrointest Liver Physiol* **290**, G640-9.

Rius, M., Nies, A. T., Hummel-Eisenbeiss, J., Jedlitschky, G., and Keppler, D. (2003). Cotransport of reduced glutathione with bile salts by MRP4 (ABCC4) localized to the basolateral hepatocyte membrane. *Hepatology* **38**, 374-84.

Roberts, L. R., Kurosawa, H., Bronk, S. F., Fesmier, P. J., Agellon, L. B., Leung, W. Y., Mao, F., and Gores, G. J. (1997). Cathepsin B contributes to bile salt-induced apoptosis of rat hepatocytes. *Gastroenterology* **113**, 1714-26.

Rose, K. A., Kostrubsky, V., and Sahi, J. (2006). Hepatobiliary disposition in primary cultures of dog and monkey hepatocytes. *Mol Pharm* **3**, 266-74.

Sampath, J., Adachi, M., Hatse, S., Naesens, L., Balzarini, J., Flatley, R. M., Matherly, L. H., and Schuetz, J. D. (2002). Role of MRP4 and MRP5 in biology and chemotherapy. *AAPS PharmSci* **4**, E14.

Schuetz, E. G., Strom, S., Yasuda, K., Lecureur, V., Assem, M., Brimer, C., Lamba, J., Kim, R. B., Ramachandran, V., Komoroski, B. J., Venkataramanan, R., Cai, H., Sinal, C. J., Gonzalez, F. J., and Schuetz, J. D. (2001). Disrupted bile acid homeostasis reveals an unexpected interaction among nuclear hormone receptors, transporters, and cytochrome P450. *J Biol Chem* **276**, 39411-8.

Smith, M. T. (2003). Mechanisms of troglitazone hepatotoxicity. *Chem Res Toxicol* **16**, 679-87.

Snow, K. L., and Moseley, R. H. (2006). Effect of thiazolidinediones on bile acid transport in rat liver. *Life Sci* **80**, 732-40.

Solaas, K., Ulvestad, A., Soreide, O., and Kase, B. F. (2000). Subcellular organization of bile acid amidation in human liver: a key issue in regulating the biosynthesis of bile salts. *J Lipid Res* **41**, 1154-62.

Soroka, C. J., Ballatori, N., and Boyer, J. L. (2010). Organic solute transporter, OSTalpha-OSTbeta: its role in bile acid transport and cholestasis. *Semin Liver Dis* **30**, 178-85.

Stieger, B., Fattinger, K., Madon, J., Kullak-Ublick, G. A., and Meier, P. J. (2000). Drug- and estrogen-induced cholestasis through inhibition of the hepatocellular bile salt export pump (Bsep) of rat liver. *Gastroenterology* **118**, 422-30.

Suchy, F. J., and Ananthanarayanan, M. (2006). Bile salt excretory pump: biology and pathobiology. *J Pediatr Gastroenterol Nutr* **43 Suppl 1**, S10-6.

Tagliacozzi, D., Mozzi, A. F., Casetta, B., Bertucci, P., Bernardini, S., Di Ilio, C., Urbani, A., and Federici, G. (2003). Quantitative analysis of bile acids in human plasma by liquid chromatography-electrospray tandem mass spectrometry: a simple and rapid one-step method. *Clin Chem Lab Med* **41**, 1633-41.

Thomas, C., Pellicciari, R., Pruzanski, M., Auwerx, J., and Schoonjans, K. (2008). Targeting bile-acid signalling for metabolic diseases. *Nat Rev Drug Discov* **7**, 678-93.

Trauner, M., and Boyer, J. L. (2003). Bile salt transporters: molecular characterization, function, and regulation. *Physiol Rev* **83**, 633-71.

Uhal, B. D., and Roehrig, K. L. (1982). Effect of dietary state on hepatocyte size. *Biosci Rep* **2**, 1003-7.

Watanabe, Y., Nakajima, M., and Yokoi, T. (2002). Troglitazone glucuronidation in human liver and intestine microsomes: high catalytic activity of UGT1A8 and UGT1A10. *Drug Metab Dispos* **30**, 1462-9.

Wolkoff, A. W., and Cohen, D. E. (2003). Bile acid regulation of hepatic physiology: I. Hepatocyte transport of bile acids. *Am J Physiol Gastrointest Liver Physiol* **284**, G175-9.

Wolters, H., Spiering, M., Gerding, A., Slooff, M. J., Kuipers, F., Hardonk, M. J., and Vonk, R. J. (1991). Isolation and characterization of canalicular and basolateral plasma membrane fractions from human liver. *Biochim Biophys Acta* **1069**, 61-9.

Yamazaki, H., Shibata, A., Suzuki, M., Nakajima, M., Shimada, N., Guengerich, F. P., and Yokoi, T. (1999). Oxidation of troglitazone to a quinone-type metabolite catalyzed by cytochrome P-450 2C8 and P-450 3A4 in human liver microsomes. *Drug Metab Dispos* **27**, 1260-6.

Yoshigae, Y., Konno, K., Takasaki, W., and Ikeda, T. (2000). Characterization of UDP-glucuronosyltransferases (UGTs) involved in the metabolism of troglitazone in rats and humans. *J Toxicol Sci* **25**, 433-41.

Zelcer, N., Reid, G., Wielinga, P., Kuil, A., van der Heijden, I., Schuetz, J. D., and Borst, P. (2003a). Steroid and bile acid conjugates are substrates of human multidrug-resistance protein (MRP) 4 (ATP-binding cassette C4). *Biochem J* **371**, 361-7.

Zelcer, N., Saeki, T., Bot, I., Kuil, A., and Borst, P. (2003b). Transport of bile acids in multidrug-resistance-protein 3-overexpressing cells co-transfected with the ileal Na<sup>+</sup>-dependent bile-acid transporter. *Biochem J* **369**, 23-30.

Zollner, G., Fickert, P., Silbert, D., Fuchsbichler, A., Marschall, H. U., Zatloukal, K., Denk, H., and Trauner, M. (2003). Adaptive changes in hepatobiliary transporter expression in primary biliary cirrhosis. *J Hepatol* **38**, 717-27.

Zollner, G., and Trauner, M. (2008). Mechanisms of cholestasis. *Clin Liver Dis* **12**, 1-26, vii.

## **CHAPTER 2**

# **Differential Disposition of Chenodeoxycholic Acid versus Taurocholic Acid in Response to Acute Troglitazone Exposure in Rat Sandwich-Cultured Hepatocytes**

## Abstract

Inhibition of bile acid (BA) transport may contribute to the hepatotoxicity of troglitazone (TRO), a peroxisome proliferator-activated receptor gamma (PPAR $\gamma$ ) agonist. Typically, studies use taurocholic acid (TCA) as a model substrate to investigate the effects of xenobiotics on BA disposition; however, TRO may differentially affect the transport of individual BAs, potentially causing the accumulation of more cytotoxic BAs. The effects of TRO on the disposition of [ $^{14}\text{C}$ ]-labeled chenodeoxycholic acid ([ $^{14}\text{C}$ ]CDCA), an unconjugated, cytotoxic BA, were determined in rat suspended hepatocytes and sandwich-cultured hepatocytes (SCH). MK571, a multidrug resistance-associated protein (MRP) inhibitor, was included to evaluate involvement of MRPs in CDCA disposition. Accumulation in cells + bile of total [ $^{14}\text{C}$ ]CDCA species in SCHs was 6-fold greater than for [ $^3\text{H}$ ]TCA, and was unaffected by 1 and 10  $\mu\text{M}$  TRO. Both 100  $\mu\text{M}$  TRO and 50  $\mu\text{M}$  MK571 ablated biliary excretion and significantly increased intracellular accumulation of total [ $^{14}\text{C}$ ]CDCA species. Results were similar in Mrp2-deficient TR $^-$  rat hepatocytes. LC-MS/MS analysis revealed that taurine- and glycine-conjugated CDCA, in addition to unconjugated CDCA, were present in cells at the end of the 10-min incubation. In suspended rat hepatocytes, initial uptake of [ $^3\text{H}$ ]TCA was primarily Na $^+$ -dependent, whereas initial [ $^{14}\text{C}$ ]CDCA uptake was primarily Na $^+$ -independent. TRO and MK571 decreased [ $^{14}\text{C}$ ]CDCA uptake to a lesser extent than [ $^3\text{H}$ ]TCA uptake. Differential effects on uptake and efflux of individual BAs may contribute to the hepatotoxic effect of TRO. Although TCA is the prototypic BA used to investigate the effect of xenobiotics on BA transport, it may not be reflective of other BAs.

## Introduction

Troglitazone (TRO) is a peroxisome proliferator-activated receptor gamma (PPAR $\gamma$ ) agonist used clinically to treat noninsulin-dependent type II diabetes until it was removed from the market following a number of cases of severe, idiosyncratic hepatotoxicity. Much research has focused on determining the mechanisms of TRO-mediated hepatotoxicity. One hypothesis is that TRO inhibits hepatic bile acid (BA) transport; inhibition of the bile salt export pump (BSEP) may cause intracellular accumulation of BAs (reviewed in Masubuchi, 2006) and subsequent toxicity due to detergent effects (Delzenne *et al.* 1992; Pauli-Magnus *et al.* 2005). Impaired BSEP function is a significant medical issue (reviewed in Pauli-Magnus *et al.* 2010); however, drug-mediated inhibition of hepatic BA transport as a mechanism of drug-induced liver injury is poorly understood.

Normally, BA disposition is tightly controlled, and hepatic BA concentrations are governed by the rate of synthesis and by basolateral (sinusoidal) and apical (canalicular) transport proteins. On the basolateral membrane, the Na<sup>+</sup>-taurocholate cotransporting polypeptide (NTCP) mediates Na<sup>+</sup>-dependent uptake of BAs, while organic anion transporting polypeptide (OATP) isoforms mediate Na<sup>+</sup>-independent uptake of BAs, organic anions, some organic cations, and neutral species (Trauner and Boyer 2003). On the apical membrane, BSEP is the major canalicular transport protein that mediates biliary excretion of monomeric BAs, while multidrug resistance-associated protein 2 (MRP2/Mrp2) transports divalent BAs into the bile canaliculi (Kullak-Ublick *et al.* 2000). Together, NTCP and BSEP represent the major transport proteins responsible for the vectorial transport of BAs from blood to bile. The

basolateral efflux transporters MRP3, MRP4, and the organic solute transporter, OST $\alpha/\beta$  may also be involved in the excretion of BAs from hepatocytes back into the blood under cholestatic conditions (reviewed in Borst *et al.* 2007; Soroka *et al.* 2010).

Taurocholic acid (TCA) is the taurine conjugate of the primary BA cholic acid (CA) that is present in both rats and humans. TCA is utilized commonly as a prototypic BA to study the effect of xenobiotics and drugs, including TRO, on BA transport both in vivo and in vitro. TRO caused the accumulation of [ $^{14}\text{C}$ ]TCA in rat liver tissue (Funk *et al.* 2001b), and inhibited Bsep-mediated TCA transport in rat canalicular membrane vesicles (Funk *et al.* 2001a) and in membrane vesicles from Sf9 cells overexpressing Bsep from different species (Kis *et al.* 2009). TRO inhibited TCA uptake and biliary excretion in primary rat SCH (Kemp *et al.* 2005), and inhibited TCA transport in both basolateral and canalicular rat liver membrane vesicles (Snow and Moseley 2006). Studies by our group in human SCH showed that TRO decreased TCA biliary excretion in a concentration-dependent manner, consistent with BSEP inhibition; Na $^{+}$ -dependent initial uptake of TCA also was inhibited in rat and human suspended hepatocytes (Marion *et al.* 2007). TRO also caused intracellular retention of preloaded [ $^3\text{H}$ ]TCA in human hepatocytes (Jemnitz *et al.* 2010).

BAs perform important physiological roles, but are cytotoxic and may cause mitochondrial dysfunction and trigger apoptosis or necrosis if they accumulate to high intracellular concentrations. The hydrophobicity of individual BAs is inversely proportional to the number and orientation of hydroxyl groups on the steroid nucleus,

and is predictive of toxicity (reviewed in Thomas *et al.* 2008). Individual BAs also have different affinities for some BA transporters (Byrne *et al.* 2002; Gerloff *et al.* 1998; Noe *et al.* 2001); thus, perturbation of BA transport resulting in increased intracellular BAs may cause a disproportionate accumulation of more cytotoxic BAs through competition for transport.

The primary BA chenodeoxycholic acid (CDCA) comprises an estimated 10.5% (Tagliacozzi *et al.* 2003) to 37% (McRae *et al.* 2010) of the BAs in human plasma, compared to 3% (Tagliacozzi *et al.* 2003) to 3.6% (McRae *et al.* 2010) for TCA. CDCA is more cytotoxic to hepatocytes than TCA (Miyazaki *et al.* 1984), and concentrations in human liver can reportedly increase 20-fold following extrahepatic biliary obstruction (Greim *et al.* 1973). Hepatic uptake of CDCA reportedly involves both Na<sup>+</sup>-dependent (NTCP-mediated) and -independent (*i.e.*, OATP1B1 and OATP1B3) transport mechanisms (Maglova *et al.* 1995; Van Dyke *et al.* 1982); OATP1B1 and OATP1B3 also can transport a fluorescent CDCA analog (Yamaguchi *et al.* 2006). The present study compared the effects of TRO on the disposition of CDCA versus TCA in rat SCH and suspended hepatocytes. Experiments were designed to determine whether TRO differentially affects the hepatobiliary disposition of individual BAs resulting in greater intracellular accumulation of CDCA compared to TCA, and to examine the mechanism(s) of potential alterations. MK571, an MRP inhibitor, was included to investigate the potential involvement of MRPs in CDCA and TCA hepatobiliary disposition.

## Materials and Methods

**Chemicals.** [ $^{14}\text{C}$ ]CDCA (50 mCi/mmol; purity > 97%) and [ $^{14}\text{C}$ ]inulin (2.8 mCi/g, purity > 97%) were purchased from American Radiolabeled Chemicals, Inc. (St. Louis, MO), and [ $^3\text{H}$ ]TCA (5 Ci/mmol; purity > 97%) was purchased from Perkin Elmer (Waltham, MA). TRO was purchased from Biomol (Plymouth Meeting, PA). MK571 sodium salt was obtained from Cayman Chemical (Ann Arbor, MI). Dexamethasone, Hanks' balanced salt solution (HBSS) premix, HBSS modified (without calcium chloride, magnesium sulfate, phenol red and sodium bicarbonate) premix, and collagenase (type IV) were purchased from Sigma-Aldrich (St. Louis, MO). Collagenase (type I, class I) was obtained from Worthington Biochemical (Freehold, NJ) and dimethyl sulfoxide (DMSO) was purchased from Fisher Scientific (Fairlawn, NJ). GIBCO brand fetal bovine serum, recombinant human insulin, and Dulbecco's modified Eagle's medium (DMEM) were purchased from Invitrogen (Carlsbad, CA). ITS (insulin, transferrin, selenium) Universal Culture Supplement Premix and Matrigel™ Basement Membrane Matrix were obtained from BD Biosciences (Palo Alto, CA). All other chemicals and reagents were of analytical grade and were readily available from commercial sources.

**Hepatocyte Isolation and Culture.** Hepatocytes were isolated from wild-type (WT) male Wistar rats (250-300 g; Charles River Laboratories, Inc., Raleigh, NC) or male Mrp2-deficient TR<sup>-</sup> rats (250-300 g; UNC colony) using a two-step collagenase perfusion method previously described (Liu *et al.*, 1998; Annaert *et al.*, 2001). Rats were maintained on a 12-h light/dark cycle with free access to water and standard rodent chow, and allowed to acclimate for at least 5 days before experimentation.

The Institutional Animal Care and Use Committee of the University of North Carolina at Chapel Hill approved all procedures.

Hepatocytes were seeded at a density of  $1.75 \times 10^6$  cells per well on 6-well BioCoat™ plates with Collagen type I substratum in 1.5 ml DMEM supplemented with 5% (v/v) fetal bovine serum, 10  $\mu$ M insulin, 1  $\mu$ M dexamethasone, 2 mM L-glutamine, 1% (v/v) MEM nonessential amino acids, 100 units penicillin G sodium and 100  $\mu$ g streptomycin sulfate. Cells were incubated at 37°C in a humidified incubator and allowed to attach for 2 h, after which time the medium was aspirated to remove unattached cells, and replaced with fresh medium. Twenty-four hours later, on day 1 of culture, hepatocytes were overlaid with BD Matrigel™ basement membrane matrix at a concentration of 0.25 mg/ml in ice-cold DMEM supplemented with 1% (v/v) ITS+ Premix, 0.1  $\mu$ M dexamethasone, 2 mM L-glutamine, 1% (v/v) MEM nonessential amino acids, 100 units penicillin G sodium and 100  $\mu$ g streptomycin sulfate. Cells were cultured for 3 additional days to allow for the formation of canalicular networks between cells. Culture medium was replaced daily.

**Accumulation of CDCA and TCA in WT and TR<sup>-</sup> Rat SCH.** On day 4 of culture, hepatocytes were rinsed 3 times (20 s per each rinse) with 2 ml per well of warm standard HBSS with Ca<sup>2+</sup> (three wells) or HBSS without Ca<sup>2+</sup> (three wells). Following the washes, 2 ml of warm HBSS with or without Ca<sup>2+</sup> were added, and cells were incubated at 37°C for 10 min. Incubation of SCH with Ca<sup>2+</sup>-containing HBSS maintains the tight junctions between cells, and the bile canalicular structures formed between cells remain intact. Incubation of cells in Ca<sup>2+</sup>-free HBSS disrupts the tight junctions, allowing the contents of the canaliculi to be washed away. After

incubation, the HBSS was double-aspirated from each well and 1.5 ml of dosing solution consisting of HBSS with  $\text{Ca}^{2+}$ , substrate (1  $\mu\text{M}$  unlabeled CDCA plus 0.2  $\mu\text{M}$  [ $^{14}\text{C}$ ]CDCA, or 1  $\mu\text{M}$  TCA plus trace [ $^3\text{H}$ ]TCA), or inhibitor (specified concentrations of TRO or MK571, or vehicle [0.1% (v/v) DMSO]) were added. Cells were incubated at 37°C for 10 min. Following incubation, the dosing solution was aspirated from the cells and uptake was stopped by rinsing cells 3 times for 20 s each with 2 ml ice-cold HBSS with  $\text{Ca}^{2+}$  per wash. After washing, the HBSS was aspirated and 1 ml of lysis buffer (0.5% [v/v] Triton X-100 in phosphate-buffered saline) was added to each well and plates were shaken on a rotating plate shaker for 20 min. Aliquots (500  $\mu\text{l}$ ) of sample and 100  $\mu\text{l}$  aliquots of dosing solution were collected for quantification of radioactivity by liquid scintillation counting; 500  $\mu\text{l}$  aliquots were reserved for protein quantification using the Pierce BCA™ Protein Assay Kit (Thermo Scientific, Rockford, IL). Accumulation of [ $^{14}\text{C}$ ]CDCA and [ $^3\text{H}$ ]TCA in BioCoat™ plates without cells was subtracted to correct for nonspecific binding to the collagen substratum.

**Temperature-dependent Accumulation of CDCA and TCA in WT Rat SCH.** Accumulation in WT rat SCH of [ $^{14}\text{C}$ ]CDCA and [ $^3\text{H}$ ]TCA in the presence of vehicle was measured at 37°C using the above method. Accumulation at 4°C was carried out using the same method, except that all reagents were kept at 4°C and all incubations were performed on ice.

**Measurement of Taurine- and Glycine-conjugated CDCA Species in WT Rat SCH.** In order to determine the extent of CDCA metabolism to taurine or glycine conjugates (TCDCA or GCDCA, respectively) during the 10-min incubation in the accumulation studies, WT rat SCH were treated using the above method for

measuring accumulation of CDCA at 37°C, except that the dosing solution contained either vehicle (0.1% DMSO) or 1 µM unlabeled CDCA only. Following the final washes, wells were aspirated and plates were stored at -70°C until analysis by LC-MS/MS for TCDCA and GCDCA, as well as for the rodent-specific BAs tauromuricholic acid (TMCA) and glycomuricholic acid (GMCA), which are metabolites of CDCA. CDCA, TCDCA, and GCDCA were measured using standard curves prepared with stable isotope equivalents; TMCA and GMCA were estimated from standard curves for TCA and glycocholic acid (GCA). Ten microliters of d<sub>4</sub>-TCDCA, d<sub>4</sub>-GCDCA, d<sub>8</sub>-TCA, and d<sub>4</sub>-GCA solutions in methanol were added to previously frozen, untreated rat SCH plates to yield a final concentration of 0.5-100 pmol/well (0.5-200 pmol/well for TCA) as standards. Lysis solution (750 µL; 70:30 [v/v] methanol:water containing 19 pmol/well d<sub>8</sub> TCA as an internal standard) was added to each well of study plates and to the plates containing standards. Plates were shaken on a rotating plate shaker at a speed of 500 rpm for 15 min. The total contact time of the lysis solution with cells, prior to filtration, was ~20-30 min. The cell lysates were transferred to a Whatman 96-well Unifilter Plate (Whatman, Florham Park, NJ) with 25 µm melt blown polypropylene over 0.45 µm polypropylene membrane. Lysate was filtered into a Greiner 96-well Deepwell Plate by centrifugation at 2000 x g for 5 min. Filtrate was evaporated to dryness under nitrogen gas, reconstituted in 200 µL of sample diluent (60:40 [v/v] methanol:10 mM ammonium acetate [native pH]), and mixed for 15 min on the plate shaker at 500 rpm. The reconstituted samples were transferred to a Whatman 96-well Unifilter Plate with 0.45 µm PVDF (polyvinylidene fluoride) membrane and collected into a

Costar 3956 96-well plate (Corning, Corning NY) by centrifugation at 2000 x g for 5 min. The 96-well plate was sealed with a silicone capmat prior to LC-MS/MS analysis. Liquid handling during these procedures was accomplished using a Hamilton Microlab<sup>®</sup> STAR liquid handling workstation and Tomtec Quadra 96<sup>®</sup> 320 96-well simultaneous pipetting workstation.

**LC-MS/MS Analysis.** Chromatographic separation of a 10  $\mu$ L sample injection volume was accomplished using a Shimadzu binary high-performance liquid chromatography system (Columbia, MD) incorporating LC-10ADvp pumps, a CTO-10Avp oven, a Shimadzu HTc 96-well autosampler, and a Thermo Scientific Hypersil GOLD C18 column (100 x 1.0 mm, 3  $\mu$ m) with matching guard and pre-column filter. The mobile phase was initially 70% [60% 0.5 mM ammonium acetate (native pH):40% methanol]:30% [20% 0.5 mM ammonium acetate (native pH):80% methanol]. From 2-15 min, the gradient was ramped to 100% [20% 0.5 mM ammonium acetate (native pH):80% methanol], then stepped back to initial conditions [60% 0.5 mM ammonium acetate (native pH):40% methanol] over 1 min. The flow rate through the column was 50  $\mu$ L/min, and the column was maintained at 35°C. The autosampler was maintained at 4°C and rinsed with 1500  $\mu$ L of 50:50 (v/v) methanol:water after aspiration. Methanol (100%; 10  $\mu$ L/min) was added as a post-column solvent to the MS. A Thermo Electron TSQ Quantum Discovery MAX (Thermo Fisher Scientific) with an Ion Max ESI source in negative ion electrospray ionization mode was used for tandem mass spectrometry. The scan type was selected reaction monitoring (SRM). The transitions monitored at unit resolution are listed in **Table 2.1**.

**Initial Uptake of CDCA and TCA in WT Rat Suspended Hepatocytes.** The initial uptake of substrate (0.5  $\mu\text{M}$  unlabeled CDCA plus 0.5  $\mu\text{M}$  [ $^{14}\text{C}$ ]CDCA, 25 nCi/ml, or 1  $\mu\text{M}$  TCA plus trace [ $^3\text{H}$ ]TCA, 60 nCi/ml) in WT rat suspended hepatocytes was measured in the presence of vehicle, 10  $\mu\text{M}$  TRO, or 50  $\mu\text{M}$  MK571 using standard methods (Leslie *et al.* 2007) with modifications. Uptake was performed in  $\text{Na}^+$ -containing buffer to measure total uptake ( $\text{Na}^+$ -dependent and -independent), and in  $\text{Na}^+$ -free, choline-containing buffer to measure  $\text{Na}^+$ -independent uptake.  $\text{Na}^+$ -dependent uptake was calculated as the difference in uptake between the two conditions. The viability of freshly isolated hepatocytes was >90% as measured by trypan blue exclusion. Briefly, cells were washed 2 x in ice-cold buffer containing sodium chloride, or in buffer in which choline chloride was substituted for sodium chloride (137 mM NaCl or choline chloride, 0.8 mM  $\text{MgSO}_4$ , 10 mM HEPES, 1.2 mM  $\text{CaSO}_4$ , 0.86 mM  $\text{K}_2\text{HPO}_4$ , 0.14 mM  $\text{KH}_2\text{PO}_4$ , and 5 mM glucose, pH 7.4). Cells were resuspended at  $1.0 \times 10^6$  cells/ml in the same buffer and kept on ice for immediate use. Aliquots of cells (4 ml) in bottom-inverted Erlenmeyer flasks were preincubated at  $37^\circ\text{C}$  in a shaking water bath for 5 min. Vehicle (0.3% DMSO), 10  $\mu\text{M}$  TRO, or 50  $\mu\text{M}$  MK571 was added 15 s prior to the addition of [ $^{14}\text{C}$ ]CDCA or [ $^3\text{H}$ ]TCA. At 15, 30, and 45 s, 200  $\mu\text{L}$  samples of the cell suspension were removed, placed in a 0.4 ml polyethylene tube over a top layer of silicone oil:mineral oil (82:18 [v/v], 100  $\mu\text{L}$ ) and a bottom layer of 3M KOH (50  $\mu\text{L}$ ), and immediately centrifuged. Radioactivity in the cell pellet and in the supernatant was measured by liquid scintillation counting. Adherent fluid volume was determined by incubating cells with [ $^{14}\text{C}$ ]inulin (60 nCi/ml) using the method of Baur *et al.* (Baur

*et al.* 1975). Uptake was normalized to protein concentrations in the incubation mixtures as measured at the end of each experiment using the BCA assay (Pierce Biotechnology, Inc., Rockford, IL).

**Data Analysis.** The biliary excretion index (BEI), which represents the percentage of accumulated substrate that is excreted into bile canaliculi, was calculated using B-CLEAR<sup>®</sup> technology (Qualyst, Inc., Durham, NC) from the following equation:  $BEI = [(Accumulation_{standard\ buffer} - Accumulation_{Ca^{2+}\text{-free}\ buffer}) / Accumulation_{standard\ buffer}] * 100\%$  (Liu *et al.* 1999). Statistical analysis (one-way analysis of variance [ANOVA] and Dunnett's multiple comparison test, or two-way ANOVA with Bonferroni's multiple comparison test) was performed using GraphPad Prism 5.03. In all cases, a *p* value < 0.05 was considered statistically significant.

## Results

**Accumulation of CDCA Species in WT and TR<sup>-</sup> Rat SCH.** Accumulation of [<sup>14</sup>C]CDCA species in cells + bile and cells was compared in WT and TR<sup>-</sup> rat SCH, respectively, following a 10-min co-incubation with 1.2 μM [<sup>14</sup>C]CDCA and vehicle control (CTL), increasing concentrations of TRO (1-100 μM), or 50 μM MK571. In WT rat SCH, 1 and 10 μM TRO had no significant effect on accumulation of [<sup>14</sup>C]CDCA species in cells + bile or cells compared to CTL, but 100 μM TRO significantly decreased cell + bile accumulation, increased cellular accumulation nearly two-fold compared to CTL, and markedly inhibited the biliary excretion of [<sup>14</sup>C]CDCA species; the BEI was reduced from ~60 to ~3% (**Figure 2.1**). MK571 completely inhibited the biliary excretion and significantly increased cellular accumulation of [<sup>14</sup>C]CDCA species 2.8-fold over CTL.

Accumulation of [<sup>14</sup>C]CDCA species and [<sup>3</sup>H]TCA also was measured in TR<sup>-</sup> rat SCH (**Figure 2.2**) to determine whether loss of Mrp2 alters the biliary excretion of [<sup>14</sup>C]CDCA species. **Figure 2.2A** shows that accumulation of [<sup>14</sup>C]CDCA species in CTL TR<sup>-</sup> cells + bile and cells was similar to WT CTL values (**Figure 2.1**). TRO (10 and 100 μM) significantly decreased cells + bile accumulation of [<sup>14</sup>C]CDCA species. Cellular accumulation of [<sup>14</sup>C]CDCA species was notably increased in the presence of 100 μM TRO and 50 μM MK571, consistent with inhibition of the biliary excretion of [<sup>14</sup>C]CDCA species (BEI values decreased from ~56 to 10%). For comparison, TCA accumulation was also measured in TR<sup>-</sup> SCH (**Figure 2.2B**). [<sup>3</sup>H]TCA accumulation in CTL cells + bile was ~8.5-fold lower than the accumulation of [<sup>14</sup>C]CDCA species in cells + bile of TR<sup>-</sup> rat SCH, similar to differences in CDCA and

TCA accumulation in WT rat SCH as shown in **Figure 2.1** and published previously (Marion *et al.* 2007). Both 10 and 100  $\mu\text{M}$  TRO, as well as 50  $\mu\text{M}$  MK571, significantly decreased cells + bile accumulation of [ $^3\text{H}$ ]TCA; although there was a trend towards decreased cellular accumulation of TCA in TR $^-$  rat SCH, the differences were not statistically significant.

The BEI of [ $^{14}\text{C}$ ]CDCA species was similar between CTL WT and TR $^-$  rat SCH; TRO appeared to decrease the BEI of [ $^{14}\text{C}$ ]CDCA species and [ $^3\text{H}$ ]TCA in a concentration-dependent manner. While MK571 ablated the biliary excretion of [ $^{14}\text{C}$ ]CDCA in WT cells, the effect in TR $^-$  rat SCH was not as pronounced. BEI values for [ $^3\text{H}$ ]TCA in TR $^-$  rat SCH also were decreased by TRO and MK571, but the decreases in BEI observed with 100  $\mu\text{M}$  TRO and MK571 for [ $^3\text{H}$ ]TCA were less than the decreases in BEI for [ $^{14}\text{C}$ ]CDCA species at the same concentrations.

**MK571-Mediated Inhibition of TCA Accumulation is Concentration Dependent.** Increasing MK571 concentrations (10, 20, and 50  $\mu\text{M}$ ) significantly inhibited [ $^3\text{H}$ ]TCA accumulation in cells + bile in WT rat SCH in a concentration-dependent manner (**Figure 2.3**), and there was a clear trend towards increased cellular accumulation of [ $^3\text{H}$ ]TCA at higher MK571 concentrations. The BEI of [ $^3\text{H}$ ]TCA also was decreased in a concentration-dependent manner; 50  $\mu\text{M}$  MK571 completely ablated biliary excretion of [ $^3\text{H}$ ]TCA.

**Accumulation of [ $^{14}\text{C}$ ]CDCA Species and [ $^3\text{H}$ ]TCA is Temperature Dependent.** The accumulation of [ $^{14}\text{C}$ ]CDCA species and [ $^3\text{H}$ ]TCA was measured at 4 $^\circ\text{C}$  in WT rat SCH in order to rule out passive uptake. As expected, the uptake of [ $^{14}\text{C}$ ]CDCA species and [ $^3\text{H}$ ]TCA into cells + bile and cells was almost entirely

ablated at 4°C, and biliary excretion was negligible, consistent with temperature-dependent, active transport processes for both BAs (data not shown).

**Unconjugated CDCA is Metabolized in WT Rat SCH.** In order to determine the extent of CDCA metabolism during the 10-min incubation period in the accumulation studies, BAs were measured by LC-MS/MS in rat SCH incubated with vehicle (0.1% DMSO; CTL) or 1 µM unlabeled CDCA; results are shown in **Figure 2.4**. Analysis revealed that endogenous unconjugated CDCA was below the limit of quantification in both cells + bile and cells in CTL SCH. In CTL cells, modest amounts of endogenous TCDCA (6% of total), and small amounts of GCDCA and GMCA (1% and 3% of total, respectively), were measured, while TMCA was the most abundant BA measured (90% of total) (**Table 2.2**). TMCA was extensively excreted into bile (86% of total), while TCDCA was excreted into bile to a lesser extent (11% of total); GCDCA and GMCA accounted for 1% and 2%, respectively, of the BAs in bile (**Table 2.2**).

Following a 10-min incubation of WT rat SCH with exogenously administered CDCA, unconjugated CDCA accumulated in cells; cellular TCDCA increased ~15-fold, GCDCA increased ~14-fold, and GMCA increased ~3-fold compared to CTL values (**Figure 2.4**). Biliary excretion of CDCA and GMCA in the bile of cells exposed to exogenous CDCA was negligible, while TCDCA in bile increased ~4-fold. Interestingly, although cells + bile accumulation of TMCA did not change between CTL and treated cells, cellular accumulation increased ~2-fold and accumulation in bile decreased 21%. Overall, following the 10-min incubation, the accumulation in cells + bile exogenously administered unlabeled CDCA including its conjugates (the

difference in total BAs before and after exogenous CDCA exposure) was about 322 pmols/mg protein, which is consistent with the accumulation of [<sup>14</sup>C]CDCA species in cells + bile in WT CTL SCH (~325 pmol/mg protein, **Figure 2.1**). This indicates that the CDCA species detected by LC-MS/MS represent the majority, if not all, of the parent and metabolites. As summarized in **Table 2.2**, following exogenous exposure to CDCA, the amount of TCDCA, GCDCA and unconjugated CDCA increased as a percentage of the total BAs measured in cells and bile, while the percentage of TMCA and GMCA within the cells and bile decreased as a percentage of the total.

**Initial Uptake of [<sup>14</sup>C]CDCA is Primarily Na<sup>+</sup>-Independent, While [<sup>3</sup>H]TCA Uptake is Primarily Na<sup>+</sup>-Dependent.** Initial uptake of [<sup>14</sup>C]CDCA and [<sup>3</sup>H]TCA was measured in WT rat suspended hepatocytes at 15, 30, and 45 s (**Figure 2.5**). Pilot studies indicated that uptake of both BAs was linear through 90 s (data not shown). TRO and MK571 significantly inhibited total [<sup>14</sup>C]CDCA uptake to a similar extent when compared to CTL (**Figure 2.5A**). Na<sup>+</sup>-independent uptake of [<sup>14</sup>C]CDCA at 45 s in CTL cells (**Figure 2.5B**) was 65 ± 5% of total uptake in CTL cells (set at 100%), which was double the Na<sup>+</sup>-independent uptake of TCA in CTL cells (**Figure 2.5E**). Both TRO and MK571 significantly inhibited Na<sup>+</sup>-independent (**Figure 2.5B**) and Na<sup>+</sup>-dependent (**Figure 2.5C**) [<sup>14</sup>C]CDCA uptake. For comparison, initial uptake of [<sup>3</sup>H]TCA also was measured under the same conditions as [<sup>14</sup>C]CDCA. TRO and MK571 significantly inhibited total [<sup>3</sup>H]TCA uptake to a similar extent at all time points (**Figure 2.5D**). Na<sup>+</sup>-independent uptake of [<sup>3</sup>H]TCA in CTL cells (**Figure 2.5E**) was 34 ± 12% of total uptake in CTL cells at 45 s (set at 100%) (**Figure 2.5D**), consistent with previous reports demonstrating that TCA uptake in rat hepatocytes is

mediated primarily by a Na<sup>+</sup>-dependent process (Kemp *et al.* 2005; Van Dyke *et al.* 1982). Both TRO and MK571 significantly inhibited Na<sup>+</sup>-independent (**Figure 2.5E**) and Na<sup>+</sup>-dependent (**Figure 2.5F**) [<sup>3</sup>H]TCA uptake.

## Discussion

The intracellular disposition of a substrate is dependent upon both its uptake and efflux. In hepatocytes, inhibition of substrate uptake or increased basolateral efflux may lead to decreased intracellular concentrations, whereas impaired biliary or basolateral excretion may cause increased intracellular concentrations. Several studies have shown that 10  $\mu\text{M}$  TRO inhibits the uptake, intracellular accumulation, and biliary excretion of TCA in rat hepatocytes (Ansedè *et al.* 2010; Kemp *et al.* 2005; Marion *et al.* 2007) and human SCH (Marion *et al.* 2007). Collectively, these data suggest that TRO-mediated inhibition of TCA uptake by NTCP/Ntcp prevents the intracellular accumulation of TCA *in vitro*.

The uptake of CDCA reportedly occurs partially by a nonsaturable  $\text{Na}^+$ -independent mechanism, hypothesized to be passive diffusion, and partially by a saturable process (Bartholomew and Billing 1983; Iga and Klaassen 1982; Van Dyke *et al.* 1982). In cultured rat hepatocytes, uptake of CDCA was significantly, but not completely, reduced by the removal of  $\text{Na}^+$ , and also by ouabain, a  $\text{Na}^+$ - $\text{K}^+$ -ATPase inhibitor (Van Dyke *et al.* 1982), suggesting a  $\text{Na}^+$ -dependent component of uptake. The rate of uptake of CDCA in suspended rat hepatocytes was reportedly ~10-fold greater than the rate of TCA uptake (Iga and Klaassen 1982). In the present study, the accumulation of [ $^{14}\text{C}$ ]CDCA into cells + bile in WT rat SCH was ~6-fold higher than accumulation of [ $^3\text{H}$ ]TCA in cells + bile (historically ~40-70 pmol/mg protein) (Lee *et al.* 2010; McRae *et al.* 2006; Wolf *et al.* 2010). Unlike our previous reports using [ $^3\text{H}$ ]TCA as a substrate in SCH (Kemp *et al.* 2005; Marion *et al.* 2007), 10  $\mu\text{M}$  TRO did not decrease accumulation of [ $^{14}\text{C}$ ]CDCA species in cells + bile or in cells.

However, treatment with 100  $\mu$ M TRO caused significant intracellular accumulation and completely ablated the biliary efflux of [ $^{14}$ C]CDCA species. These results are significant because, to the best of our knowledge, they are the first to show that TRO causes an increase in the in vitro intracellular accumulation of a BA without uncoupling uptake from efflux, as discussed below with TCA.

Additionally, MK571 inhibited biliary excretion and caused significant cellular accumulation of [ $^{14}$ C]CDCA species. Hepatic MRP3/Mrp3 and MRP4/Mrp4 are upregulated under cholestatic conditions in both rat (Denk *et al.* 2004; Donner and Keppler 2001) and human (Gradhand *et al.* 2008; Scheffer *et al.* 2002) liver, and are postulated compensatory routes for basolateral BA efflux. MK571 was expected to increase intracellular CDCA accumulation by inhibiting basolateral efflux via Mrps; complete ablation of biliary efflux was not anticipated because BSEP/Bsep transports both conjugated and unconjugated BAs into bile, and MK571 has not been reported to inhibit BSEP/Bsep. In contrast to BSEP/Bsep, which transports monovalent BAs, Mrp2 transports sulfate- and glucuronide-conjugated (divalent) BAs (Konig *et al.* 1999). Initially, impaired biliary excretion of CDCA by MK571 suggested that unconjugated CDCA was either completely metabolized to an Mrp2 substrate (*i.e.*, sulfated or glucuronidated) during the 10-min incubation, or that MK571 inhibited Bsep-mediated biliary excretion of [ $^{14}$ C]CDCA species in rat SCH. Therefore, Mrp2-deficient TR<sup>-</sup> rat hepatocytes were utilized to elucidate a potential role for Mrp2 in the transport of [ $^{14}$ C]CDCA species, and to compare the effect of MK571 on transport of [ $^{14}$ C]CDCA species versus [ $^3$ H]TCA. Accumulation of [ $^{14}$ C]CDCA species in cells + bile and cells and BEI were similar in vehicle-treated

TR<sup>-</sup> compared to WT rat SCH, indicating that the lack of Mrp2 did not affect the disposition of [<sup>14</sup>C]CDCA species in rat SCH. Furthermore, MK571 and TRO had similar effects on intracellular accumulation of [<sup>14</sup>C]CDCA species in WT and TR<sup>-</sup> rat SCH. These data suggest that CDCA and/or CDCA metabolites are Bsep substrates, and that TRO and MK571 inhibited Bsep-mediated biliary excretion. In contrast to [<sup>14</sup>C]CDCA species, 10 μM and 100 μM TRO, as well as MK571, significantly and substantially decreased accumulation of [<sup>3</sup>H]TCA in cells + bile, but had no significant effect on cellular accumulation.

Recently, Jemnitz *et al.* (2010) used the method of Lengyel *et al.* (2008) to assess the effects of TRO on basolateral and canalicular efflux of TCA in SCH. In these studies, [<sup>3</sup>H]TCA was preloaded into rat and human SCH by incubating them with [<sup>3</sup>H]TCA in the absence of inhibitor; then, [<sup>3</sup>H]TCA was washed off, and cells were incubated with various inhibitors or vehicle in standard HBSS or in Ca<sup>2+</sup>- and Mg<sup>2+</sup>-free HBSS buffer. At the end of the 10-min incubation, effluxed [<sup>3</sup>H]TCA was measured in the buffer and in cells + bile or in cells. Using this method, 100 μM TRO decreased biliary excretion and increased intracellular accumulation of [<sup>3</sup>H]TCA in both rat and human SCH without affecting basolateral efflux of [<sup>3</sup>H]TCA into the medium. These results established that TRO can cause the intracellular accumulation of TCA, which had not been shown using other methods in SCH. Previous studies in rat and human SCH did not report this effect because TRO inhibits TCA uptake into hepatocytes. By preloading hepatocytes with TCA, any inhibitory effects of compounds on BA uptake are bypassed, as in the study by Jemnitz *et al.* (2010). However, this paradigm does not realistically represent the in

vivo situation. BAs are highly conserved through enterohepatic cycling; basolateral reuptake of BAs from the blood greatly exceeds BA synthesis, and intracellular BAs are excreted rapidly into the bile canaliculi. This vectorial transport of BAs from blood to bile represents the normal circulation of BAs. In our previous studies using TCA to examine the disposition of BAs following TRO exposure, it appears that TRO-mediated inhibition of [<sup>3</sup>H]TCA uptake precluded any effects on intracellular [<sup>3</sup>H]TCA accumulation (Kemp *et al.* 2005; Marion *et al.* 2007).

In rats, ~95-98% of BAs are conjugated to taurine, and the remainder to glycine, whereas in humans, 75% of BAs are conjugated to glycine and 25% to taurine (Alvaro *et al.* 1986); conjugation confers a negative charge, lowers the pK<sub>a</sub>, and increases aqueous solubility, facilitating biliary excretion (Kullak-Ublick *et al.* 2004). LC-MS/MS analysis revealed that when CDCA was administered exogenously to SCH, 88% of total biliary BAs were taurine conjugates with 4% as unconjugated CDCA and the remainder as glycine conjugates (**Table 2.2**). The present results are consistent with data from Hoffman *et al.* (1975), showing that when unconjugated CDCA was injected into rats, >90% was excreted into the bile as the taurine conjugate, <5% as unconjugated CDCA, and a small amount was excreted as the glycine conjugate (Hoffman *et al.* 1975). TRO- and MK571 increased cellular accumulation of [<sup>14</sup>C]CDCA species in WT and TR<sup>-</sup> rat SCH. These results raise the possibility that in humans, TRO may cause intracellular accumulation of CDCA/CDCA species. GCDCA has been shown to induce apoptosis in primary rat hepatocytes (Kaplowitz 2003).

Based on results in SCH, TRO and MK571 were expected to have little, if any, effect on initial uptake of CDCA in suspended rat hepatocytes. Results confirmed that the majority of [<sup>3</sup>H]TCA uptake was Na<sup>+</sup>-dependent, while [<sup>14</sup>C]CDCA uptake was primarily Na<sup>+</sup>-independent. Surprisingly, both TRO and MK571 decreased Na<sup>+</sup>-dependent and -independent initial uptake of [<sup>14</sup>C]CDCA. TRO inhibits TCA uptake in suspended rat (Kemp *et al.* 2005) and human (Marion *et al.* 2007) hepatocytes, and in basolateral membrane vesicles (Snow and Moseley 2006). MK571 reportedly inhibits OATP1B3 (Letschert *et al.* 2005) and OATP2B1 (Letschert *et al.* 2006), which would explain inhibition of the Na<sup>+</sup>-independent component of CDCA uptake. MK571 inhibited Na<sup>+</sup>-dependent TCA uptake into hepatocytes. To our knowledge, there are no prior reports of MK571-mediated inhibition of NTCP/Ntcp. Decreased initial uptake of [<sup>14</sup>C]CDCA in suspended rat hepatocytes is compatible with results in SCH. Given that total intracellular accumulation of BAs is dependent on uptake processes as well as canalicular and basolateral efflux processes, then total accumulation of [<sup>14</sup>C]CDCA species in cells in the presence of 10 μM TRO may be the result of decreased uptake coupled with decreased efflux, resulting in no change in net accumulation relative to CTL. However, the increased intracellular [<sup>14</sup>C]CDCA accumulation with 100 μM TRO may indicate that 100 μM TRO does not decrease [<sup>14</sup>C]CDCA uptake further, but further inhibits the biliary excretion of [<sup>14</sup>C]CDCA (decreased BEI) compared with 10 μM TRO. Thus, TRO may have different effects on uptake and efflux depending on the concentration at the site of transport.

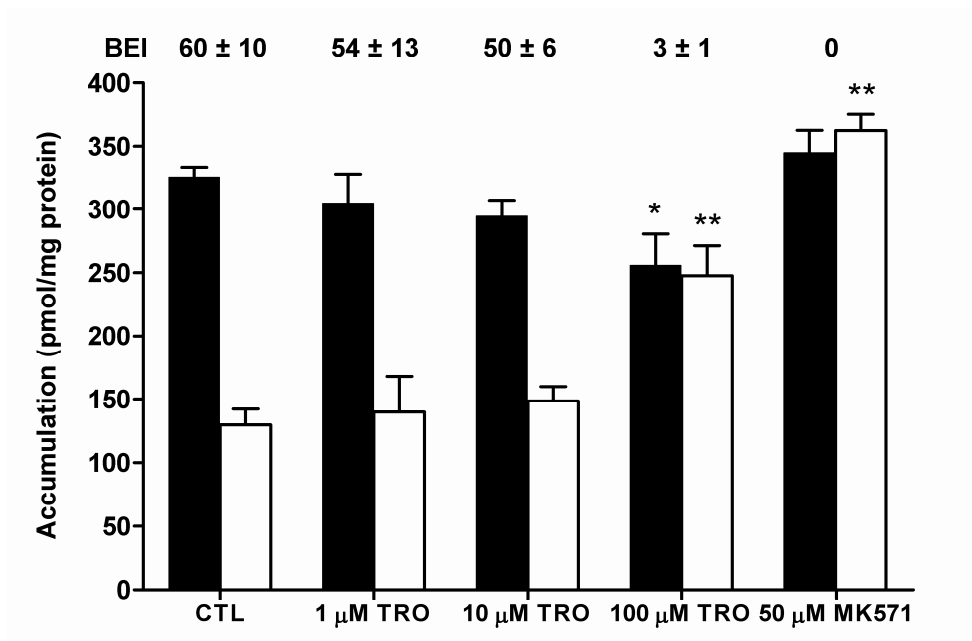
In conclusion, TRO differentially affects the uptake and accumulation of CDCA species compared to TCA in rat SCH, causing an intracellular increase in CDCA species but not TCA. In addition to the known inhibitory effect of MK571 on MRPs, our results suggest that MK571 also inhibits Ntcp and Bsep. Overall, these results demonstrate that inhibitors of BA transport proteins may have differential effects on the disposition of individual BAs, and suggest that use of a single BA substrate for transport studies (*i.e.*, TCA) may yield an incomplete picture of a compound's effects on overall BA disposition.

Analyte	Molecular Weight	Salt	Retention Time (min)	Precursor m/z	Product m/z	Calibration Curve Range
TCA	515.7	none	5.7	514	124	n/a
d <sub>4</sub> -TCA	519.73	none	5.7	518	124	Internal Standard
d <sub>8</sub> -TCA	545.73	Na <sup>+</sup>	5.7	522	128	0.5 – 200 pmol/well
GCA	465.62	none	5.8	464	74	n/a
d <sub>4</sub> -GCA	469.65	none	5.8	468	74	0.5 – 100 pmol/well
TCDCA	499.73	none	8.1	498	80	n/a
d <sub>4</sub> -TCDCA	503.73	none	8.1	502	80	0.5 – 100 pmol/well
GCDCA	449.62	none	8.1	448	74	n/a
d <sub>4</sub> -GCDCA	453.65	none	8.1	452	74	0.5 – 100 pmol/well
CDCA	392.57	none	10.2			5 – 1000 pmol/well

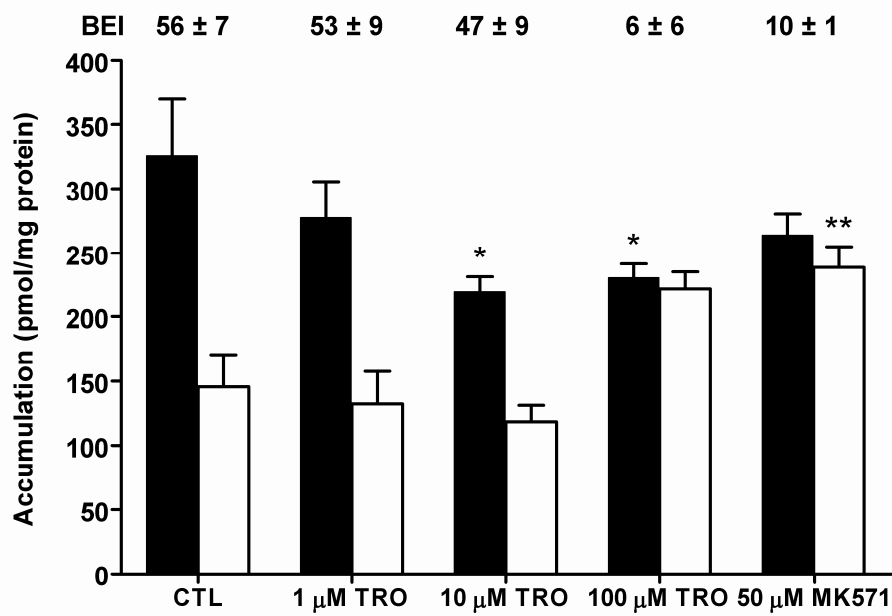
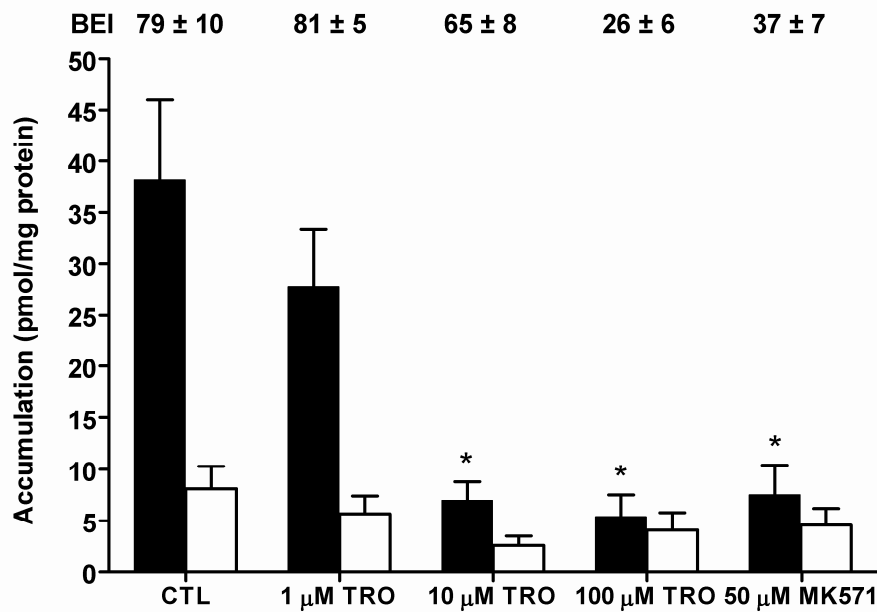
**Table 2.1:** Transitions monitored at unit resolution for LC-MS/MS analysis of parent CDCA and taurine- and glycine-conjugated CDCA metabolites in cell lysates from WT rat SCH following a 10-min incubation with 1  $\mu$ M CDCA.

% of total	CTL		Treated	
	cells	bile	cells	bile
CDCA	0	0	22	4
TCDCA	6	11	21	34
GCDCA	1	1	5	6
TMCA	90	86	50	54
GMCA	3	2	2	2

**Table 2.2:** Accumulation (% total) of CDCA, TCDCA, GCDCA, TMCA, and GMCA in cells and bile in rat SCH following a 10-min incubation with vehicle (0.1% DMSO; CTL) or treated with 1  $\mu$ M exogenous CDCA (Treated).



**Figure 2.1:** Accumulation of [<sup>14</sup>C]CDCA species in cells+bile (black bars) or cells (white bars) in WT rat SCH following a 10-min incubation with 1 μM [<sup>14</sup>C]CDCA and vehicle control (0.1% DMSO; CTL), 1, 10, or 100 μM TRO, or 50 μM MK571. The biliary excretion index (BEI) was calculated as described in Materials and Methods. Data represent the mean ± SEM of triplicate determinations in at least n = 3 livers; \* *p* < 0.05 vs CTL cells+bile; \*\* *p* < 0.05 vs CTL cells.

**A****B**

**Figure 2.2:** Accumulation of (A) [<sup>14</sup>C]CDCA species and (B) [<sup>3</sup>H]TCA in cells + bile (black bars) or cells (white bars) in TR<sup>-</sup> rat SCH following a 10-min incubation with 1.2 μM [<sup>14</sup>C]CDCA or 1 μM [<sup>3</sup>H]TCA and vehicle control (0.1% DMSO; CTL), 1, 10,

or 100  $\mu\text{M}$  TRO, or 50  $\mu\text{M}$  MK571. The biliary excretion index (BEI) was calculated as described in Materials and Methods. Data represent the mean  $\pm$  SEM of triplicate determinations in at least  $n = 3$  livers; \*  $p < 0.05$  vs CTL cells+bile; \*\*  $p < 0.05$  vs CTL cells.

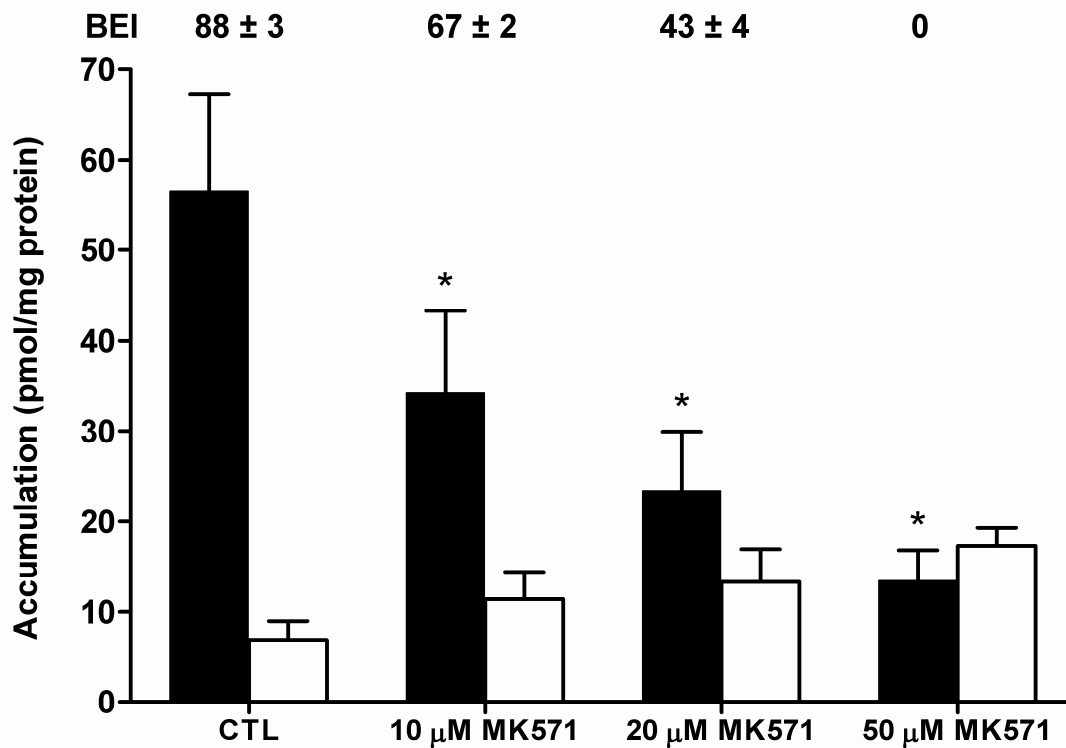


**Figure 2.3:** Accumulation of [<sup>3</sup>H]TCA in cells + bile (black bars) or cells (white bars) in WT rat SCH following a 10-min incubation with 1 μM [<sup>3</sup>H]TCA and vehicle control (0.1% DMSO; CTL), or 10, 20, or 50 μM MK571. The biliary excretion index (BEI) was calculated as described in Materials and Methods. Data represent the mean ± SEM of triplicate determinations in n = 3 livers; \* *p* < 0.05 vs CTL.

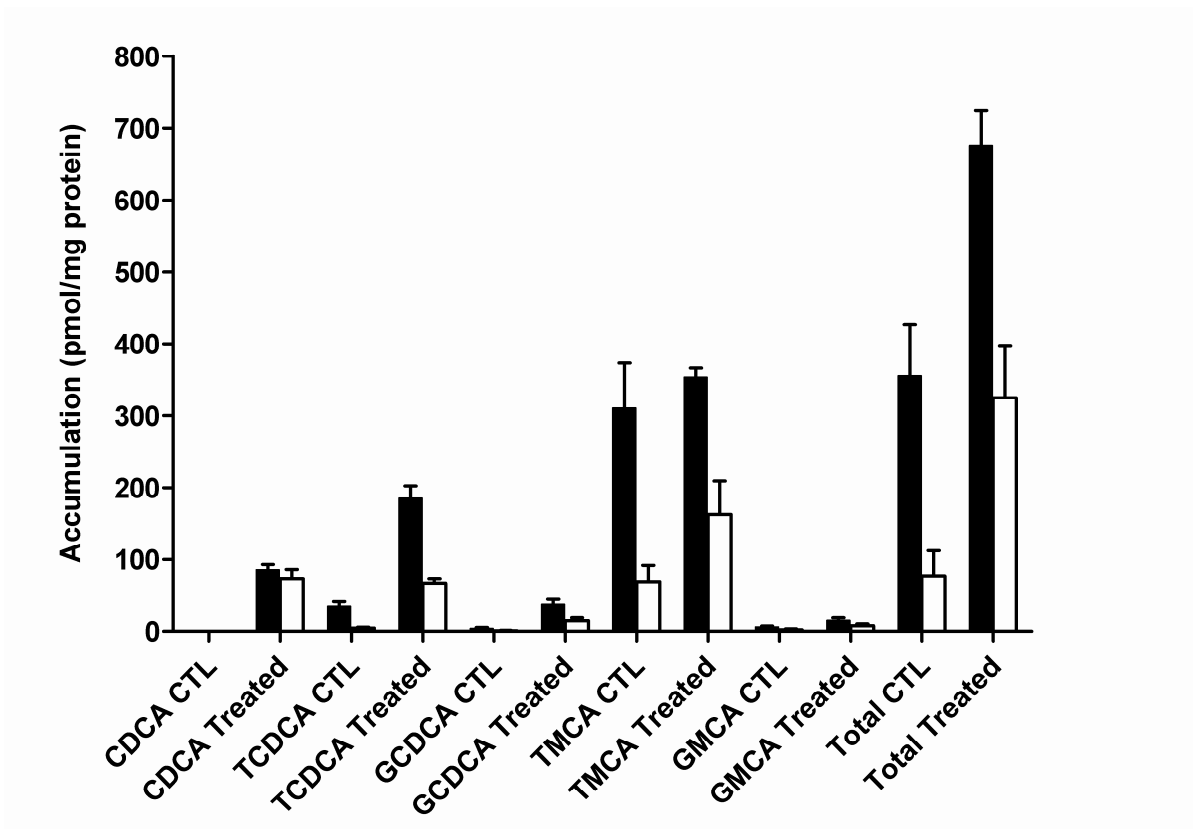


**Figure 2.4:** Parent CDCA and formed CDCA species (taurine- and glycine-conjugated CDCA); TMCA, and GMCA (pmol/mg protein) in cells + bile (solid bars) and cells (white bars) in WT rat SCH following a 10-min incubation with vehicle CTL (0.1% DMSO; CTL) or 1  $\mu$ M unlabeled CDCA (Treated). Data represent the mean  $\pm$  SD of triplicate determinations in n = 1 liver.

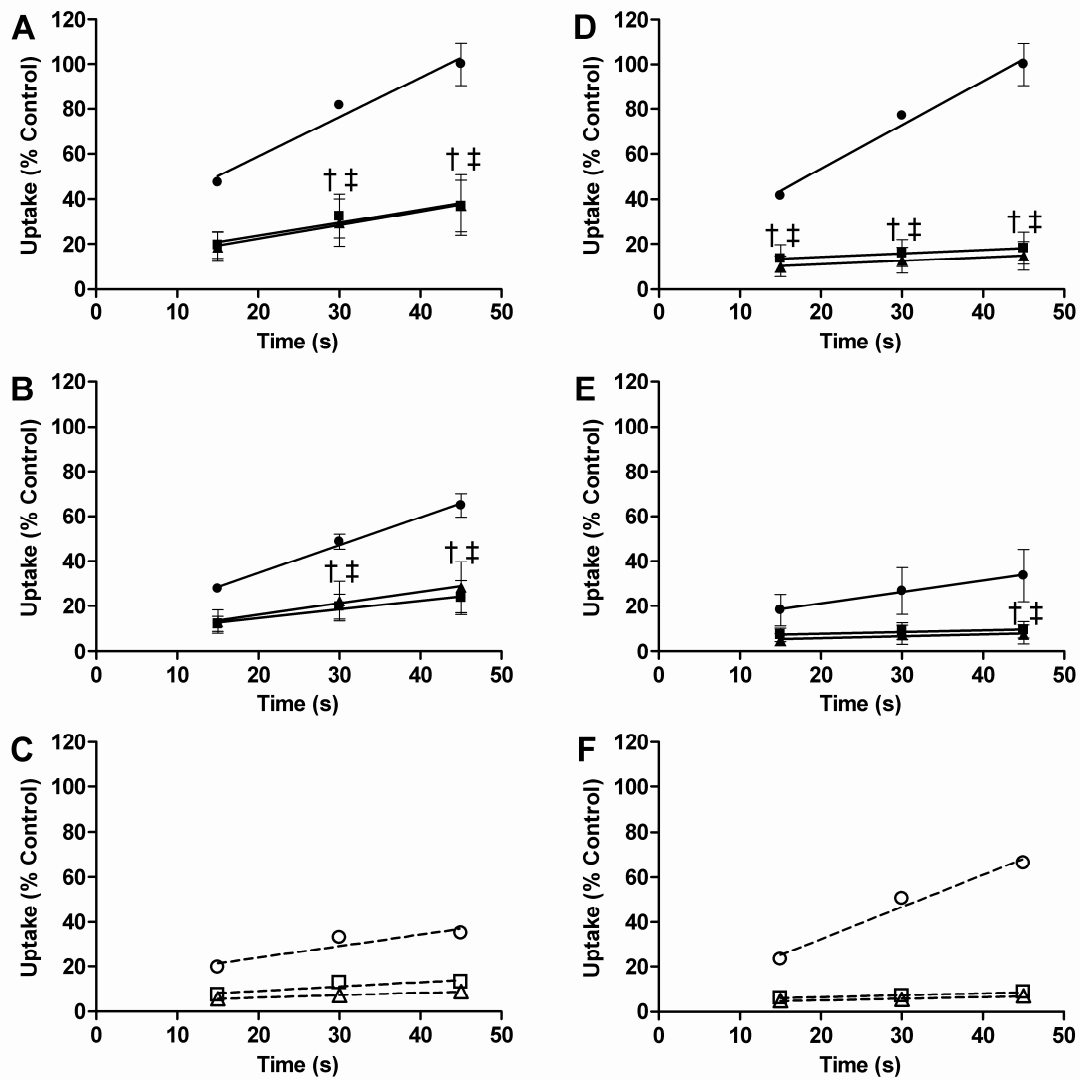


**Figure 2.5:** Accumulation of  $[^{14}\text{C}]\text{CDCA}$  (A, B, C) or  $[^3\text{H}]\text{TCA}$  (D, E, F) in suspended rat hepatocytes in the presence of 1  $\mu\text{M}$   $[^{14}\text{C}]\text{CDCA}$  or 1  $\mu\text{M}$   $[^3\text{H}]\text{TCA}$ , and vehicle (● 0.3% DMSO; CTL), 10  $\mu\text{M}$  TRO (■), or 50  $\mu\text{M}$  MK571 (▲). Lines represent the linear regression of the data using GraphPad Prism 5.03. Total accumulation (Na<sup>+</sup>-dependent and independent) was measured in Na<sup>+</sup>-containing buffer (A, D). Na<sup>+</sup>-independent uptake was measured in choline-containing buffer (B, E). Na<sup>+</sup>-

dependent uptake (dashed lines) was calculated by subtracting Na<sup>+</sup>-independent accumulation from total accumulation (C, F, open symbols, dashed line). Data represent the mean ± SEM of triplicate determinations in n = 3 experiments; †  $p < 0.05$  vs CTL for TRO, and ‡  $p < 0.05$  vs CTL for MK571.

## REFERENCES

- Alvaro, D., Cantafora, A., Attili, A. F., Ginanni Corradini, S., De Luca, C., Minervini, G., Di Biase, A., and Angelico, M. (1986). Relationships between bile salts hydrophilicity and phospholipid composition in bile of various animal species. *Comp Biochem Physiol B* **83**, 551-4.
- Ansele, J. H., Smith, W. R., Perry, C. H., St Claire, R. L., 3rd, and Brouwer, K. R. (2010). An in vitro assay to assess transporter-based cholestatic hepatotoxicity using sandwich-cultured rat hepatocytes. *Drug Metab Dispos* **38**, 276-80.
- Bartholomew, T. C., and Billing, B. H. (1983). The effect of 3-sulphation and taurine conjugation on the uptake of chenodeoxycholic acid by rat hepatocytes. *Biochim Biophys Acta* **754**, 101-9.
- Baur, H., Kasperek, S., and Pfaff, E. (1975). Criteria of viability of isolated liver cells. *Hoppe Seylers Z Physiol Chem* **356**, 827-38.
- Borst, P., de Wolf, C., and van de Wetering, K. (2007). Multidrug resistance-associated proteins 3, 4, and 5. *Pflugers Arch* **453**, 661-73.
- Byrne, J. A., Strautnieks, S. S., Mieli-Vergani, G., Higgins, C. F., Linton, K. J., and Thompson, R. J. (2002). The human bile salt export pump: characterization of substrate specificity and identification of inhibitors. *Gastroenterology* **123**, 1649-58.
- Delzenne, N. M., Calderon, P. B., Taper, H. S., and Roberfroid, M. B. (1992). Comparative hepatotoxicity of cholic acid, deoxycholic acid and lithocholic acid in the rat: in vivo and in vitro studies. *Toxicol Lett* **61**, 291-304.
- Denk, G. U., Soroka, C. J., Takeyama, Y., Chen, W. S., Schuetz, J. D., and Boyer, J. L. (2004). Multidrug resistance-associated protein 4 is up-regulated in liver but down-regulated in kidney in obstructive cholestasis in the rat. *J Hepatol* **40**, 585-91.
- Donner, M. G., and Keppler, D. (2001). Up-regulation of basolateral multidrug resistance protein 3 (Mrp3) in cholestatic rat liver. *Hepatology* **34**, 351-9.
- Funk, C., Pantze, M., Jehle, L., Ponelle, C., Scheuermann, G., Lazendic, M., and Gasser, R. (2001a). Troglitazone-induced intrahepatic cholestasis by an interference with the hepatobiliary export of bile acids in male and female rats. Correlation with the gender difference in troglitazone sulfate formation and the inhibition of the

canalicular bile salt export pump (Bsep) by troglitazone and troglitazone sulfate. *Toxicology* **167**, 83-98.

Funk, C., Ponelle, C., Scheuermann, G., and Pantze, M. (2001b). Cholestatic potential of troglitazone as a possible factor contributing to troglitazone-induced hepatotoxicity: in vivo and in vitro interaction at the canalicular bile salt export pump (Bsep) in the rat. *Mol Pharmacol* **59**, 627-35.

Gerloff, T., Stieger, B., Hagenbuch, B., Madon, J., Landmann, L., Roth, J., Hofmann, A. F., and Meier, P. J. (1998). The sister of P-glycoprotein represents the canalicular bile salt export pump of mammalian liver. *J Biol Chem* **273**, 10046-50.

Gradhand, U., Lang, T., Schaeffeler, E., Glaeser, H., Tegude, H., Klein, K., Fritz, P., Jedlitschky, G., Kroemer, H. K., Bachmakov, I., Anwald, B., Kerb, R., Zanger, U. M., Eichelbaum, M., Schwab, M., and Fromm, M. F. (2008). Variability in human hepatic MRP4 expression: influence of cholestasis and genotype. *Pharmacogenomics J* **8**, 42-52.

Greim, H., Czygan, P., Schaffner, F., and Popper, H. (1973). Determination of bile acids in needle biopsies of human liver. *Biochem Med* **8**, 280-6.

Hoffman, N. E., Iser, J. H., and Smallwood, R. A. (1975). Hepatic bile acid transport: effect of conjugation and position of hydroxyl groups. *Am J Physiol* **229**, 298-302.

Iga, T., and Klaassen, C. D. (1982). Uptake of bile acids by isolated rat hepatocytes. *Biochem Pharmacol* **31**, 211-6.

Jemnitz, K., Veres, Z., and Vereczkey, L. (2010). Contribution of high basolateral bile salt efflux to the lack of hepatotoxicity in rat in response to drugs inducing cholestasis in human. *Toxicol Sci* **115**, 80-8.

Kaplowitz, N., DeLeve, L.D. (2003). *Drug-Induced Liver Disease*. Marcel Dekker, New York.

Kemp, D. C., Zamek-Gliszczynski, M. J., and Brouwer, K. L. (2005). Xenobiotics inhibit hepatic uptake and biliary excretion of taurocholate in rat hepatocytes. *Toxicol Sci* **83**, 207-14.

Kis, E., Iojă, E., Nagy, T., Szente, L., Heredi-Szabo, K., and Krajcsi, P. (2009). Effect of membrane cholesterol on BSEP/Bsep activity: species specificity studies for substrates and inhibitors. *Drug Metab Dispos* **37**, 1878-86.

König, J., Nies, A. T., Cui, Y., Leier, I., and Keppler, D. (1999). Conjugate export pumps of the multidrug resistance protein (MRP) family: localization, substrate specificity, and MRP2-mediated drug resistance. *Biochim Biophys Acta* **1461**, 377-94.

Kullak-Ublick, G. A., Stieger, B., Hagenbuch, B., and Meier, P. J. (2000). Hepatic transport of bile salts. *Semin Liver Dis* **20**, 273-92.

Kullak-Ublick, G. A., Stieger, B., and Meier, P. J. (2004). Enterohepatic bile salt transporters in normal physiology and liver disease. *Gastroenterology* **126**, 322-42.

Lee, J. K., Paine, M. F., and Brouwer, K. L. (2010). Sulindac and its metabolites inhibit multiple transport proteins in rat and human hepatocytes. *J Pharmacol Exp Ther* **334**, 410-8.

Leslie, E. M., Watkins, P. B., Kim, R. B., and Brouwer, K. L. (2007). Differential Inhibition of Rat and Human Na<sup>+</sup>-dependent Taurocholate Co-transporting Polypeptide (NTCP/SLC10A1) by Bosentan: A Mechanism for Species Differences in Hepatotoxicity. *J Pharmacol Exp Ther* **321**, 1170-8.

Letschert, K., Faulstich, H., Keller, D., and Keppler, D. (2006). Molecular characterization and inhibition of amanitin uptake into human hepatocytes. *Toxicol Sci* **91**, 140-9.

Letschert, K., Komatsu, M., Hummel-Eisenbeiss, J., and Keppler, D. (2005). Vectorial transport of the peptide CCK-8 by double-transfected MDCKII cells stably expressing the organic anion transporter OATP1B3 (OATP8) and the export pump ABCB2. *J Pharmacol Exp Ther* **313**, 549-56.

Liu, X., LeCluyse, E. L., Brouwer, K. R., Lightfoot, R. M., Lee, J. I., and Brouwer, K. L. (1999). Use of Ca<sup>2+</sup> modulation to evaluate biliary excretion in sandwich-cultured rat hepatocytes. *J Pharmacol Exp Ther* **289**, 1592-9.

Maglova, L. M., Jackson, A. M., Meng, X. J., Carruth, M. W., Schteingart, C. D., Ton-Nu, H. T., Hofmann, A. F., and Weinman, S. A. (1995). Transport characteristics of

three fluorescent conjugated bile acid analogs in isolated rat hepatocytes and couplets. *Hepatology* **22**, 637-47.

Marion, T. L., Leslie, E. M., and Brouwer, K. L. (2007). Use of sandwich-cultured hepatocytes to evaluate impaired bile acid transport as a mechanism of drug-induced hepatotoxicity. *Mol Pharm* **4**, 911-8.

McRae, M., Rezk, N. L., Bridges, A. S., Corbett, A. H., Tien, H. C., Brouwer, K. L., and Kashuba, A. D. (2010). Plasma bile acid concentrations in patients with human immunodeficiency virus infection receiving protease inhibitor therapy: possible implications for hepatotoxicity. *Pharmacotherapy* **30**, 17-24.

McRae, M. P., Lowe, C. M., Tian, X., Bourdet, D. L., Ho, R. H., Leake, B. F., Kim, R. B., Brouwer, K. L. R., and Kashuba, A. D. (2006). Ritonavir, saquinavir, and efavirenz, but not nevirapine, inhibit bile acid transport in human and rat hepatocytes. *J Pharmacol Exp Ther* **318**, 1068-75.

Miyazaki, K., Nakayama, F., and Koga, A. (1984). Effect of chenodeoxycholic and ursodeoxycholic acids on isolated adult human hepatocytes. *Dig Dis Sci* **29**, 1123-30.

Noe, J., Hagenbuch, B., Meier, P. J., and St-Pierre, M. V. (2001). Characterization of the mouse bile salt export pump overexpressed in the baculovirus system. *Hepatology* **33**, 1223-31.

Pauli-Magnus, C., Meier, P. J., and Stieger, B. (2010). Genetic determinants of drug-induced cholestasis and intrahepatic cholestasis of pregnancy. *Semin Liver Dis* **30**, 147-59.

Pauli-Magnus, C., Stieger, B., Meier, Y., Kullak-Ublick, G. A., and Meier, P. J. (2005). Enterohepatic transport of bile salts and genetics of cholestasis. *J Hepatol* **43**, 342-57.

Scheffer, G. L., Kool, M., de Haas, M., de Vree, J. M., Pijnenborg, A. C., Bosman, D. K., Elferink, R. P., van der Valk, P., Borst, P., and Scheper, R. J. (2002). Tissue distribution and induction of human multidrug resistant protein 3. *Lab Invest* **82**, 193-201.

Snow, K. L., and Moseley, R. H. (2006). Effect of thiazolidinediones on bile acid transport in rat liver. *Life Sci* **80**, 732-40.

Soroka, C. J., Ballatori, N., and Boyer, J. L. (2010). Organic solute transporter, OSTalpha-OSTbeta: its role in bile acid transport and cholestasis. *Semin Liver Dis* **30**, 178-85.

Tagliacozzi, D., Mozzi, A. F., Casetta, B., Bertucci, P., Bernardini, S., Di Ilio, C., Urbani, A., and Federici, G. (2003). Quantitative analysis of bile acids in human plasma by liquid chromatography-electrospray tandem mass spectrometry: a simple and rapid one-step method. *Clin Chem Lab Med* **41**, 1633-41.

Thomas, C., Pellicciari, R., Pruzanski, M., Auwerx, J., and Schoonjans, K. (2008). Targeting bile-acid signalling for metabolic diseases. *Nat Rev Drug Discov* **7**, 678-93.

Trauner, M., and Boyer, J. L. (2003). Bile salt transporters: molecular characterization, function, and regulation. *Physiol Rev* **83**, 633-71.

Van Dyke, R. W., Stephens, J. E., and Scharschmidt, B. F. (1982). Bile acid transport in cultured rat hepatocytes. *Am J Physiol* **243**, G484-92.

Wolf, K. K., Vora, S., Webster, L. O., Generaux, G. T., Polli, J. W., and Brouwer, K. L. (2010). Use of cassette dosing in sandwich-cultured rat and human hepatocytes to identify drugs that inhibit bile acid transport. *Toxicol In Vitro* **24**, 297-309.

Yamaguchi, H., Okada, M., Akitaya, S., Ohara, H., Mikkaichi, T., Ishikawa, H., Sato, M., Matsuura, M., Saga, T., Unno, M., Abe, T., Mano, N., Hishinuma, T., and Goto, J. (2006). Transport of fluorescent chenodeoxycholic acid via the human organic anion transporters OATP1B1 and OATP1B3. *J Lipid Res* **47**, 1196-202.

## **CHAPTER 3**

### **Endogenous Bile Acid Disposition in Rat and Human Sandwich-Cultured Hepatocytes: Effect of Troglitazone**

## Abstract

Inhibition of hepatic transport proteins may mediate drug-induced liver injury by increasing the intracellular accumulation of potentially toxic compounds such as bile acids (BAs). Therefore, drug-induced changes in hepatic BA disposition may be potential indicators of hepatotoxicity. In this study, differences in the endogenous BA pool in primary rat and human sandwich-cultured hepatocytes (SCH) was compared, and the effects of troglitazone (TRO)-mediated inhibition of BA transport proteins on cellular BA accumulation and biliary excretion was determined in this in vitro model. Using the B-CLEAR<sup>®</sup> method, four BAs common to both rat and human—taurocholic acid (TCA), glycocholic acid (GCA), taurochenodeoxycholic acid (TCDCA), and glycochenodeoxycholic acid (GCDCA)—were measured in cells + bile canaliculi and cells of SCH by LC-MS/MS following 24-h treatment with vehicle or 10  $\mu$ M TRO, an inhibitor of the bile salt export pump (BSEP) and the Na<sup>+</sup>-taurocholate cotransporting polypeptide (NTCP). Total BAs were ~12-fold greater in human SCH than in rat SCH. Similar to in vivo reports, ~90% of BAs in rat SCH were taurine-conjugated, while in human SCH, 99% of BAs were glycine-conjugated. There was a trend toward decreased cellular accumulation of BAs in human SCH treated with TRO, but because variability between donors was high, differences failed to reach statistical significance. In rat SCH, TRO decreased biliary excretion of TCA 3%, GCA 12%, TCDCA 15%, and GCDCA 27%. Interestingly, in human SCH, TRO had no effect on GCA but decreased biliary excretion of TCA 43%, TCDCA 67%, and GCDCA 48%; this differential effect may be attributable to differences in intracellular concentrations of TRO/metabolites. Total BAs in TRO-treated human SCH were decreased by 19%

compared to control, suggesting that TRO may affect BA synthesis pathways.

Together, these data demonstrate that BA synthesis and secretion occurs in SCH similarly to in vivo, and suggest that TRO differentially affects BA disposition in rat and human SCH.

## Introduction

Drug-induced hepatotoxicity remains the most common reason for the withdrawal of drugs from the market (Kaplowitz 2001). Unfortunately, this toxicity is frequently idiosyncratic, occurring with no clear relationship to dose or duration of treatment (Roth and Ganey 2010). The difficulty in predicting idiosyncratic hepatotoxicity necessitates further study regarding mechanisms and identification of potential biomarkers of injury. Recent research suggests that interference with normal BA transport processes may be an important mechanism of drug- and xenobiotic-induced hepatotoxicity (Pauli-Magnus and Meier 2006). Drugs, xenobiotics, or hormones can cause noninflammatory cholestasis through the inhibition of BA transport proteins or the retrieval of transporters from the hepatocyte plasma membrane (Zollner and Trauner 2008). Inhibition of these transport proteins may mediate drug-induced liver injury by increasing the intracellular accumulation of potentially toxic compounds (parent drug/xenobiotic and/or metabolites), as well as endogenous BAs, which can cause toxicity through detergent effects on cellular membranes, mitochondrial dysfunction, and ultimately cellular apoptosis or necrosis (Delzenne *et al.* 1992; Desmet 1995; Gores *et al.* 1998; Pauli-Magnus *et al.* 2005). Clinically, diagnosis of cholestasis includes measuring levels of alkaline phosphatase (ALP), gamma-glutamyl transpeptidase (GGT), conjugated bilirubin, and total BAs in the blood (Pauli-Magnus and Meier 2006). The measurement of serum BAs has long been considered a specific and sensitive indicator of liver function (Barnes *et al.* 1975; Kaplowitz *et al.* 1973; Korman *et al.* 1974). Altered BA

disposition also may be an indicator for impaired BA transport and potential toxicity in vitro.

Primary hepatocytes in a sandwich-culture configuration continue to synthesize and secrete BAs, as well as albumin, urea, transferrin and fibrinogen; however, when cultured using conventional methods (*i.e.*, on a rigid substratum or on collagen-coated plates), cells de-differentiate and rapidly lose hepatocyte-specific functions (Dunn *et al.* 1991). The advantage of hepatocytes cultured in a sandwich configuration between layers of gelled collagen or extracellular matrix is that they begin to repolarize hours after plating, CYP450 enzymes are expressed, transport proteins traffic to their proper membrane domains and are functional over days in culture, and adjacent cells form intact, sealed bile-canaliculi-like structures over time into which BAs are secreted (LeCluyse *et al.* 1994; Liu *et al.* 1999a; Liu *et al.* 1999b; Liu *et al.* 1999c). BA synthesis and efflux into the culture medium in SCH has been shown to remain relatively steady for up to 42 days in culture (Shibukawa *et al.* 1995). Modulation of the integrity of the tight junctions that seal the bile canaliculi by washing cells in buffer with or without  $\text{Ca}^{2+}$  and  $\text{Mg}^{2+}$  allows quantification of cellular and biliary BAs.

The vectorial, active uptake and efflux of hepatic BAs, as well as other endobiotics and xenobiotics, are mediated by a number of transport proteins which are expressed in polarized hepatocytes on the basolateral (sinusoidal) or apical (canalicular) membrane domains. On the basolateral membrane,  $\text{Na}^+$ -taurocholate cotransporting polypeptide (NTCP) is a sodium-dependent transporter that is primarily responsible for the uptake of conjugated BAs from the blood, while

isoforms of the Na<sup>+</sup>-independent organic anion transporting polypeptide (OATP/Oatp) take up conjugated and unconjugated BAs and other organic anions; OATP/Oatp isoforms also may function as bi-directional transporters (Trauner and Boyer 2003). In humans, the efflux transporters multidrug resistance-associated proteins 3 and 4 (MRP3, MRP4), as well as organic solute transporter OST $\alpha/\beta$  also are localized to the basolateral membrane and may function as BA efflux transporters when intracellular BA concentrations are increased (Borst *et al.* 2007; Geier *et al.* 2007; Soroka *et al.* 2010). On the apical membrane, BSEP and multidrug resistance-associated protein 2 (MRP2/Mrp2) efflux monovalent and divalent BAs, respectively, into the bile canaliculi (Keppler *et al.* 1999; Keppler and Konig 2000).

A number of drugs inhibit rat and/or human Bsep/BSEP-mediated biliary secretion of TCA in vitro including cyclosporin, glibenclamide, rifampin, bosentan, ritonavir, saquinavir, efavirenz, and TRO (Fattinger *et al.* 2001; Funk *et al.* 2001a; Kemp *et al.* 2005; McRae *et al.* 2006; Pauli-Magnus and Meier 2006; Stieger *et al.* 2000). The PPAR $\gamma$  agonist TRO, the first thiazolidinedione insulin-sensitizing drug introduced to treat type II diabetes, was removed from the market because of hepatotoxicity, but preclinical safety testing did not predict toxicity in humans. A number of studies have demonstrated that TRO, and particularly its major metabolite, troglitazone sulfate (TS), inhibit BA transport (Funk *et al.* 2001a; Funk *et al.* 2001b; Kemp *et al.* 2005; Preininger *et al.* 1999). The hepatotoxicity observed in humans following TRO treatment may not have been observed in rats during preclinical testing due to species differences in the composition of the BA pools, and differential effects on the hepatobiliary transport of BAs.

Drug-induced changes in the intra- and/or extracellular disposition of individual BAs may be indicators of a the hepatotoxic potential of a compound. The goals of this study were to profile the endogenous BA pool in an in vitro model—primary rat and human SCH—in which the medium, intracellular, and biliary compartments are accessible, in order to (1) compare species differences between rat and human in the disposition of hepatic BAs common to both, (2) determine whether TRO-mediated inhibition of transport proteins causes the intracellular accumulation of endogenous BAs, and (3) elucidate whether distinct changes in intra- and extracellular accumulation and biliary excretion of individual BA species occur such that a particular BA would be a marker for transport inhibition. In order to accomplish these goals, the mass of taurocholic acid (TCA), glycocholic acid (GCA), taurochenodeoxycholic acid (TCDCA), and glycochenodeoxycholic acid (GCDCA), accumulated in cells + bile canaliculi, cells, and medium of SCH following 24-h treatment with vehicle or 10  $\mu$ M TRO were quantified by LC-MS/MS using the B-CLEAR<sup>®</sup> method. Furthermore, intracellular and biliary concentrations of BAs were calculated using estimated cell volumes for human and rat hepatocytes.

## Materials and Methods

**Chemicals.** Troglitazone was purchased from Biomol (Plymouth Meeting, PA). MK571 sodium salt was obtained from Cayman Chemical (Ann Arbor, MI). Dexamethasone, Hanks' balanced salt solution (HBSS) premix, HBSS without calcium chloride, magnesium sulfate, phenol red and sodium bicarbonate premix, and collagenase (type IV) were purchased from Sigma-Aldrich (St. Louis, MO). Collagenase (type I, class I) was obtained from Worthington Biochemical (Freehold, NJ). DMSO was purchased from Fisher Scientific (Fairlawn, NJ). GIBCO brand Fetal bovine serum, insulin, and Dulbecco's modified Eagle's medium were obtained from Invitrogen (Carlsbad, CA). ITS+ Premix (insulin, transferrin, selenium) and BD Matrigel™ Basement Membrane Matrix were purchased from BD Biosciences (Palo Alto, CA). All other chemicals and reagents were of analytical grade and were readily available from commercial sources.

**Hepatocyte Isolation and Culture.** Hepatocytes were isolated from male Wistar rats (250-300 g; Charles River Laboratories, Inc., Raleigh, NC) using a two-step collagenase perfusion method previously described (Liu *et al.*, 1998; Annaert *et al.*, 2001). Rats were maintained on a 12 h light/dark cycle with free access to water and standard rodent chow, and were allowed to acclimate for at least 5 days before experimentation. The Institutional Animal Care and Use Committee of the University of North Carolina at Chapel Hill approved all procedures. Human hepatocytes were obtained from CellzDirect (Durham, NC) pre-plated on 6-well BioCoat plates with collagen type I substratum (BD Biosciences, Bedford, MA). Donor information is listed in **Table 3.1**.

Rat hepatocytes were seeded at a density of  $1.75 \times 10^6$  cells per well on 6-well BioCoat plates in 1.5 ml DMEM supplemented with 5% (v/v) fetal bovine serum, 10  $\mu$ M insulin, and 1  $\mu$ M dexamethasone, 2 mM L-glutamine, 1% (v/v) MEM non-essential amino acids, 100 units penicillin G sodium and 100  $\mu$ g streptomycin sulfate. Cells were incubated at 37°C, 5% CO<sub>2</sub> in a humidified incubator and allowed to attach for 2 h, after which time the medium was aspirated to remove unattached cells, and replaced with fresh medium. Twenty-four hours later, on day 1 of culture, rat and human hepatocytes were overlaid with BD Matrigel™ basement membrane matrix at a concentration of 0.25 mg/ml in ice-cold DMEM supplemented with 1% (v/v) ITS™+ Premix, 0.1  $\mu$ M dexamethasone, 2 mM L-glutamine, 1% (v/v) MEM non-essential amino acids, 100 units penicillin G sodium and 100  $\mu$ g streptomycin sulfate. Rat and human hepatocytes were cultured for up to 3 and 6 more days, respectively, to allow for the formation of canalicular networks between cells. Culture medium was replaced daily.

**Determination of BAs in Cells + Bile, Cells, and Culture Medium of Untreated Rat SCH over Days in Culture.** At 24, 48, 72, and 96 h post-seeding, 1 ml aliquots of culture medium were collected from each of 6 wells of rat SCH and stored at <-70°C until analysis. The remaining 0.5 ml of the culture medium was aspirated and duplicate wells were rinsed briefly with 1.5 ml/well of warmed HBSS containing Ca<sup>2+</sup> (cells + bile condition), while two wells were rinsed with HBSS without Ca<sup>2+</sup> (cells only condition), and the wash buffer was aspirated. Following the wash, 1.5 ml of HBSS with or without Ca<sup>2+</sup> was added again to wells, and cells were incubated for 4 min at 37°C. Incubation of SCH with Ca<sup>2+</sup>-containing buffer

maintained the tight junctions between cells so that the bile canalicular structures formed between cells remained intact. Incubation of cells in  $\text{Ca}^{2+}$ -free buffer disrupted the tight junctions and opened the bile canalicular structures between cells, allowing the contents to be washed away. Following incubation, the HBSS was aspirated from each well and plates were sealed and stored at  $<-70^{\circ}\text{C}$  until analysis.

**Accumulation of BAs in Cells + Bile, Cells, and Culture Medium of Rat and Human SCH.** On day 3 (rat) or 6 (human) of culture, medium was aspirated from each well of rat SCH and replaced with 1.5 ml medium containing vehicle (0.1% DMSO) or 10  $\mu\text{M}$  TRO. Cells were incubated at  $37^{\circ}\text{C}$  for an additional 24 h. Following incubation, 1 ml aliquots of the culture medium were collected for analysis of BAs in the medium, and the remaining 0.5 ml was aspirated. Triplicate wells were briefly rinsed 2 times with 2 ml per well of warmed HBSS with or without  $\text{Ca}^{2+}$ . After the washes, 2 ml of HBSS with or without  $\text{Ca}^{2+}$  was added, and cells were incubated at  $37^{\circ}\text{C}$  for 4 min. Following the 4-min incubation, the HBSS was aspirated, and plates were stored at  $<-70^{\circ}\text{C}$  until analysis. Human and rat SCH were handled identically except that human SCH were treated on day 6 of culture, and samples were collected 24 h later on day 7.

**Sample Preparation for LC-MS/MS Analysis of BAs in Cell Lysates.**

Endogenous BAs were measured using standard curves prepared with stable isotope equivalents. Ten microliters of deuterated BAs [ $\text{d}_8$ -taurocholic acid ( $\text{d}_8$ -TCA),  $\text{d}_4$ -glycocholic acid ( $\text{d}_4$ -GCA),  $\text{d}_4$ -taurochenodeoxycholic acid ( $\text{d}_4$ -TCDCA), and  $\text{d}_4$ -glycochenodeoxycholic acid ( $\text{d}_4$ -GCDCA)] solutions in methanol were added to previously frozen, untreated rat and human SCH plates. The final concentration

range for rat cell lysate analysis was 0.5 - 100 pmol/well and for human cell lysate analysis was 0.5 – 50 pmol/well for taurine conjugates and 10 – 1000 pmol/well for glycine conjugates. Lysis solution (750  $\mu$ l; 70:30 methanol:water [v/v] containing 25 nM  $d_4$ -TCA as an internal standard) were added to each well of study plates and to plates containing standards. Plates were shaken on a rotating plate shaker (Lab-Line Instruments Model 4625) at a speed of 500 rpm for 15 min. The total contact time of the lysis solution with cells, prior to filtration, was ~20–30 min. The cell lysates were transferred to a Whatman 96-well Unifilter Plate (Whatman, Florham Park, NJ) with 25  $\mu$ m melt blown polypropylene over 0.45  $\mu$ m polypropylene membrane. Lysate was filtered into a Greiner 96-well Deepwell Plate by centrifugation at 2000 rcf for 5 min. Filtrate was evaporated to dryness under nitrogen gas and then reconstituted in 200  $\mu$ l of sample diluent (60:40 methanol:10 mM ammonium acetate [native pH]) and mixed for 15 min on the plate shaker at 500 rpm. Reconstituted samples were transferred to a Whatman 96-well Unifilter Plate with 0.45  $\mu$ m polyvinylidene fluoride (PVDF) membrane and collected into a Costar 3956 96-well plate (Corning, Corning NY) by centrifugation at 2000 rcf for 5 min. The 96-well plate was sealed with a silicone capmat prior to LC-MS/MS analysis. Liquid handling during these procedures was accomplished using a Hamilton Microlab<sup>®</sup> STAR 12-pipetting channel liquid handling workstation and Tomtec Quadra 96<sup>®</sup> 320 96-well simultaneous pipetting workstation.

**Sample Preparation for LC-MS/MS Analysis of BAs in Culture Medium.** A volume of 300  $\mu$ l of 100% methanol containing 25 nM  $d_4$ -TCA as an internal standard was added to a well within a Millipore 96-well MultiScreen Deep Well

Solvinert filter plate. This was followed by the addition of 100  $\mu$ l of medium study sample and mixing on the plate shaker at a speed of 500 rpm for 15 min. Following protein precipitation, the filter plate was stacked on a deep well plate and centrifuged at 2000  $\times$  rcf for 5 minutes. Filtrate was evaporated to dryness under nitrogen gas and reconstituted in 200  $\mu$ l of sample diluent (60:40 [v/v] methanol:10 mM ammonium acetate [native pH]) and mixed for 15 min on the plate shaker at 500 rpm. Reconstituted samples were transferred to a Whatman 96-well Unifilter Plate with 0.45  $\mu$ m PVDF membrane and collected into a Costar 3956 96-well plate (Corning, Corning NY) by centrifugation at 2000  $\times$  rcf for 5 min. The 96-well plate was sealed with a silicone capmat prior to LC-MS/MS analysis. Liquid handling during these procedures was accomplished using a Hamilton Microlab<sup>®</sup> STAR 12-pipetting channel liquid handling workstation and Tomtec Quadra 96<sup>®</sup> 320 96-well simultaneous pipetting workstation.

Endogenous BAs were measured using standard curves prepared with stable isotope equivalents. Ten microliters of deuterated BAs ( $d_8$ -TCA,  $d_4$ -GCA,  $d_4$ -TCDCa,  $d_4$ -GCDCA) solutions in methanol were added to 300  $\mu$ l of 100% methanol containing 25 nM internal standard within a Millipore 96-well filter plate. The final concentration range for rat culture medium analysis was 0.5 - 50 pmol/100  $\mu$ l for each deuterated BA and for human culture analysis was 0.5 – 50 pmol/100  $\mu$ l for  $d_8$ TCA,  $d_4$ -TCDCa, and  $d_4$ -GCDCA and 100 – 5000 pmol/100  $\mu$ l for  $d_4$ -GCA. This was followed by the addition of 90  $\mu$ l cell culture medium and then mixing on the plate shaker for 15 min. Further processing of medium standard was completed as described for medium study samples described above.

**LC-MS/MS Analysis.** Chromatographic separation of a 10 µl sample injection volume was accomplished using a Shimadzu binary high-performance liquid chromatography system (Columbia, MD) incorporating LC-10ADvp pumps, a CTO-10Avp oven, a Shimadzu HTc 96-well autosampler, and a Thermo Scientific Hypersil GOLD C18 column (100 x 1.0 mm, 3 µm) with matching guard and pre-column filter. The mobile phase was initially 70% [60% 0.5 mM ammonium acetate (native pH):40% methanol]:30% [20% 0.5 mM ammonium acetate (native pH):80% methanol]. From 2-15 min, the gradient was ramped to 100% [20% 0.5 mM ammonium acetate (native pH):80% methanol], then stepped back to initial conditions [60% 0.5 mM ammonium acetate (native pH):40% methanol] over 1 min. The flow rate through the column was 50 µl/min, and the column was maintained at 35°C. The autosampler was maintained at 4°C and rinsed with 1500 µl of 50:50 (v/v) methanol:water after aspiration. Methanol (10 µl/min; 100%) was added as a post-column solvent to the MS. A Thermo Electron TSQ Quantum Discovery MAX (Thermo Fisher Scientific) with an Ion Max ESI source in negative ion electrospray ionization mode was used for tandem mass spectrometry. The scan type was selected reaction monitoring (SRM). The transitions monitored at unit resolution are listed in **Table 3.2**.

## Results

**Determination of BAs in Cells + Bile, Cells, and Medium of Untreated Rat SCH over Days in Culture.** Total BAs (sum of TCA, GCA, TCDCA, and GCDCA) were measured in cells + bile, cells, and medium in rat SCH over days 1 to 4 of culture (**Figure 3.1**). BAs in cells + bile and in cells tended to decrease over days 1 to 4 in culture, while the mass of total BAs in the bile (cells + bile minus cells) remained relatively constant. These data confirm that BAs do not accumulate in the cells over days in culture. Unlike cells + bile and cells, total BAs in the culture medium remained relatively equal over days 1 and 2, but increased 2.6-fold from day 2 to day 3, and increased 3.1-fold from day 2 to day 4.

**Accumulation of BAs in Cells + Bile, Cells, and Medium of Rat and Human SCH.** Experiments were designed to compare the BA pools between rat and human SCH. **Figures 3.2 – 3.5** show the accumulation of TCA, GCA, TCDCA, and GCDCA, respectively, in cells + bile, cells, and medium of rat and human SCH following 24-h treatment with vehicle or 10  $\mu$ M TRO. In controls, accumulation of TCA in cells + bile, cells, and medium in rat SCH was about 3-fold, 2-fold, and 20-fold higher, respectively, than in human SCH (**Figure 3.2**). Treatment with TRO appeared to decrease TCA accumulation in cells + bile and cells in human, but not rat SCH; however, because of variability, the differences were not statistically significant. In rat SCH, TRO treatment decreased the BEI of TCA by 3% compared to control (**Table 3.3**) whereas in human SCH, TRO decreased the BEI of TCA by 43% compared to control (**Table 3.4**). In contrast, accumulation of GCA in cells + bile, cells, and medium in human SCH was over 1000-fold, 1300-fold, and 80-fold

higher, respectively, than in rat SCH (**Figure 3.3**). Treatment with TRO appeared to decrease GCA accumulation in cells + bile and cells in human SCH, but the effect was not statistically significant. GCA was the only BA to accumulate within cells following TRO treatment; the effect was only observed in rat SCH. Overall accumulation of GCA was quantitatively far less than the other BAs. TRO treatment decreased the BEI of GCA by 12% compared to control in rat SCH (**Table 3.3**), but had no inhibitory effect on the BEI of GCA in human SCH (**Table 3.4**). The relative abundance of TCA versus GCA in rat versus human SCH was consistent with published reports: taurine conjugation of BAs is greater in the rat, and conjugation of BAs to glycine is greater in humans.

The trends observed with TCA and GCA also were observed with TCDCA and GCDCA. In controls, accumulation of TCDCA in cells + bile, cells, and medium in rat SCH was about 2.5-fold, 2.4-fold, and 12-fold higher, respectively, than in human SCH (**Figure 3.4**). Treatment with TRO also appeared to decrease TCDCA accumulation in cells + bile and cells in both human and rat; however, because of variability, the differences were not statistically significant. TRO treatment decreased the BEI of TCDCA by 15% compared to control in rat SCH (**Table 3.3**), and by 67% compared to control in human SCH (**Table 3.4**). Accumulation of GCDCA in cells + bile, cells, and medium in human SCH was over 400-fold, 450-fold, and 30-fold higher, respectively, than in rat SCH (**Figure 3.5**). Treatment with TRO appeared to decrease GCDCA accumulation in cells + bile and cells in human, but the effect was not statistically significant. In rat SCH, TRO treatment decreased the BEI of GCDCA

by 27% compared to control (**Table 3.3**), while in human, TRO decreased the BEI of GCDCA by 48% compared to control (**Table 3.4**).

Accumulation of total BAs (the sum of all BAs measured) in rat and human SCH are shown in **Figure 3.6**. The medium accumulation of total BAs was about 9-fold higher in human than in rat SCH; likewise, cells + bile and cell accumulation of total BAs were about 57-fold and 70-fold higher, respectively, in human than rat SCH. Total BAs in cells + bile plus medium of human SCH treated with TRO were decreased by 19% of control, suggesting that TRO might affect BA synthesis pathways. **Figure 3.7** shows the contribution of each individual BA species as a percentage of the total in cells + bile, cells, bile, and medium of rat and human SCH. Overall, about 90% of BAs in rat SCH were conjugated to taurine, and 10% to glycine. In human SCH, about 99% of BAs were conjugated to glycine and 1% to taurine. In rat SCH, TCDCA was the predominant BA in cells, while TCA was the most abundant BA in the bile and medium. GCA and GCDCA together comprised 16% or less of the total BAs in all compartments in both control and TRO-treated rat SCH. TRO appeared to have little effect on the relative percentages of the individual BAs in each compartment of rat SCH. In human SCH, GCDCA was the most abundant BA in cells, while GCA was predominant in bile and medium. TCA and TCDCA comprised less than 1% of the total BAs in all compartments in both control and TRO-treated human SCH. TRO appeared to increase GCDCA in cells, at the same time decreasing GCDCA in the bile, although due to variability, these differences were not statistically significant.

Estimates for individual and total BA concentrations in cells + bile and cells were calculated based on estimates of hepatocyte intracellular volume and the number of cells/well (6.83  $\mu$ l cells/well for rat SCH, 6.79  $\mu$ l cells/well for human) (Lee *et al.*, 2010), (**Tables 3.3 and 3.4**); concentrations for total cholic acid (CA) species (TCA + GCA) and total chenodeoxycholic acid species (TCDCA + GCDCA) are presented in **Table 3.5**. Concentrations of BAs in the medium were calculated using a volume of 1.5 ml/well. Based on these estimates, intracellular concentrations of the total BAs measured were about 70-fold higher in human than in rat SCH, while concentrations in the medium were only about 8-fold higher in human than in rat SCH. BA concentrations in the bile compartment were not estimated because the volume of the bile canalicular spaces is not known.

## Discussion

**BA s Decreased in Cells + Bile and Cells, but Increased in Medium, of Untreated Rat SCH over Days in Culture.** Initial experiments were carried out in order to characterize the disposition of BAs over time in culture in the intracellular, biliary, and medium compartments of rat SCH. The mass of total BAs in cells + bile and cells decreased over time while total BAs in bile remained relatively constant; thus it appears that the increase in BAs in the culture medium over time may be due to increased BA synthesis starting on day 3 of culture. Whether the increase is a recovery of normal synthesis capability following the isolation process, or a response to culture conditions, is unclear. However, it has been reported that cholesterol 7 $\alpha$ -hydroxylase (the rate-limiting enzyme for BA synthesis) mRNA levels increased several-fold from day 2 to day 4 and then declined in human SCH (Ellis *et al.* 1998). While our studies only measured BAs up to day 4 in rat, Sauter *et al.* (1996) reported that total BA efflux into the culture medium by human SCH remained relatively constant from days 4-12 of culture (Sauter *et al.* 1996).

Importantly, these data also demonstrate that in this *in vitro* model, BAs do not accumulate in hepatocytes over time in culture, indicating that efflux mechanisms are functional and that the model is not inherently cholestatic. However, it is not clear whether increasing BAs in the medium over time are preferentially effluxed into the medium from the basolateral membrane (*i.e.*, by Mrp4), or whether BAs are effluxed into the medium from contractions of the bile canaliculi. In rat liver *in vivo*, contractions of the bile canaliculi mediated by actin filaments facilitate bile flow (Watanabe *et al.* 1991). Similar regular, ordered

contractions have been reported in the bile canaliculi of isolated hepatocyte couplets in vitro (Oshio and Phillips 1981; Phillips *et al.* 1982). Contractions of the bile canaliculi in the SCH model may release accumulated BAs into the culture medium over time.

Alternatively, while MRP4/Mrp4 normally is expressed at low levels in hepatocytes, it is induced in cholestasis, presumably as an adaptive response mechanism to compensate for increased intracellular concentrations of BAs; such induction in vivo may explain the increased excretion of BAs in the urine of patients with cholestasis (Assem *et al.* 2004; Schuetz *et al.* 2001; Zollner *et al.* 2003). If intracellular BAs increase over time, MRP4/Mrp4 protein expression and/or membrane localization may increase in order to compensate. The canalicular transport proteins P-gp, BSEP, and MRP2 reside inside intracellular compartments and are capable of trafficking, within minutes, to the canalicular membrane under increased demand for BA and organic anion efflux (reviewed in Kipp and Arias 2002). This rapid insertion of transport proteins into the membrane allows for more rapid upregulation of transport capability than would be possible through increased protein synthesis. Therefore, while basal MRP4 expression is considered low in liver, it is possible that increased membrane trafficking of the protein from cytosolic vesicular compartments may increase MRP4-mediated BA efflux.

**Clear Species Differences are Evident in BA profiles of Rat versus Human SCH.** BA profiles between rat and human SCH differed in two prominent ways. First, the total mass of BAs was about 12-fold greater in human SCH than in rat SCH. Second, taurine-conjugated BAs predominated in rat SCH, while glycine-

conjugated BAs predominated in human SCH. It has been reported that cultured human hepatocytes have a greater capacity to produce BAs than cultured rat hepatocytes, even though the synthesis of BAs in rat liver *in vivo* is 3- to 5-fold higher than that in human liver (Ellis *et al.* 1998). Although variability was high in human SCH in this study, the results were consistent with this observation. Variability was not entirely unexpected; in historic controls for human plasma BA concentrations, variability in CA and CDCA concentrations were 103-115% and 62-84% (Ahlberg *et al.* 1977; Tagliacozzi *et al.* 2003). In rodents, but not humans, CDCA can be hydroxylated and conjugated to form glyco- and tauromuricholic acids (GMCA and TMCA). Because humans do not synthesize these BAs, they were not included in this study; however, limited analysis of GMCA and TMCA in rat SCH suggested that the mass of BAs in rat including TMCA and GMCA would still have been several-fold lower than in human (data not shown).

Overall, taurine-conjugated BAs comprised 90% of BAs in the rat SCH, consistent with previous reports that ~94-98% of BAs in rats are conjugated to taurine (Alvaro *et al.* 1986; Mizuta *et al.* 1999; Pellicoro *et al.* 2007). In human SCH, 99% of BAs were conjugated to glycine and 1% to taurine; these values are considerably greater than the value of ~75% glycine conjugates and ~25% taurine conjugates in human plasma and bile reported in the literature (Alvaro *et al.* 1986; Byrne *et al.* 2002; Tagliacozzi *et al.* 2003). An explanation for the decreased taurine conjugation of BAs in human SCH is unclear. One reason could be depletion of available taurine; hepatic taurine concentrations are a major determinant of the proportion of BAs conjugated with taurine versus glycine (Hardison and Proffitt

1977). When homogenates of both human and rat liver were exposed to equimolar concentrations of taurine and glycine, conjugation of CA to taurine predominated, but when human liver homogenates were exposed to high concentrations of glycine, conjugation of CA to glycine predominated. Therefore, because glycine is easily synthesized and not readily depleted *in vivo*, the concentration of available taurine determines the amount of BAs conjugated to taurine (Gottfrieds *et al.* 1966). While both rat and human SCH were exposed to the exact same culture conditions, rat hepatocytes were treated on day 3 and collected on day 4, while human hepatocytes were treated on day 6 and collected on day 7 because bile canaliculi formation in human SCH is slower than in rat SCH. Alternatively, preferential glycine-conjugation of BAs in human SCH may be the result of altered function of bile acid-coenzyme A:amino acid N-acyltransferase (BAAT), the single enzyme responsible for the conjugation of BAs to both glycine and taurine in humans.

**Intracellular and Medium Concentrations of BAs Were Estimated Using the B-CLEAR<sup>®</sup> System.** Concentrations of BAs were estimated in cells + bile and cells using estimates for cell volume described in **Materials and Methods**, while BA concentrations in the medium were based on a volume of 1.5 ml/well. Direct comparisons of intracellular concentrations of BAs between this study and other published values are difficult; efflux of total BAs into the culture medium is most commonly reported for *in vitro* studies, and studies wherein BAs are measured in rat or human liver tissue are likely to also contain residual BAs from bile canaliculi within the tissue. Furthermore, the same BAs are not always measured in each study. However, our estimate for the concentration of total BAs (TCA + GCA + TCDCA +

GCDCA) in the medium of rat SCH ( $0.36 \pm 0.19 \mu\text{M}$ ) is comparable to the published concentration of  $0.13 \pm 0.02 \mu\text{M}$  in rat conventionally-cultured hepatocytes (Ellis *et al.* 1998). In contrast, Dunn *et al.* (1991) reported a BA secretion rate for total BAs in rat SCH of  $\sim 1.2 \text{ nmol/hr}$  in 4 ml medium; this translates to a much higher maximum concentration of  $\sim 7 \mu\text{M}$  over a 24-h period (Dunn *et al.* 1991). The concentration of BAs in the medium of human SCH ( $3.25 \pm 1.99 \mu\text{M}$ ), also is in good agreement with the published value of  $3.68 \pm 1.47 \mu\text{M}$  (Ellis *et al.* 1998), and for human plasma BA concentrations of  $\sim 3\text{-}10 \mu\text{M}$  (Ahlberg *et al.* 1977; Tagliacozzi *et al.* 2003). The intracellular concentration of total BAs in humans in vivo is thought to be maintained at  $< 3 \mu\text{M}$  through efficiently coupled uptake and efflux, as well as intracellular binding of BAs to cytosolic BA binding proteins (Hofmann 1999), although intracellular BA concentrations can be as high as  $200 \mu\text{M}$  (Blitzer and Boyer 1982). The intracellular concentration of total BAs in rat SCH ( $2.6 \pm 1.3 \mu\text{M}$ ) was comparable to this value, whereas intracellular concentrations of total BAs in human SCH were much higher than in rat ( $183.5 \pm 155.2 \mu\text{M}$ ), but variability was also quite high. It is possible that hepatocytes from individual human subjects have differing capacities for BA synthesis based on underlying genetic factors, disease states of donor tissue, or liver exposure to drugs/xenobiotics prior to tissue collection.

**TRO Displayed Minimal Effects on BA Profiles of Rat versus Human SCH.** TRO trended to decrease BA accumulation in cells of both rat and human SCH; only the intracellular accumulation of GCA was increased in rat SCH. Effects on BEI were more pronounced. In particular, in rat SCH, TRO decreased the BEI of TCDCa, which was the most abundant BA in cells, by 15%; in human SCH, TRO

decreased the BEI of GCDCA, which was the most abundant BA, by 48%. TRO-mediated inhibition of the BEI of TCDCA and GCDCA, did not increase concentrations of these BA species in cells. TRO inhibits both the NTCP/Ntcp-mediated uptake and BSEP/Bsep-mediated canalicular excretion of exogenously administered [ $^3\text{H}$ ]TCA in both rat and human hepatocytes (Kemp *et al.* 2005; Marion *et al.* 2007). Thus, even though the BEI of [ $^3\text{H}$ ]TCA is decreased, inhibition of [ $^3\text{H}$ ]TCA uptake may prevent increased intracellular accumulation of TCA. The same may be true for TCDCA and GCDCA; TRO-mediated inhibition of BA reuptake from the culture medium might also account for the decreased cellular accumulation. TRO also decreased the mass of total BAs by 19% compared to control, suggesting that overall BA synthesis was compromised. TRO has been shown to reduce cholesterol synthesis in HepG2 cells and Caco2 cells (Klopotek *et al.* 2006), which may in turn decrease BA synthesis.

Data concerning the intracellular concentrations of xenobiotics (drugs, toxins, etc.) at the target organ or tissue often are limited, especially in human studies. However, intracellular concentrations may be a critical determinant of efficacy and/or toxicity. Rat and human SCH models are useful for determining the cellular and biliary disposition of xenobiotics, as well as the targets of these xenobiotics (*i.e.*, BAs), since it is possible to measure BAs in the cells + bile, cells, and medium compartments directly, and the bile compartment indirectly. In this study, BA profiles in rat and human hepatocytes were similar to those reported in the literature. Treatment with TRO decreased the intracellular accumulation of BAs, and also decreased biliary excretion, consistent with previously published acute studies of

[<sup>3</sup>H]TCA hepatobiliary disposition in the presence of TRO. Overall, the impact of TRO on BA transport, whether endogenous or exogenous, appears to be directed towards decreased hepatic exposure to potentially cytotoxic BAs.

Donor	HU0803	HU1067	HU1184	HU1191
Age	42	61	73	19
Sex	male	male	female	male
Race	Caucasian	Caucasian	Caucasian	Caucasian
Height (in)	72	76	66	74
Weight (lb)	240	215	150	152
BMI (%)	32.6	26.2	24.2	19.5
Smoker	no	no	no	no
Alcohol Use	rare	no	rare	no
Serology	not known	not tested	Hep B and Hep C: non-reactive HIV: not tested	Hep B and Hep C: non-reactive HIV: not tested
Medications	not known	Zantac 300 mg QD Prilosec 20 mg BID Allegra 180 mg QD Diltiazem CD 180 mg QD Iron Multivitamin Vitamin D	Hydrochlorithiazide 12.5 mg QD Flagyl	none

**Table 3.1:** Demographic data for human liver donors.

Analyte	Molecular Weight	Salt	Retention Time (min)	Precursor m/z	Product m/z
TCA	515.7	none	5.7	514	124
d <sub>8</sub> -TCA	545.73	Na <sup>+</sup>	5.7	522	128
d <sub>4</sub> -TCA (IS)	519.73	none	5.7	518	124
TCDCA	499.7	none	8.1	498	80
d <sub>4</sub> -TCDCA	503.73	none	8.1	502	80
GCA	465.62	none	5.8	464	74
d <sub>4</sub> -GCA	469.65	none	5.8	468	74
GCDCA	449.62	none	8.1	448	74
d <sub>4</sub> -GCDCA	453.65	none	8.1	452	74

**Table 3.2:** Transitions monitored at unit resolution for LC-MS/MS analysis.

Rat		cells + bile ( $\mu\text{M}$ )	cells ( $\mu\text{M}$ )	medium ( $\mu\text{M}$ )	BEI (%)
TCA	CTL	2.15 $\pm$ 0.67	0.73 $\pm$ 0.14	0.252 $\pm$ 0.112	66.2
	TRO	2.17 $\pm$ 0.43	0.77 $\pm$ 0.11	0.265 $\pm$ 0.142	64.4
GCA	CTL	0.12 $\pm$ 0.04	0.06 $\pm$ 0.01	0.029 $\pm$ 0.022	50.0
	TRO	0.13 $\pm$ 0.07	0.07 $\pm$ 0.01	0.031 $\pm$ 0.025	44.1
TCDCA	CTL	2.23 $\pm$ 1.04	1.62 $\pm$ 1.01	0.054 $\pm$ 0.049	27.3
	TRO	1.64 $\pm$ 0.65	1.26 $\pm$ 0.67	0.050 $\pm$ 0.044	23.1
GCDCA	CTL	0.37 $\pm$ 0.07	0.23 $\pm$ 0.10	0.030 $\pm$ 0.010	37.3
	TRO	0.29 $\pm$ 0.03	0.21 $\pm$ 0.05	0.024 $\pm$ 0.004	27.2

**Table 3.3:** BEI (%) and concentrations ( $\mu\text{M}$ ) of BAs in cells + bile, cells, and medium in rat SCH. Calculations assume a hepatocyte volume of 6.83  $\mu\text{l}$  cells/well of a 6-well plate for rat SCH (Lee *et al.*, 2010).

Human		cells + bile ( $\mu\text{M}$ )	cells ( $\mu\text{M}$ )	medium ( $\mu\text{M}$ )	BEI (%)
TCA	CTL	$0.7 \pm 0.41$	$0.39 \pm 0.19$	$0.013 \pm 0.006$	44.3
	TRO	$0.33 \pm 0.18$	$0.25 \pm 0.08$	$0.011 \pm 0.005$	25.4
GCA	CTL	$136.6 \pm 111.5$	$78.78 \pm 64.01$	$2.341 \pm 1.359$	42.3
	TRO	$59.0 \pm 46.0$	$32.46 \pm 26.89$	$2.336 \pm 1.498$	45.0
TCDCA	CTL	$0.88 \pm 0.25$	$0.67 \pm 0.15$	$0.005 \pm 0.002$	24.0
	TRO	$0.47 \pm 0.03$	$0.43 \pm 0.06$	$0.004 \pm 0.001$	8.0
GCDCA	CTL	$142.57 \pm 130.02$	$103.63 \pm 90.89$	$0.891 \pm 0.614$	27.3
	TRO	$73.82 \pm 70.05$	$63.44 \pm 62.35$	$0.706 \pm 0.392$	14.1

**Table 3.4:** BEI (%) and concentrations ( $\mu\text{M}$ ) of BAs in cells + bile, cells, and medium in human SCH. Calculations assume a hepatocyte volume of  $6.79 \mu\text{l}$  cells/well of a 6-well plate for human SCH (Lee *et al.*, 2010).

		cells + bile ( $\mu\text{M}$ ) <sup>*</sup>	cells ( $\mu\text{M}$ ) <sup>*</sup>	medium ( $\mu\text{M}$ )
CTL Rat	CA	2.3 $\pm$ 0.7	0.8 $\pm$ 0.2	0.3 $\pm$ 0.1
	CDCA	2.6 $\pm$ 1.1	1.9 $\pm$ 1.1	0.1 $\pm$ 0.1
	total	4.9 $\pm$ 1.8	2.6 $\pm$ 1.3	0.4 $\pm$ 0.2
		cells + bile ( $\mu\text{M}$ ) <sup>**</sup>	cells ( $\mu\text{M}$ ) <sup>**</sup>	medium ( $\mu\text{M}$ )
CTL Human	CA	137.3 $\pm$ 111.9	79.2 $\pm$ 64.2	2.4 $\pm$ 1.4
	CDCA	143.5 $\pm$ 130.3	104.3 $\pm$ 91.0	0.9 $\pm$ 0.6
	total	280.8 $\pm$ 242.2	183.5 $\pm$ 155.2	3.3 $\pm$ 2.0

**Table 3.5:** Concentration ( $\mu\text{M}$ ) of total CA species (TCA + GCA) and total CDCA species (TCDCA + GCDCA) in cells + bile, cells, and medium of CTL rat and human SCH. \* Assumes a hepatocyte volume of 6.83  $\mu\text{l}$  cells/well of a 6-well plate for rat SCH; \*\* assumes a hepatocyte volume of 6.79  $\mu\text{l}$  cells/well of a 6-well plate for human SCH (Lee *et al.*, 2010).

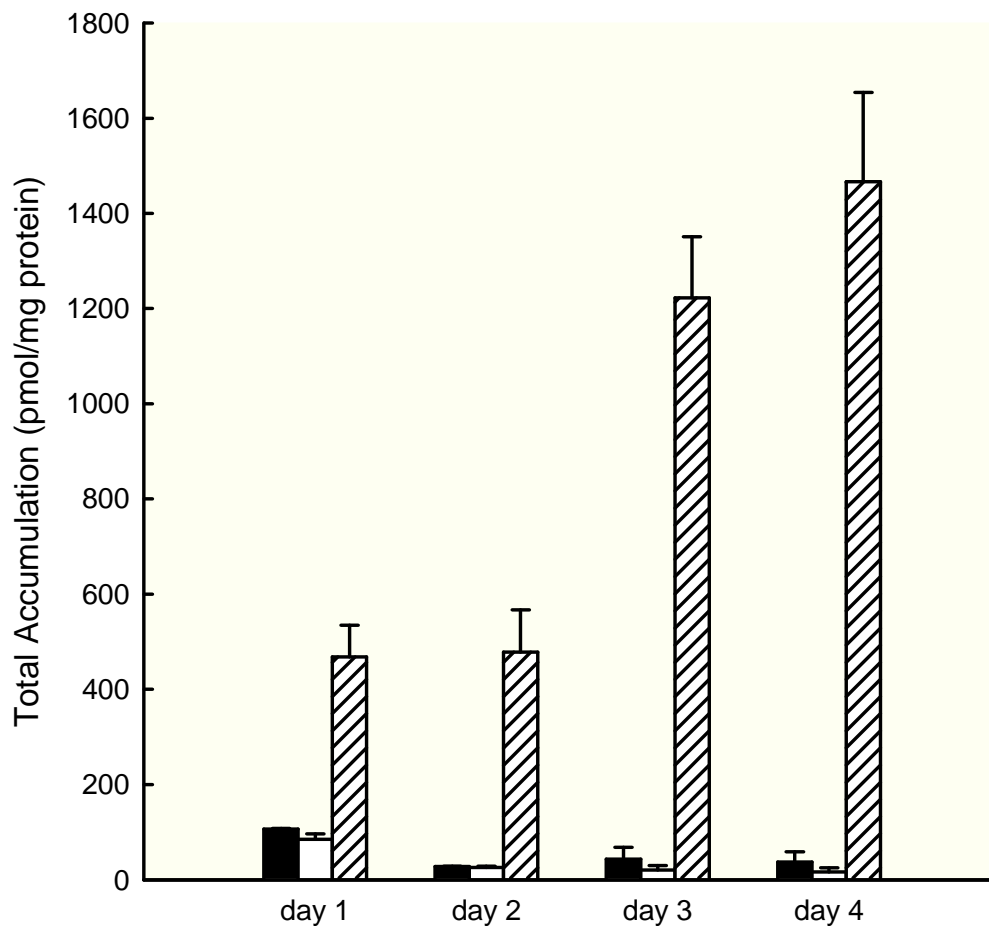


**Figure 3.1:** Total accumulation (pmol/mg protein) of total BAs in cells + bile (solid bars), cells (open bars), and medium (hatched bars) in rat SCH over days 1 through 4 of culture. Values represent mean  $\pm$  range of duplicate measurements in  $n = 2$  experiments (cells + bile and cells) or mean  $\pm$  SD of 6 individual measurements in  $n = 1$  experiment.

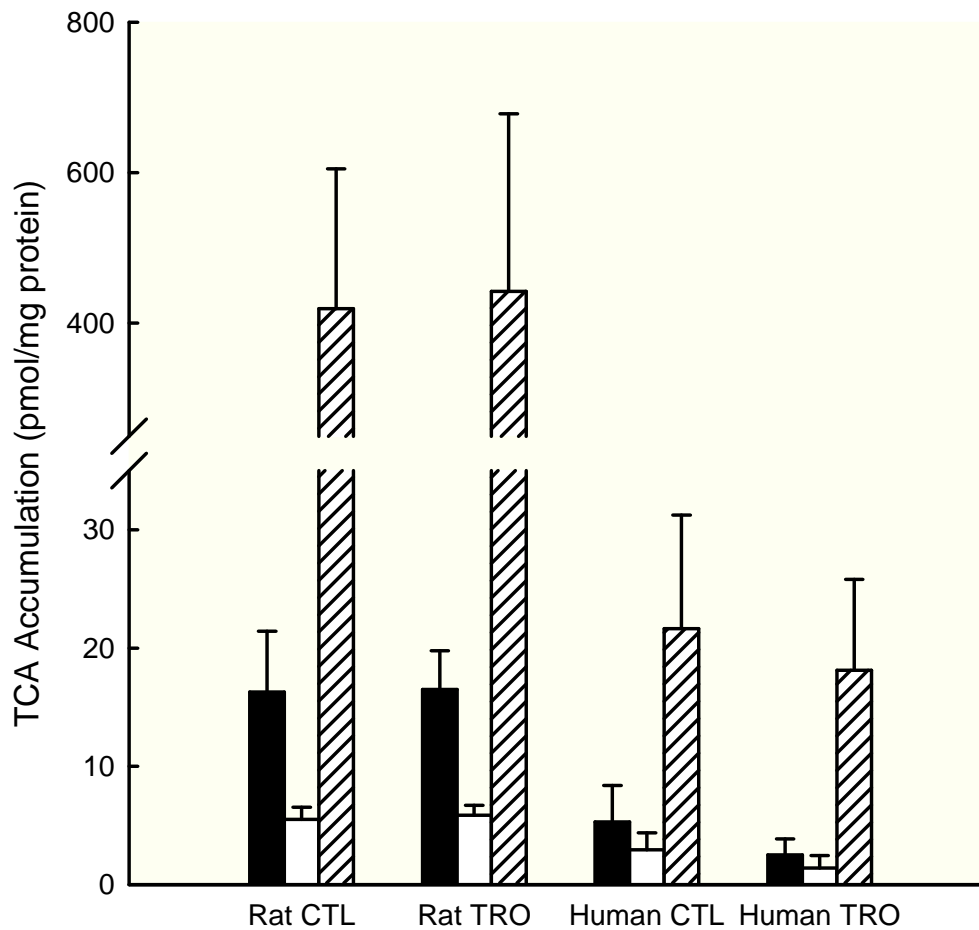


**Figure 3.2:** Accumulation (pmol/mg protein) of TCA in cells + bile (solid bars), cells (open bars), and medium (hatched bars) in rat and human SCH following 24-h treatment with vehicle (0.1% DMSO) or 10  $\mu$ M TRO. In rat SCH, values represent the mean  $\pm$  SEM of triplicate measurements (cells + bile and cells) in n = 3 experiments, and mean  $\pm$  range (medium) of 3-6 measurements in n = 2 experiments. In human SCH, values represent mean  $\pm$  SD of duplicate measurements (cells + bile and cells) in n = 4 experiments and mean  $\pm$  SD of 2-6 measurements (medium) in n = 4 experiments.

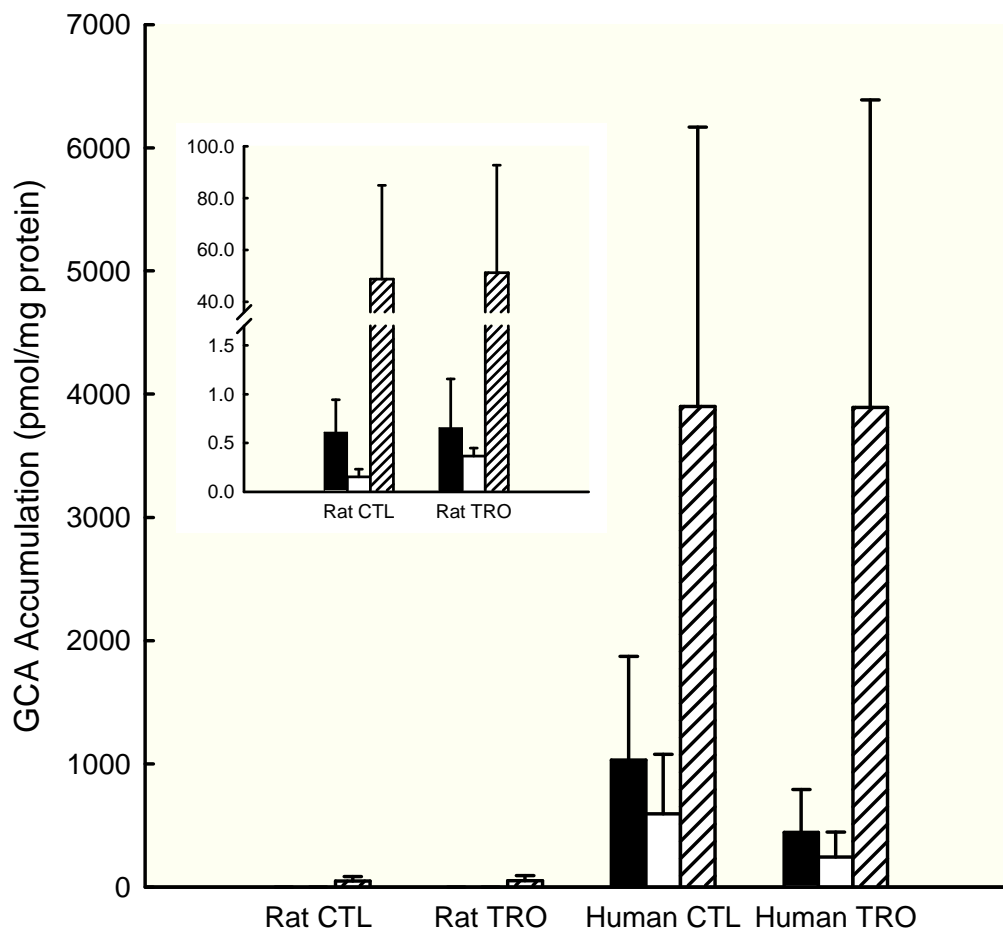


**Figure 3.3:** Accumulation (pmol/mg protein) of GCA in cells + bile (solid bars), cells (open bars), and medium (hatched bars) in rat and human SCH following 24-h treatment with vehicle (0.1% DMSO) or 10  $\mu$ M TRO. In rat SCH, values represent the mean  $\pm$  SEM of triplicate measurements (cells + bile and cells) in  $n = 3$  experiments, and mean  $\pm$  range (medium) of 3-6 measurements in  $n = 2$  experiments. In human SCH, values represent mean  $\pm$  SD of duplicate measurements (cells + bile and cells) in  $n = 4$  experiments and mean  $\pm$  SD of 2-6 measurements (medium) in  $n = 4$  experiments. Inset shows accumulation of GCA in cells + bile, cells, and medium in rat SCH with the y-axis scaled for easier visualization.

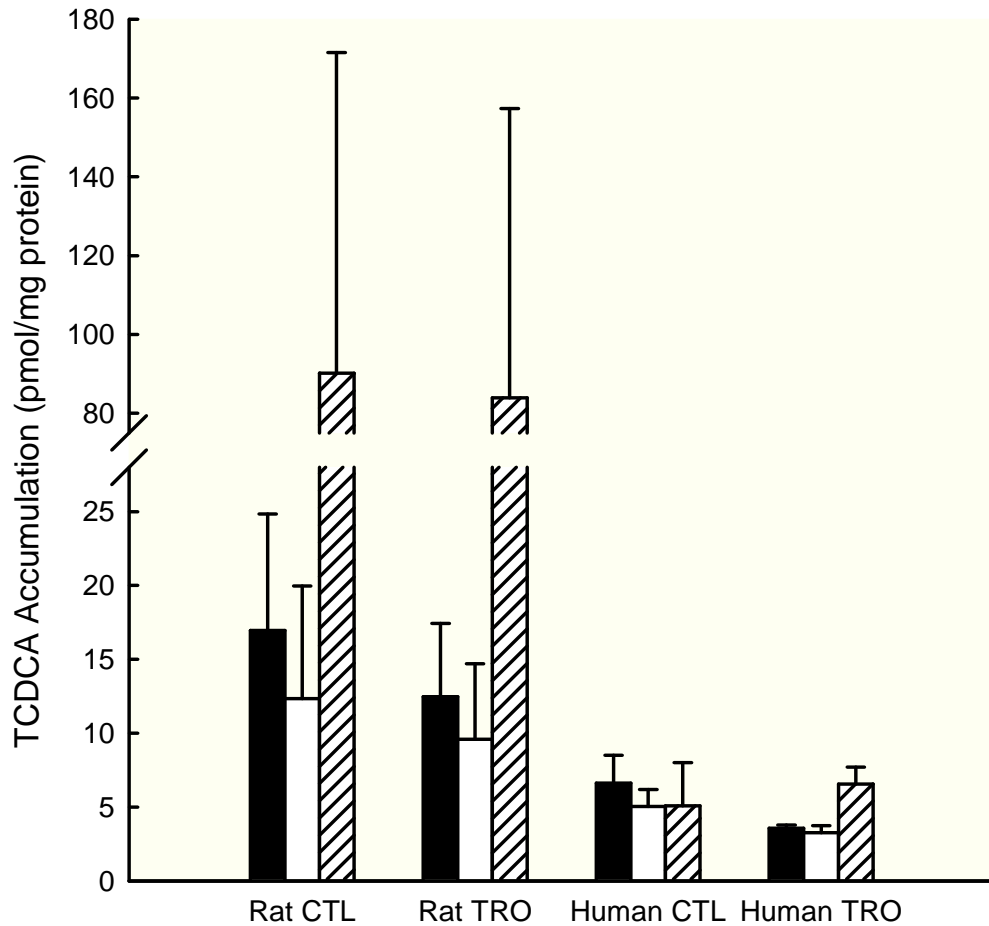


**Figure 3.4:** Accumulation (pmol/mg protein) of TCDCA in cells + bile (solid bars), cells (open bars), and medium (hatched bars) in rat and human SCH following 24-h treatment with vehicle (0.1% DMSO) or 10  $\mu$ M TRO. In rat SCH, values represent the mean  $\pm$  SEM of triplicate measurements (cells + bile and cells) in n = 3 experiments, and mean  $\pm$  range (medium) of 3-6 measurements in n = 2 experiments. In human SCH, values represent mean  $\pm$  SD of duplicate measurements (cells + bile and cells) in n = 4 experiments and mean  $\pm$  SD of 2-6 measurements (medium) in n = 4 experiments.

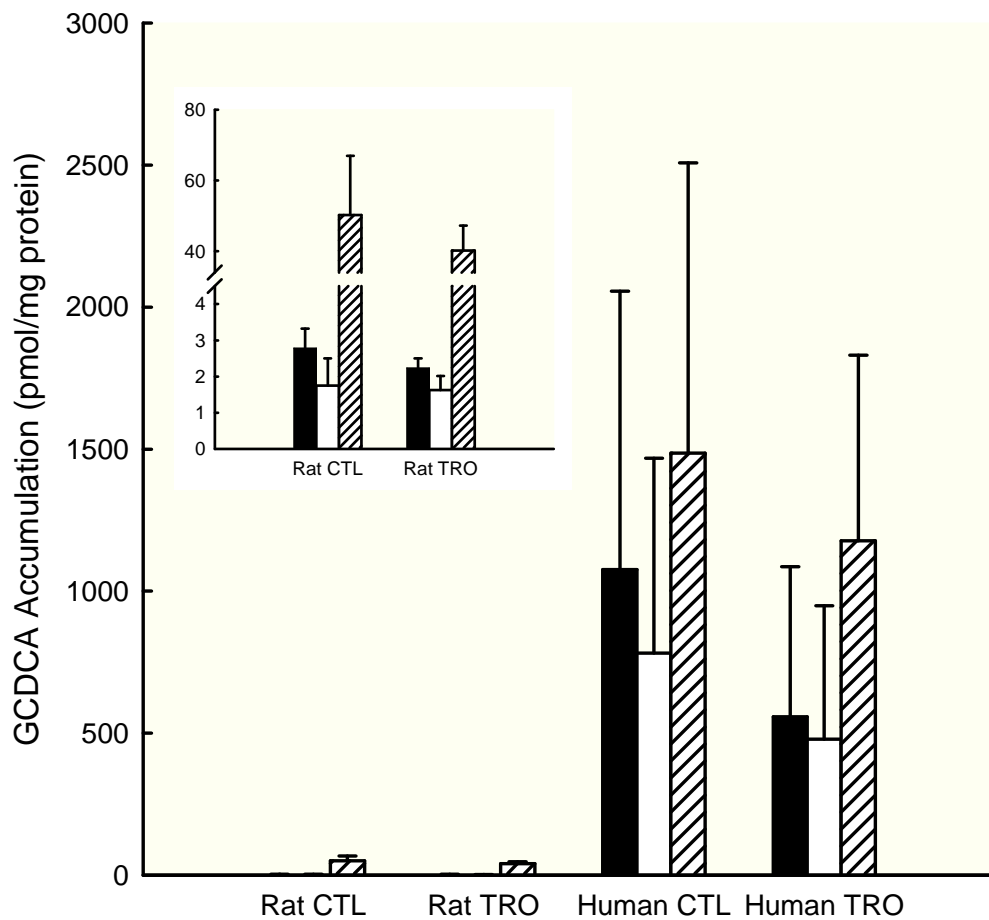


**Figure 3.5:** Accumulation (pmol/mg protein) of GCDCA in cells + bile (solid bars), cells (open bars), and medium (hatched bars) in rat and human SCH following 24-h treatment with vehicle (0.1% DMSO) or 10  $\mu$ M TRO. In rat SCH, values represent the mean  $\pm$  SEM of triplicate measurements (cells + bile and cells) in n = 3 experiments, and mean  $\pm$  range (medium) of 3-6 measurements in n = 2 experiments. In human SCH, values represent mean  $\pm$  SD of duplicate measurements (cells + bile and cells) in n = 4 experiments and mean  $\pm$  SD of 2-6 measurements (medium) in n = 4 experiments. Inset shows accumulation of GCDCA in cells + bile, cells, and medium in rat SCH with the y-axis scaled for easier visualization.

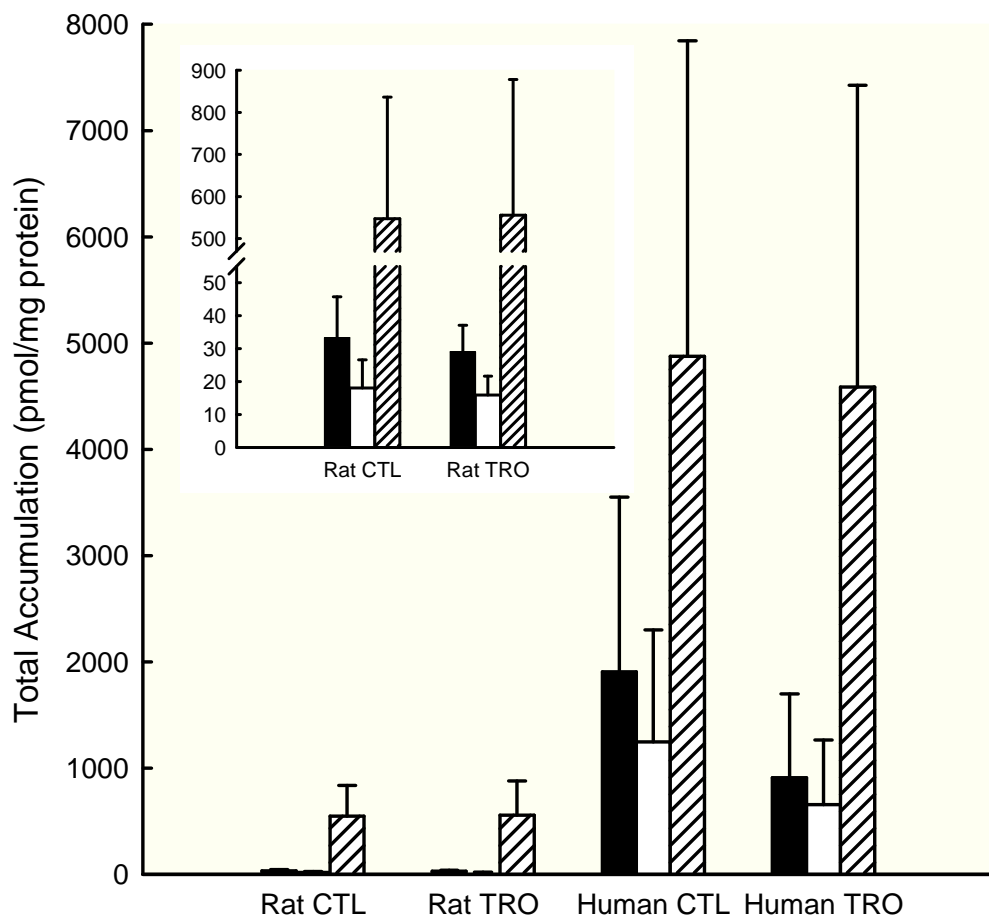


**Figure 3.6:** Accumulation (pmol/mg protein) of total BAs measured in cells + bile (solid bars), cells (open bars), and medium (hatched bars) in rat and human SCH following 24-h treatment with vehicle (0.1% DMSO) or 10  $\mu$ M TRO. In rat SCH, values represent the mean  $\pm$  SEM of triplicate measurements (cells + bile and cells) in n = 3 experiments, and mean  $\pm$  range (medium) of 3-6 measurements in n = 2 experiments. In human SCH, values represent mean  $\pm$  SD of duplicate measurements (cells + bile and cells) in n = 4 experiments and mean  $\pm$  SD of 2-6 measurements (medium) in n = 4 experiments. Inset shows accumulation of BAs in cells + bile, cells, and medium in rat SCH with the y-axis scaled for easier visualization.

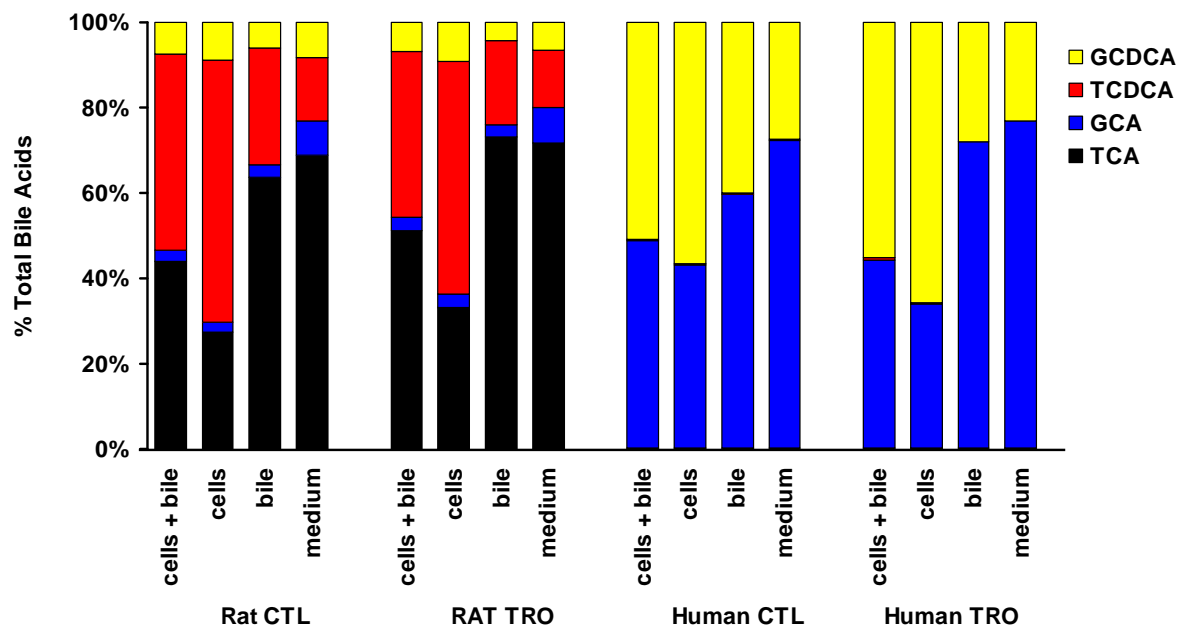


**Figure 3.7:** Accumulation of individual BA species as percent of total in cells + bile, cells, bile, and medium in rat and human SCH following 24-h treatment with vehicle (0.1% DMSO) or 10  $\mu$ M TRO.

## REFERENCES

- Ahlberg, J., Angelin, B., Bjorkhem, I., and Einarsson, K. (1977). Individual bile acids in portal venous and systemic blood serum of fasting man. *Gastroenterology* **73**, 1377-82.
- Alvaro, D., Cantafora, A., Attili, A. F., Ginanni Corradini, S., De Luca, C., Minervini, G., Di Biase, A., and Angelico, M. (1986). Relationships between bile salts hydrophilicity and phospholipid composition in bile of various animal species. *Comp Biochem Physiol B* **83**, 551-4.
- Assem, M., Schuetz, E. G., Leggas, M., Sun, D., Yasuda, K., Reid, G., Zelcer, N., Adachi, M., Strom, S., Evans, R. M., Moore, D. D., Borst, P., and Schuetz, J. D. (2004). Interactions between hepatic Mrp4 and Sult2a as revealed by the constitutive androstane receptor and Mrp4 knockout mice. *J Biol Chem* **279**, 22250-7.
- Barnes, S., Gallo, G. A., Trash, D. B., and Morris, J. S. (1975). Diagnostic value of serum bile acid estimations in liver disease. *J Clin Pathol* **28**, 506-9.
- Blitzer, B. L., and Boyer, J. L. (1982). Cellular mechanisms of bile formation. *Gastroenterology* **82**, 346-57.
- Borst, P., de Wolf, C., and van de Wetering, K. (2007). Multidrug resistance-associated proteins 3, 4, and 5. *Pflugers Arch* **453**, 661-73.
- Byrne, J. A., Strautnieks, S. S., Mieli-Vergani, G., Higgins, C. F., Linton, K. J., and Thompson, R. J. (2002). The human bile salt export pump: characterization of substrate specificity and identification of inhibitors. *Gastroenterology* **123**, 1649-58.
- Delzenne, N. M., Calderon, P. B., Taper, H. S., and Roberfroid, M. B. (1992). Comparative hepatotoxicity of cholic acid, deoxycholic acid and lithocholic acid in the rat: in vivo and in vitro studies. *Toxicol Lett* **61**, 291-304.
- Desmet, V. J. (1995). Histopathology of cholestasis. *Verh Dtsch Ges Pathol* **79**, 233-40.
- Dunn, J. C., Tompkins, R. G., and Yarmush, M. L. (1991). Long-term in vitro function of adult hepatocytes in a collagen sandwich configuration. *Biotechnol Prog* **7**, 237-45.

Ellis, E., Goodwin, B., Abrahamsson, A., Liddle, C., Mode, A., Rudling, M., Bjorkhem, I., and Einarsson, C. (1998). Bile acid synthesis in primary cultures of rat and human hepatocytes. *Hepatology* **27**, 615-20.

Fattinger, K., Funk, C., Pantze, M., Weber, C., Reichen, J., Stieger, B., and Meier, P. J. (2001). The endothelin antagonist bosentan inhibits the canalicular bile salt export pump: a potential mechanism for hepatic adverse reactions. *Clin Pharmacol Ther* **69**, 223-31.

Funk, C., Pantze, M., Jehle, L., Ponelle, C., Scheuermann, G., Lazendic, M., and Gasser, R. (2001a). Troglitazone-induced intrahepatic cholestasis by an interference with the hepatobiliary export of bile acids in male and female rats. Correlation with the gender difference in troglitazone sulfate formation and the inhibition of the canalicular bile salt export pump (Bsep) by troglitazone and troglitazone sulfate. *Toxicology* **167**, 83-98.

Funk, C., Ponelle, C., Scheuermann, G., and Pantze, M. (2001b). Cholestatic potential of troglitazone as a possible factor contributing to troglitazone-induced hepatotoxicity: in vivo and in vitro interaction at the canalicular bile salt export pump (Bsep) in the rat. *Mol Pharmacol* **59**, 627-35.

Geier, A., Wagner, M., Dietrich, C. G., and Trauner, M. (2007). Principles of hepatic organic anion transporter regulation during cholestasis, inflammation and liver regeneration. *Biochim Biophys Acta* **1773**, 283-308.

Gores, G. J., Miyoshi, H., Botla, R., Aguilar, H. I., and Bronk, S. F. (1998). Induction of the mitochondrial permeability transition as a mechanism of liver injury during cholestasis: a potential role for mitochondrial proteases. *Biochim Biophys Acta* **1366**, 167-75.

Gottfries, A., Schersten, T., and Ekdahl, P. H. (1966). The capacity of human liver homogenates to synthesize taurocholic and glycocholic acid in vitro. *Scand J Clin Lab Invest* **18**, 643-53.

Hardison, W. G., and Proffitt, J. H. (1977). Influence of hepatic taurine concentration on bile acid conjugation with taurine. *Am J Physiol* **232**, E75-9.

Hofmann, A. F. (1999). Bile acids: the good, the bad, and the ugly. *News Physiol Sci* **14**, 24-29.

Kaplowitz, N. (2001). Drug-induced liver disorders: implications for drug development and regulation. *Drug Saf* **24**, 483-90.

Kaplowitz, N., Kok, E., and Javitt, N. B. (1973). Postprandial serum bile acid for the detection of hepatobiliary disease. *Jama* **225**, 292-3.

Kemp, D. C., Zamek-Gliszczynski, M. J., and Brouwer, K. L. (2005). Xenobiotics inhibit hepatic uptake and biliary excretion of taurocholate in rat hepatocytes. *Toxicol Sci* **83**, 207-14.

Keppler, D., Cui, Y., Konig, J., Leier, I., and Nies, A. (1999). Export pumps for anionic conjugates encoded by MRP genes. *Adv Enzyme Regul* **39**, 237-46.

Keppler, D., and Konig, J. (2000). Hepatic secretion of conjugated drugs and endogenous substances. *Semin Liver Dis* **20**, 265-72.

Kipp, H., and Arias, I. M. (2002). Trafficking of canalicular ABC transporters in hepatocytes. *Annu Rev Physiol* **64**, 595-608.

Klopotek, A., Hirche, F., and Eder, K. (2006). PPAR gamma ligand troglitazone lowers cholesterol synthesis in HepG2 and Caco-2 cells via a reduced concentration of nuclear SREBP-2. *Exp Biol Med (Maywood)* **231**, 1365-72.

Korman, M. G., Hofmann, A. F., and Summerskill, W. H. (1974). Assessment of activity in chronic active liver disease. Serum bile acids compared with conventional tests and histology. *N Engl J Med* **290**, 1399-402.

LeCluyse, E. L., Audus, K. L., and Hochman, J. H. (1994). Formation of extensive canalicular networks by rat hepatocytes cultured in collagen-sandwich configuration. *Am J Physiol* **266**, C1764-74.

Lee, J., and Brouwer, K. R. (2010). Determination of Intracellular Volume of Rat and Human Sandwich-Cultured Hepatocytes. In Society of Toxicology Annual Meeting, Salt Lake City, UT, USA.

Liu, X., Chism, J. P., LeCluyse, E. L., Brouwer, K. R., and Brouwer, K. L. R. (1999a). Correlation of biliary excretion in sandwich-cultured rat hepatocytes and in vivo in rats. *Drug Metab Dispos* **27**, 637-44.

Liu, X., LeCluyse, E. L., Brouwer, K. R., Gan, L. S., Lemasters, J. J., Stieger, B., Meier, P. J., and Brouwer, K. L. (1999b). Biliary excretion in primary rat hepatocytes cultured in a collagen-sandwich configuration. *Am J Physiol* **277**, G12-21.

Liu, X., LeCluyse, E. L., Brouwer, K. R., Lightfoot, R. M., Lee, J. I., and Brouwer, K. L. (1999c). Use of Ca<sup>2+</sup> modulation to evaluate biliary excretion in sandwich-cultured rat hepatocytes. *J Pharmacol Exp Ther* **289**, 1592-9.

Marion, T. L., Leslie, E. M., and Brouwer, K. L. (2007). Use of sandwich-cultured hepatocytes to evaluate impaired bile acid transport as a mechanism of drug-induced hepatotoxicity. *Mol Pharm* **4**, 911-8.

McRae, M. P., Lowe, C. M., Tian, X., Bourdet, D. L., Ho, R. H., Leake, B. F., Kim, R. B., Brouwer, K. L. R., and Kashuba, A. D. (2006). Ritonavir, saquinavir, and efavirenz, but not nevirapine, inhibit bile acid transport in human and rat hepatocytes. *J Pharmacol Exp Ther* **318**, 1068-75.

Mizuta, K., Kobayashi, E., Uchida, H., Ogino, Y., Fujimura, A., Kawarasaki, H., and Hashizume, K. (1999). Cyclosporine inhibits transport of bile acid in rats: comparison of bile acid composition between liver and bile. *Transplant Proc* **31**, 2755-6.

Oshio, C., and Phillips, M. J. (1981). Contractility of bile canaliculi: implications for liver function. *Science* **212**, 1041-2.

Pauli-Magnus, C., and Meier, P. J. (2006). Hepatobiliary transporters and drug-induced cholestasis. *Hepatology* **44**, 778-87.

Pauli-Magnus, C., Stieger, B., Meier, Y., Kullak-Ublick, G. A., and Meier, P. J. (2005). Enterohepatic transport of bile salts and genetics of cholestasis. *J Hepatol* **43**, 342-57.

Pellicoro, A., van den Heuvel, F. A., Geuken, M., Moshage, H., Jansen, P. L., and Faber, K. N. (2007). Human and rat bile acid-CoA:amino acid N-acyltransferase are liver-specific peroxisomal enzymes: implications for intracellular bile salt transport. *Hepatology* **45**, 340-8.

Phillips, M. J., Oshio, C., Miyairi, M., Katz, H., and Smith, C. R. (1982). A study of bile canalicular contractions in isolated hepatocytes. *Hepatology* **2**, 763-8.

Preininger, K., Stingl, H., Englisch, R., Furnsinn, C., Graf, J., Waldhausl, W., and Roden, M. (1999). Acute troglitazone action in isolated perfused rat liver. *Br J Pharmacol* **126**, 372-8.

Roth, R. A., and Ganey, P. E. (2010) Intrinsic versus idiosyncratic drug-induced hepatotoxicity--two villains or one? *J Pharmacol Exp Ther* **332**, 692-7.

Sauter, G., Fischer, S., Pahernik, S., Koebe, H. G., and Paumgartner, G. (1996). Formation of cholic acid and chenodeoxycholic acid from 7 alpha-hydroxycholesterol and 27-hydroxycholesterol by primary cultures of human hepatocytes. *Biochim Biophys Acta* **1300**, 25-9.

Schuetz, E. G., Strom, S., Yasuda, K., Lecureur, V., Assem, M., Brimer, C., Lamba, J., Kim, R. B., Ramachandran, V., Komoroski, B. J., Venkataramanan, R., Cai, H., Sinal, C. J., Gonzalez, F. J., and Schuetz, J. D. (2001). Disrupted bile acid homeostasis reveals an unexpected interaction among nuclear hormone receptors, transporters, and cytochrome P450. *J Biol Chem* **276**, 39411-8.

Shibukawa, A., Sawada, T., Nakao, C., Izumi, T., and Nakagawa, T. (1995). High-performance frontal analysis for the study of protein binding of troglitazone (CS-045) in albumin solution and in human plasma. *J Chromatogr A* **697**, 337-43.

Soroka, C. J., Ballatori, N., and Boyer, J. L. (2010). Organic solute transporter, OSTalpha-OSTbeta: its role in bile acid transport and cholestasis. *Semin Liver Dis* **30**, 178-85.

Stieger, B., Fattinger, K., Madon, J., Kullak-Ublick, G. A., and Meier, P. J. (2000). Drug- and estrogen-induced cholestasis through inhibition of the hepatocellular bile salt export pump (Bsep) of rat liver. *Gastroenterology* **118**, 422-30.

Tagliacozzi, D., Mozzi, A. F., Casetta, B., Bertucci, P., Bernardini, S., Di Ilio, C., Urbani, A., and Federici, G. (2003). Quantitative analysis of bile acids in human plasma by liquid chromatography-electrospray tandem mass spectrometry: a simple and rapid one-step method. *Clin Chem Lab Med* **41**, 1633-41.

Trauner, M., and Boyer, J. L. (2003). Bile salt transporters: molecular characterization, function, and regulation. *Physiol Rev* **83**, 633-71.

Watanabe, N., Tsukada, N., Smith, C. R., and Phillips, M. J. (1991). Motility of bile canaliculi in the living animal: implications for bile flow. *J Cell Biol* **113**, 1069-80.

Zollner, G., Fickert, P., Silbert, D., Fuchsbichler, A., Marschall, H. U., Zatloukal, K., Denk, H., and Trauner, M. (2003). Adaptive changes in hepatobiliary transporter expression in primary biliary cirrhosis. *J Hepatol* **38**, 717-27.

Zollner, G., and Trauner, M. (2008). Mechanisms of cholestasis. *Clin Liver Dis* **12**, 1-26.

## **CHAPTER 4**

### **Inhibition of MRP4-Mediated Taurocholic Acid Transport by Troglitazone Sulfate**

## Abstract

Multidrug resistance-associated protein 4 (MRP4) is an efflux transport protein expressed on the basolateral (sinusoidal) membrane of hepatocytes. Because MRP4 mRNA and protein are upregulated in humans during cholestasis, MRP4 may play a role in the compensatory efflux of excess intracellular bile acids (BAs). If this compensatory efflux route is compromised, for example by xenobiotics, or a disease state, or polymorphism, cytotoxicity may ensue. Inhibition of BA transport has been hypothesized as one mechanism by which the drug troglitazone (TRO) causes hepatotoxicity. TRO inhibits basolateral uptake of BAs via Na<sup>+</sup>-taurocholate cotransporting polypeptide (NTCP/Ntcp), and inhibits canalicular BA efflux via the bile salt export pump (BSEP/Bsep); TRO also inhibits organic anion transport polypeptide (Oatp) isoforms in rat. The major metabolite of TRO, TRO-sulfate (TS), is an even more potent inhibitor of BSEP/Bsep than TRO. Whether TS inhibits MRP4-mediated BA efflux is not known. This study was designed to assess the potential for TS-mediated inhibition of compensatory BA transport by MRP4 by measuring uptake of [<sup>3</sup>H]TCA in the presence of TS in membrane vesicles from HEK293 cells overexpressing MRP4 protein. Initial pilot studies showed that TS is a substrate of MRP4, and inhibits uptake of the known MRP4 substrates methotrexate (MTX) and dehydroepiandrosterone sulfate (DHEAS). Uptake of [<sup>3</sup>H]TCA by MRP4 was linear for up to 5 min; TS inhibited [<sup>3</sup>H]TCA uptake in a concentration-dependent manner. These results suggest that, in addition to inhibition of BSEP/Bsep-mediated biliary efflux of BAs, TRO (via TS) may mediate its toxic effect through inhibition of compensatory basolateral BA efflux. Impaired MRP4 function in susceptible

individuals may cause intracellular accumulation of BAs, TS, or both.

## Introduction

Multidrug resistance-associated protein 4 (MRP4) is a member of the ATP-binding cassette (ABC) transport protein superfamily that uses the energy from the hydrolysis of ATP to transport substrates. MRP4 protein is expressed in a number of different tissues, including the liver (Rius *et al.* 2003) and kidneys (van Aobel *et al.* 2002). In the liver, MRP4 is localized to the basolateral (sinusoidal) hepatocyte membrane, and excretes substrates such as conjugated steroids, prostanoids, cyclic nucleotides, bile acids (BAs), and sulfated conjugates of xenobiotics (reviewed in Borst *et al.* 2007) from hepatocytes into the sinusoidal blood. MRP4 protein normally is expressed at low levels in hepatocytes, but is induced during cholestasis in humans (Gradhand *et al.* 2008), and also in mice (Mennone *et al.* 2006) and rats (Denk *et al.* 2004), presumably as an adaptive response mechanism to compensate for increased intracellular concentrations of BAs. Interestingly, increased MRP4 protein expression on the basolateral membrane of hepatocytes can occur without concurrent increased MRP4 mRNA (Denk *et al.* 2004), suggesting that post-translational mechanisms participate in increased protein mobilization to the membrane.

Troglitazone (TRO), a peroxisome proliferator-activated receptor  $\gamma$  (PPAR $\gamma$ ) agonist marketed for the treatment of noninsulin-dependent type II diabetes, was removed from the U.S. market three years after its release following numerous reports of idiosyncratic hepatotoxicity. Inhibition of BA transport leading to cholestatic liver injury is one proposed mechanism for TRO's hepatotoxicity. TRO is metabolized primarily to a sulfate conjugate (TS) in humans (Honma *et al.* 2002;

Kawai *et al.* 1997), and to a quinone (TQ) (Yamazaki *et al.* 1999); a glucuronide conjugate (TG) also is formed to a lesser extent (Watanabe *et al.* 2002; Yoshigae *et al.* 2000). Of the metabolites detected in human plasma at steady-state after multiple oral dosing for 7 days, the sulfate and quinone metabolites of TRO predominated, making up 70% and 10%, respectively (Loi *et al.* 1999a; Loi *et al.* 1997), while the glucuronide conjugate was a minor metabolite in plasma (Loi *et al.* 1999b; Parke-Davis 1998). TRO inhibits both basolateral BA uptake in human and rat hepatocytes via NTCP/Ntcp and canalicular BA efflux via BSEP/Bsep (Kemp *et al.* 2005; Marion *et al.* 2007); however, TS, the major metabolite of TRO, is an even more potent inhibitor of BSEP/Bsep than TRO (Funk *et al.* 2001a; Funk *et al.* 2001b).

Studies examining the disposition of TRO in rats showed that there was a high degree of TS accumulation in liver; accumulation was greater in males, and was attributed to an increased rate of sulfation in male rats as compared to females (Funk *et al.* 2001a). In *in vitro* studies using rat sandwich-cultured hepatocytes (SCH), TS also accumulated within hepatocytes to a greater extent than TRO or its glucuronide or quinone metabolites (Lee *et al.* 2009). Under cholestatic conditions, BAs, especially sulfated BAs, increase in the plasma and urine (Assem *et al.* 2004; Schuetz *et al.* 2001; Zollner *et al.* 2003). Induction of MRP4 may account for these changes in BA disposition, since MRP4 effluxes sulfated steroids (Zelcer *et al.* 2003), and both unsulfated and sulfated BAs into the blood (Geier *et al.* 2007). Sulfated BAs in particular are not substrates of BSEP, so removal from the liver by MRP4 presents a potential mechanism for protecting the liver from further damage (Assem *et al.* 2004). Therefore, TS and BAs may compete for transporter-mediated

efflux from the hepatocyte. If basolateral efflux is compromised (*i.e.*, due to impaired MRP4 function), then toxicity may be exacerbated if TS and/or BAs accumulate.

In this study, a role for MRP4 in the efflux of TS and BAs was explored. Membrane vesicles were prepared from untransfected (CTL) or transfected HEK293 cells overexpressing MRP4 protein. Pilot studies determined that TS was both a substrate of MRP4 and inhibited uptake of known MRP4 substrates. MRP4-mediated uptake of [<sup>3</sup>H]TCA was measured in the presence of increasing concentrations of TS to assess inhibition of BA transport; data revealed that TS inhibited [<sup>3</sup>H]TCA transport in a concentration-dependent manner. This interaction between TS, BAs, and MRP4 provides another potential mechanism by which TRO can cause the intrahepatic accumulation of BAs.

## Materials and Methods

**Chemicals.** [ $^3\text{H}$ ]TCA (5 Ci/mmol; purity > 97%) and [ $^3\text{H}$ ]dehydroepiandrosterone sulfate (DHEAS) (63 Ci/mmol; purity > 97%) were purchased from Perkin Elmer (Waltham, MA). [ $^3\text{H}$ ]Methotrexate (MTX) (24 Ci/mmol; purity > 97%) was acquired from Moravek (Brea, CA). TS was a gift from Daiichi Sankyo Co., LTD., Tokyo, Japan. Dulbecco's modified Eagle's medium (DMEM) with phenol red, and MAX Efficiency<sup>®</sup> DH5 $\alpha$ <sup>™</sup> Competent Cells were purchased from Invitrogen (Carlsbad, CA). Cellgro<sup>®</sup> fetal bovine serum (FBS) was acquired from Mediatech, Inc. (Manassas, VA). Dimethyl sulfoxide (DMSO) was purchased from Fisher Scientific (Fairlawn, NJ). Type A/E glass fiber filters were acquired from Pall Corporation (Ann Arbor, MI). Creatine kinase, FuGENE<sup>®</sup> 6 transfection reagent, and Complete Mini EDTA-free protease inhibitor cocktail tablets were purchased from Roche Applied Science (Mannheim, Germany). All other chemicals and reagents were of analytical grade and were readily available from commercial sources.

**MRP4 Expression Vector and Transfection in HEK293 Cells.** The pcDNA3.1/Hygro-ABCC4 cDNA vector was a kind gift from Dr. Deitrich Keppler. Construction of the expression vector pcDNA3.1/Hygro-ABCC4 cDNA encoding MRP4 (ABCC4) has been described previously (Rius *et al.* 2003). Amplification of the cDNA was performed as follows: 10  $\mu\text{l}$  of *E. coli* competent cells were heat-transformed using 100 ng of plasmid DNA stock and cultured overnight on Luria Bertani (LB) agar plates containing 50  $\mu\text{g}/\text{ml}$  ampicillin. Colonies were selected 12 h later and incubated in 2 ml sterile LB broth containing ampicillin for 8 h at 37°C with vigorous shaking. The entire volume of the starter culture was added to 60 ml of LB

broth containing ampicillin and grown at 37°C for an additional 8–10 h with vigorous shaking. Cell cultures were centrifuged at 1200 × g for 10-min. Plasmid DNA was purified from the transformed *E. coli* cell pellets using the QIAGEN Plasmid Maxi Kit (QIAGEN, Valencia, CA), and purity and concentration were measured spectrophotometrically using a NanoDrop spectrophotometer (Thermo Scientific, Wilmington, DE).

Human HEK293 cells were cultured in BD Falcon 175 cm<sup>2</sup> tissue culture treated flasks (Fisher Scientific, Pittsburgh, PA) in DMEM with phenol red supplemented with 10% (v/v) FBS and incubated at 37°C and 5% CO<sub>2</sub> in a humidified incubator. The HEK293 cells were transfected with the pcDNA3.1/Hygro-ABCC4 cDNA construct using FuGENE<sup>®</sup> 6 transfection reagent. Untransfected HEK293 cells served as controls, and were otherwise treated identically, concurrently with transfected cells. After 72 h, the culture medium was aspirated, cells were rinsed 1x with 10 ml ice-cold phosphate-buffered saline (PBS), and scraped into 5 ml/flask of ice-cold PBS on ice. Cells from 8 flasks were consolidated into a single 50 ml conical tube and centrifuged at 800 × g for 5 min at 4°C, and the supernatant was removed. Cell pellets were washed 2x by resuspending in 10 ml buffer containing 250 mM sucrose, 50 mM tris(hydroxymethyl)aminomethane (Tris), and 0.25 mM CaCl<sub>2</sub>, pH 7.4, and centrifuging at 800 × g for 5 min. Following the final centrifugation step, the wash buffer was aspirated and cell pellets were resuspended in buffer containing 250 mM sucrose, 50 mM Tris, 0.25 mM CaCl<sub>2</sub>, 10 µl of 200 mg/ml benzamidine, and one Complete mini EDTA-free protease inhibitor cocktail

tablet per tube, pH 7.4. Pellets were snap-frozen using liquid nitrogen and stored at -80°C until preparation of membrane vesicles.

**Membrane Vesicle Preparation and Immunoblotting.** Plasma membrane vesicles were prepared as described with modifications (Loe *et al.* 1996). Briefly, transfected and untransfected (control) HEK293 cell pellets were thawed on ice, resuspended, and membranes disrupted by N<sub>2</sub> cavitation. The exploded cell suspension was centrifuged for 10 min at 800 × g at 4°C and the supernatant was layered over a cushion of 35% (w/v) sucrose, 1 mM EDTA, and 50 mM Tris, pH 7.4, and centrifuged at 100,000 × g at 4°C for 1 h. Following centrifugation, the interface was removed and placed in a buffer solution containing 25 mM sucrose and 50 mM Tris, pH 7.4 and centrifuged at 100,000 × g for 30 min. The pelleted membranes were washed with buffer containing 250 mM sucrose, 50 mM Tris, pH 7.4, and resuspended and vesicularized by passing through a 27-gauge needle and syringe 20 times. Aliquots of vesicles were stored at -80°C until use. Relative expression of MRP4 protein in the membrane fractions was determined by immunoblot. Protein (2-10 µg total protein/well) was resolved by electrophoresis on NuPAGE<sup>®</sup> Novex<sup>®</sup> 4% to 20% Bis-Tris gels (Invitrogen, Carlsbad, CA), and following transfer to nitrocellulose membranes, blots were blocked overnight with 5% (w/v) skim milk powder in Tris-buffered saline with 0.1% Tween 20 (TBS-T) buffer, pH 7.4, rinsed 3 x, and incubated with the M<sub>4</sub>I-10 rat monoclonal antibody (Alexis Biochemicals, San Diego, CA) at a dilution of 1:1000 for 2 h. After washing, blots were incubated with horseradish peroxidase-conjugated goat anti-rat antibody (Sigma-Aldrich, St. Louis, MO) followed by application of SuperSignal West Dura (Thermo Scientific,

Wilmington, DE) enhanced duration chemiluminescent substrate. Bands were visualized using a VersaDoc 1000 imaging system (Bio-Rad Laboratories, Hercules, CA), and relative band density was determined using Quantity One 1-D Analysis Software v4.4.0 (Bio-Rad Laboratories, Hercules, CA).

**Transport Studies.** All transport assays were performed using a rapid filtration method as described (Loe *et al.* 1996). Membrane vesicles (10  $\mu$ g protein) were incubated at 37°C in a 50  $\mu$ l total reaction volume containing 4 mM ATP or AMP, 10 mM MgCl<sub>2</sub>, 10 mM dithiothreitol (DTT), 10 mM creatine phosphate, 100 mg/ml creatine kinase, 3 mM GSH, 5  $\mu$ M TCA, and substrate (10  $\mu$ M TS, 10  $\mu$ M MTX plus 60 nCi/reaction [<sup>3</sup>H]MTX, trace [<sup>3</sup>H]DHEAS, or 5  $\mu$ M TCA plus 100 nCi/reaction [<sup>3</sup>H]TCA). MK571 (18 or 50  $\mu$ M) was included as a positive control for MRP4 inhibition. At selected timepoints, the uptake reaction was stopped by adding 800  $\mu$ l ice-cold buffer containing 250 mM sucrose, 50 mM Tris, pH 7.4. The entire 850  $\mu$ l aliquot was filtered through glass fiber type A/E filters and washed 2x with the same ice-cold buffer. Filters were allowed to dry 1 h, and radioactivity trapped within the filters was quantitated by liquid scintillation counting in the case of [<sup>3</sup>H]MTX, [<sup>3</sup>H]DHEAS, and [<sup>3</sup>H]TCA, while TS was measured by LC-MS/MS. Transport in the presence of AMP was subtracted from transport in the presence of ATP and reported as ATP-dependent uptake. Transport also was measured in membrane vesicles prepared from untransfected HEK293 cells. The inhibitory effect of TS on MRP4-mediated TCA uptake was determined using the same method as described above; the initial rate of [<sup>3</sup>H]TCA uptake was measured at a single timepoint (2 min) in the presence of increasing concentrations of TS (0-100  $\mu$ M).

**Data Analysis.** Statistical analysis (one-way analysis of variance [ANOVA] and Dunnett's multiple comparison test, or two-way ANOVA with Bonferroni's multiple comparison test) was performed using GraphPad Prism 5.03. In all cases, a  $p$  value  $< 0.05$  was considered statistically significant.

## Results

Pilot studies were undertaken to determine whether TS is a substrate for MRP4, and whether TS inhibits uptake of the known MRP4 substrates MTX and DHEAS. **Figure 4.1** shows uptake (nM) at 1 and 5 min of TS into MRP4-expressing membrane vesicles incubated with 10  $\mu$ M TS. Uptake at 5 min was almost 2.5-fold higher than at 1 min, showing that uptake of TS increased over time. **Figure 4.2** shows uptake of [ $^3$ H]MTX (pmol/mg protein/90 s) into MRP4-expressing membrane vesicles in the presence of vehicle (0.1% DMSO; CTL), 1 or 10  $\mu$ M TS, or 18  $\mu$ M MK571. MK571 inhibited [ $^3$ H]MTX uptake; TS also inhibited [ $^3$ H]MTX uptake in a concentration-dependent manner. Uptake of the MRP4 substrate [ $^3$ H]DHEAS ( $\mu$ l/min/mg protein) was measured in the presence of vehicle (0.1% DMSO; CTL), 50  $\mu$ M TS, or 50  $\mu$ M MK571 (**Figure 4.3**). As with [ $^3$ H]MTX, both TS and MK571 inhibited MRP4-mediated [ $^3$ H]DHEAS uptake. These pilot studies established that TS is a substrate for MRP4, and that TS inhibits the transport of known MRP4 substrates.

ATP-dependent uptake of [ $^3$ H]TCA in CTL and MRP4-expressing membrane vesicles over time is shown in **Figure 4.4**. Uptake was linear up to ~5 min; the 2 min timepoint was chosen for subsequent experiments. At 2 min, the uptake rate of [ $^3$ H]TCA in MRP4-expressing membrane vesicles was ~56 pmol/mg protein/min, while the uptake rate in CTL vesicles was ~29 pmol/mg protein/min. The ATP-dependent uptake rate (pmol/mg protein/min) of [ $^3$ H]TCA in CTL membrane vesicles (solid circles) and MRP4-expressing membrane vesicles (open squares) in the presence of increasing concentrations of TS (0-100  $\mu$ M) is plotted in **Figure 4.5**. The

uptake rate of [<sup>3</sup>H]TCA in the MRP4-expressing membrane vesicles without TS (~50 pmol/mg protein/min) was consistent with results from the uptake time course (**Figure 4.4**), while uptake in CTL vesicles was higher (~38 pmol/mg protein/min vs ~29 pmol/mg protein/min). At the maximum TS concentration used (100 μM), uptake in MRP4 vesicles was reduced by 72% to ~14 pmol/mg protein/min. In CTL vesicles, uptake in the presence of 100 μM TS was reduced by 71% to ~11 pmol/mg protein/min.

Immunoblot analysis of MRP4 protein expression in membrane vesicles from CTL (untransfected) HEK293 cells and in membrane vesicles from MRP4-transfected HEK293 cells was performed; a representative blot is shown in **Figure 4.7**. While overexpression of MRP4 protein was detected in the membrane vesicles from transfected HEK293 cells, endogenous MRP4 expression in the untransfected HEK293 cells was high.

## Discussion

A number of studies have examined the role of impaired BA transport in the idiosyncratic hepatotoxicity observed with TRO. While TRO-mediated inhibition of BSEP/Bsep- and NTCP/Ntcp-mediated BA transport has been reported using multiple model systems, we believe this is the first study to specifically explore the potential role of the basolateral efflux transport protein MRP4 in the toxicity of TRO. Jemnitz *et al.* reported that in rat SCH, 100  $\mu\text{M}$  TRO had no effect on basolateral efflux of *preloaded* [ $^3\text{H}$ ]TCA, but decreased [ $^3\text{H}$ ]TCA canalicular efflux and increased [ $^3\text{H}$ ]TCA intracellular accumulation; in human SCH, 100  $\mu\text{M}$  TRO decreased basolateral [ $^3\text{H}$ ]TCA efflux slightly, markedly decreased canalicular [ $^3\text{H}$ ]TCA efflux, and almost doubled [ $^3\text{H}$ ]TCA intracellular accumulation (Jemnitz *et al.* 2010). The authors concluded that TRO had no effect on basolateral efflux of [ $^3\text{H}$ ]TCA in rats. Because canalicular and basolateral efflux of TCA were the same magnitude in human hepatocytes, the authors concluded that greater inhibition of canalicular efflux caused the increased intracellular accumulation of [ $^3\text{H}$ ]TCA, and not impaired basolateral efflux. However, the present data challenge this observation, and instead indicate that the major metabolite of TRO, TS, is capable of inhibiting MRP4-mediated BA transport, as well as the transport of other known MRP4 substrates including MTX and DHEAS.

TS has been shown to accumulate in the livers of rats to levels 20-fold higher than parent TRO (Funk *et al.* 2001b). TS also accumulated within rat and human hepatocytes *in vitro*; following a 2-h incubation with 10  $\mu\text{M}$  TRO, the intracellular concentration of TS ranged from 132 to 222  $\mu\text{M}$  in rat SCH and from 136 to 160  $\mu\text{M}$

in human SCH (Lee *et al.* 2009). Our results indicate that MRP4-mediated TCA transport is inhibited by TS at concentrations well below those measured within cells. Sulfation of xenobiotics in general renders compounds more hydrophilic and less toxic, but whether or not TS is in itself inherently hepatotoxic is unclear; in HEPG2 cells, only parent TRO and its quinone derivative were cytotoxic (Yamamoto *et al.* 2001). Inhibition of TRO sulfation resulted in increased cytotoxicity in human and porcine hepatocyte cultures (Kostrubsky *et al.* 2000). However, in immortalized human hepatocyte-derived THLE-2 cells, TS caused greater oxidative stress than parent TRO (Saha *et al.* 2010). BAs, on the other hand, are known to be cytotoxic, and can induce apoptosis or necrosis if they accumulate within hepatocytes. Therefore, competition between BAs and TS for transport out of the cell may exacerbate toxicity if normal compensatory efflux routes are impaired.

Research indicates that MRP4 compensates for impaired canalicular BA excretion. Gradhand *et al.* (2008) found that although MRP4 protein expression varied 45-fold in humans, expression was increased in patients with cholestasis (Gradhand *et al.* 2008). While MRP3 is also upregulated under cholestatic conditions, MRP4 probably plays a more significant role in basolateral BA efflux. Human MRP3 protein expressed in Sf9 vesicles did not transport TCA to a significant extent (Akita *et al.* 2002). In Mrp3 knockout mice, Mrp4 expression between knockout mice and WT mice was similar, and enterohepatic circulation of BAs was unaffected by the loss of Mrp3 (Belinsky *et al.* 2005). Similarly, Mrp3 knockout mice exhibited normal BA transport, but altered hepatic transport of hepatic glucuronides (Zelcer *et al.* 2006). Mrp4, but not Mrp3, protein was upregulated in

common bile duct-ligated (CBDL) WT mice; CBDL Mrp4 knockout mice had more severe liver injury caused by the intracellular accumulation of BAs than WT CBDL mice, suggesting that increased Mrp4 protein in cholestasis protects against damage caused by BA accumulation (Mennone *et al.* 2006).

In addition to cholestasis, MRP4 appears to be involved in hepatoprotection from multiple types of toxic insult. In rats treated with carbon tetrachloride (CCl<sub>4</sub>), decreased Bsep and Mrp2 mRNA expression and increased Mrp3 and Mrp4 mRNA expression were observed (Okumura *et al.* 2007). When mice were treated with toxic doses of CCl<sub>4</sub> or acetaminophen (APAP), CCl<sub>4</sub> induced Mrp4 mRNA 26-fold but reduced Mrp3 mRNA to 20% of control, whereas APAP increased Mrp3 mRNA by 3.5-fold, and Mrp4 mRNA by 16-fold (Aleksunes *et al.* 2006). In humans, APAP-induced liver failure was associated with increased mRNA and protein expression of MRP4, but not MRP3 (Barnes *et al.* 2007). Champion *et al.* (2008) reported that induction of Mrp4 protein in mouse following APAP treatment was dependent on Kupffer cell derived/released mediators, potentially TNF- $\alpha$  and IL-1 $\beta$  (Champion *et al.* 2008).

In humans, increased MRP4 protein expression may overcome TS-mediated BA transport inhibition, and may decrease intracellular accumulation of TS. However, if individuals are unable to increase the amount of functional MRP4 protein on the membrane, perhaps because of a disease state alteration or a genetic polymorphism, then hepatotoxicity may ensue due to increased intracellular BAs or TS. Gradhand *et al.* found two single-nucleotide polymorphisms (SNPs) in the MRP4 gene in humans that resulted in significantly lower or significantly higher protein

expression, although the authors could not associate these mutations with decreased or increased MRP4 function (Gradhand *et al.* 2008). However, during a screen of SNPs in MRP4 in an ethnically diverse human population, Abia *et al.* identified two variants that resulted in a significant reduction in function and caused increased cellular accumulation of the antiviral agents azidothymidine (AZT) and adefovir in HEK293T cells transiently transfected with MRP4 (Abia *et al.* 2008). The effect of TRO on MRP4 mRNA or protein in humans has not been examined. Lee *et al.* reported that treatment of rat SCH with BSO, an inhibitor of glutathione synthesis, induced Mrp4 protein expression and decreased trabectedin toxicity (Lee *et al.* 2008). In the present rat SCH studies, treatment with 100  $\mu$ M TRO increased Mrp4 protein expression 63% over control in one experiment, but no change in Mrp4 protein was observed in a second experiment, although BSO increased Mrp4 protein in both experiments (data not shown).

One clear limitation of the studies presented here is the high level of substrate transport by the untransfected control membrane vesicles from HEK293 cells. While untransfected HEK293 cells do not express endogenous MRP3 (data not shown), it cannot be ruled out that another BA transport protein is expressed in these parent cells. However, the high expression of MRP4 protein in membrane vesicles from untransfected cells implicates MRP4 as the protein responsible for transport. Interestingly, an unidentified protein that reacted with the MRP4 antibody consistently appeared on immunoblots of CTL and MRP4-transfected vesicles that increased in intensity with increased MRP4 protein expression. Clearly, a parent cell line that expressed no, or very little, MRP4 would be more desirable, but is beyond

the scope of this dissertation project. These are the first studies to suggest that TS inhibits MRP4-mediated BA transport. Future goals of this research include the development and characterization of a more specific MRP4 protein-expressing cell line.

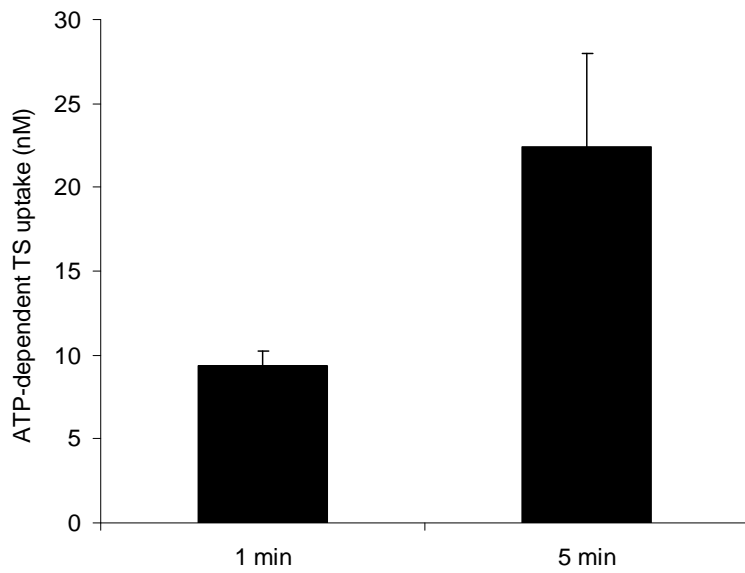


**Figure 4.1:** ATP-dependent uptake (nM) at 1 and 5 min of TS into MRP4-expressing membrane vesicles incubated with 10  $\mu$ M TS. Bars represent mean  $\pm$  SD of triplicate determinations in n = 1 experiment.

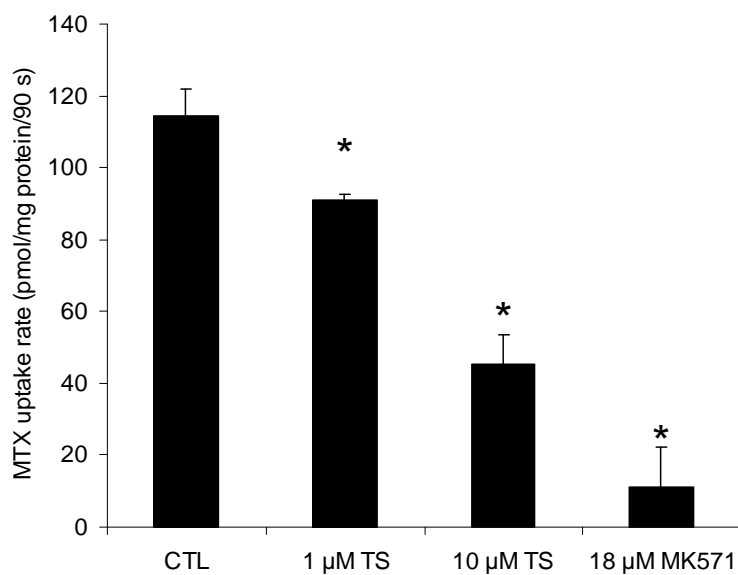


**Figure 4.2:** Uptake of [<sup>3</sup>H]MTX (pmol/mg protein/90 s) into MRP4-expressing membrane vesicles in the presence of vehicle (0.1% DMSO; CTL), 1 or 10 μM TS, or 18 μM MK571. Bars represent mean ± SD of triplicate determinations in n = 1 experiment. \*  $p < 0.05$  vs CTL.

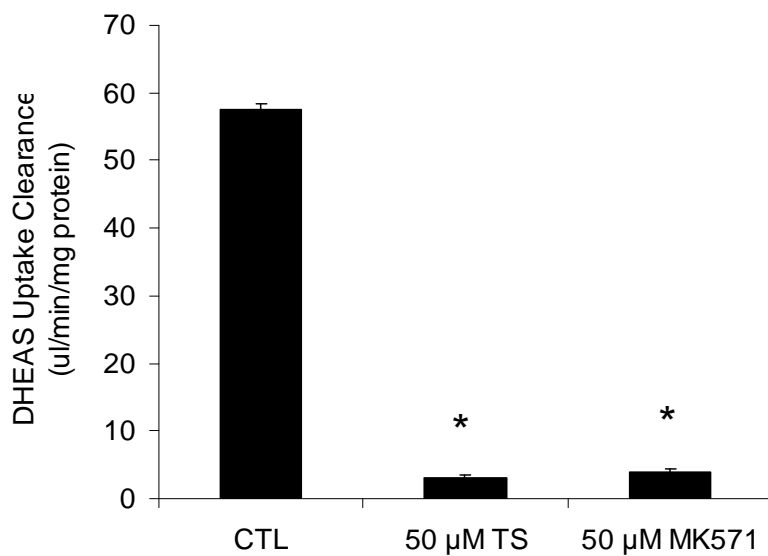


**Figure 4.3:** Uptake clearance ( $\mu\text{l}/\text{min}/\text{mg}$  protein) of DHEAS into MRP4-expressing membrane vesicles in the presence of vehicle (0.1% DMSO; CTL), 50  $\mu\text{M}$  TS, or 50  $\mu\text{M}$  MK571. Bars represent mean  $\pm$  SD of triplicate determinations in  $n = 1$  experiment. \*  $p < 0.05$  vs CTL.

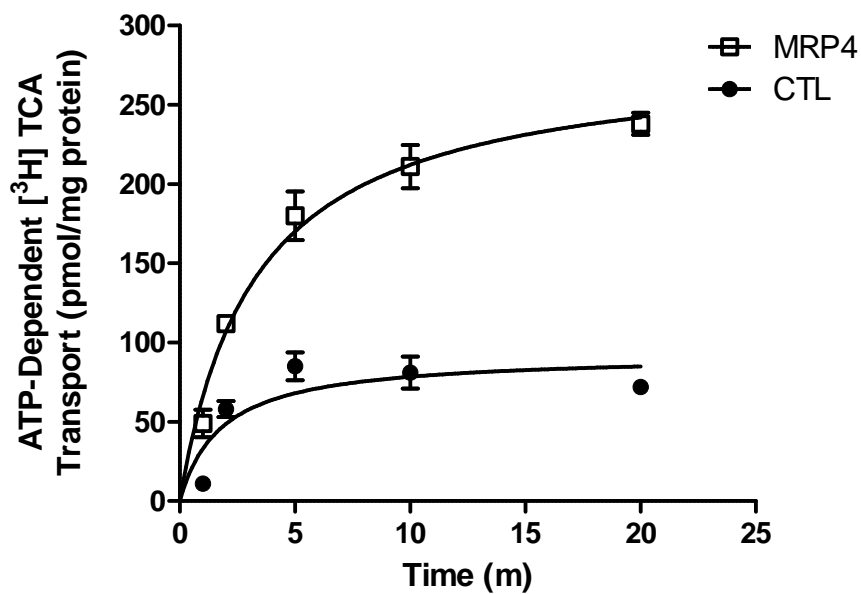


**Figure 4.4:** Time-dependent uptake (pmol/mg protein) of [<sup>3</sup>H]TCA in CTL (solid circles) and MRP4-expressing (open squares) membrane vesicles. Symbols represent mean  $\pm$  range of duplicate determinations in n = 1 experiment.

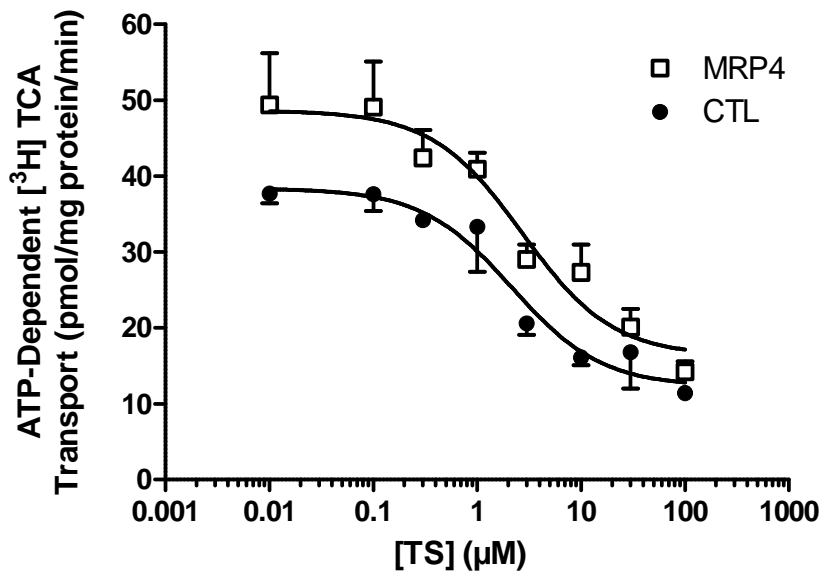


**Figure 4.5:** ATP-dependent uptake rate (pmol/mg protein/min) of [<sup>3</sup>H]TCA in CTL membrane vesicles (solid circles) and MRP4-expressing membrane vesicles (open squares) in the presence of increasing concentrations of TS (0-100 μM). Symbols represent mean ± SEM of triplicate determinations in n = 3 experiments; *p* > 0.05 vs CTL at all concentrations of TS.

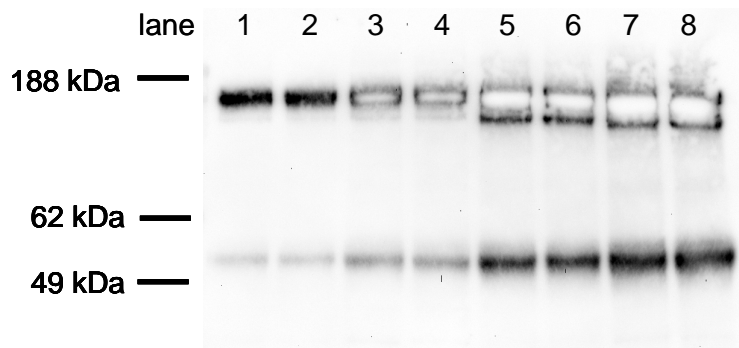


**Figure 4.6:** MRP4 protein expression (~180 kDa) in membrane vesicles from CTL (untransfected) HEK293 cells (lanes 1 and 2, 2  $\mu$ g protein/lane; lanes 5 and 6, 10  $\mu$ g protein/lane) and in membrane vesicles from MRP4-transfected HEK293 cells (lanes 3 and 4, 2  $\mu$ g protein/lane; lanes 7 and 8, 10  $\mu$ g protein/lane). Unidentified protein bands consistently appeared at ~52 kDa in vesicles from both untransfected CTL and MRP4-transfected HEK293 cells.

## REFERENCES

- Abla, N., Chinn, L. W., Nakamura, T., Liu, L., Huang, C. C., Johns, S. J., Kawamoto, M., Stryke, D., Taylor, T. R., Ferrin, T. E., Giacomini, K. M., and Kroetz, D. L. (2008). The human multidrug resistance protein 4 (MRP4, ABCC4): functional analysis of a highly polymorphic gene. *J Pharmacol Exp Ther* **325**, 859-68.
- Akita, H., Suzuki, H., Hirohashi, T., Takikawa, H., and Sugiyama, Y. (2002). Transport activity of human MRP3 expressed in Sf9 cells: comparative studies with rat MRP3. *Pharm Res* **19**, 34-41.
- Aleksunes, L. M., Scheffer, G. L., Jakowski, A. B., Pruijboom-Brees, I. M., and Manautou, J. E. (2006). Coordinated expression of multidrug resistance-associated proteins (Mrps) in mouse liver during toxicant-induced injury. *Toxicol Sci* **89**, 370-9.
- Assem, M., Schuetz, E. G., Leggas, M., Sun, D., Yasuda, K., Reid, G., Zelcer, N., Adachi, M., Strom, S., Evans, R. M., Moore, D. D., Borst, P., and Schuetz, J. D. (2004). Interactions between hepatic Mrp4 and Sult2a as revealed by the constitutive androstane receptor and Mrp4 knockout mice. *J Biol Chem* **279**, 22250-7.
- Barnes, S. N., Aleksunes, L. M., Augustine, L., Scheffer, G. L., Goedken, M. J., Jakowski, A. B., Pruijboom-Brees, I. M., Cherrington, N. J., and Manautou, J. E. (2007). Induction of hepatobiliary efflux transporters in acetaminophen-induced acute liver failure cases. *Drug Metab Dispos* **35**, 1963-9.
- Belinsky, M. G., Dawson, P. A., Shchaveleva, I., Bain, L. J., Wang, R., Ling, V., Chen, Z. S., Grinberg, A., Westphal, H., Klein-Szanto, A., Lerro, A., and Kruh, G. D. (2005). Analysis of the in vivo functions of Mrp3. *Mol Pharmacol* **68**, 160-8.
- Borst, P., de Wolf, C., and van de Wetering, K. (2007). Multidrug resistance-associated proteins 3, 4, and 5. *Pflugers Arch* **453**, 661-73.
- Campion, S. N., Johnson, R., Aleksunes, L. M., Goedken, M. J., van Rooijen, N., Scheffer, G. L., Cherrington, N. J., and Manautou, J. E. (2008). Hepatic Mrp4 induction following acetaminophen exposure is dependent on Kupffer cell function. *Am J Physiol Gastrointest Liver Physiol* **295**, G294-304.
- Denk, G. U., Soroka, C. J., Takeyama, Y., Chen, W. S., Schuetz, J. D., and Boyer, J. L. (2004). Multidrug resistance-associated protein 4 is up-regulated in liver but down-regulated in kidney in obstructive cholestasis in the rat. *J Hepatol* **40**, 585-91.

Funk, C., Pantze, M., Jehle, L., Ponelle, C., Scheuermann, G., Lazendic, M., and Gasser, R. (2001a). Troglitazone-induced intrahepatic cholestasis by an interference with the hepatobiliary export of bile acids in male and female rats. Correlation with the gender difference in troglitazone sulfate formation and the inhibition of the canalicular bile salt export pump (Bsep) by troglitazone and troglitazone sulfate. *Toxicology* **167**, 83-98.

Funk, C., Ponelle, C., Scheuermann, G., and Pantze, M. (2001b). Cholestatic potential of troglitazone as a possible factor contributing to troglitazone-induced hepatotoxicity: in vivo and in vitro interaction at the canalicular bile salt export pump (Bsep) in the rat. *Mol Pharmacol* **59**, 627-35.

Geier, A., Wagner, M., Dietrich, C. G., and Trauner, M. (2007). Principles of hepatic organic anion transporter regulation during cholestasis, inflammation and liver regeneration. *Biochim Biophys Acta* **1773**, 283-308.

Gradhand, U., Lang, T., Schaeffeler, E., Glaeser, H., Tegude, H., Klein, K., Fritz, P., Jedlitschky, G., Kroemer, H. K., Bachmakov, I., Anwald, B., Kerb, R., Zanger, U. M., Eichelbaum, M., Schwab, M., and Fromm, M. F. (2008). Variability in human hepatic MRP4 expression: influence of cholestasis and genotype. *Pharmacogenomics J* **8**, 42-52.

Honma, W., Shimada, M., Sasano, H., Ozawa, S., Miyata, M., Nagata, K., Ikeda, T., and Yamazoe, Y. (2002). Phenol sulfotransferase, ST1A3, as the main enzyme catalyzing sulfation of troglitazone in human liver. *Drug Metab Dispos* **30**, 944-9.

Jemnitz, K., Veres, Z., and Vereczkey, L. (2010). Contribution of high basolateral bile salt efflux to the lack of hepatotoxicity in rat in response to drugs inducing cholestasis in human. *Toxicol Sci* **115**, 80-8.

Kawai, K., Kawasaki-Tokui, Y., Odaka, T., Tsuruta, F., Kazui, M., Iwabuchi, H., Nakamura, T., Kinoshita, T., Ikeda, T., Yoshioka, T., Komai, T., and Nakamura, K. (1997). Disposition and metabolism of the new oral antidiabetic drug troglitazone in rats, mice and dogs. *Arzneimittelforschung* **47**, 356-68.

Kemp, D. C., Zamek-Gliszczynski, M. J., and Brouwer, K. L. (2005). Xenobiotics inhibit hepatic uptake and biliary excretion of taurocholate in rat hepatocytes. *Toxicol Sci* **83**, 207-14.

Kostrubsky, V. E., Sinclair, J. F., Ramachandran, V., Venkataramanan, R., Wen, Y. H., Kindt, E., Galchev, V., Rose, K., Sinz, M., and Strom, S. C. (2000). The role of

conjugation in hepatotoxicity of troglitazone in human and porcine hepatocyte cultures. *Drug Metab Dispos* **28**, 1192-7.

Lee, J. K., Leslie, E. M., Zamek-Gliszczynski, M. J., and Brouwer, K. L. (2008). Modulation of trabectedin (ET-743) hepatobiliary disposition by multidrug resistance-associated proteins (Mrps) may prevent hepatotoxicity. *Toxicol Appl Pharmacol* **228**, 17-23.

Lee, J. K., Marion, T., Abe, K., Lim, C., Pollack, G. M., and Brouwer, K. L. (2009). Hepatobiliary disposition of troglitazone and metabolites in rat and human sandwich-cultured hepatocytes: use of Monte Carlo simulations to assess the impact of changes in biliary excretion on troglitazone sulfate accumulation. *J Pharmacol Exp Ther* **332**, 26-34.

Loe, D. W., Almquist, K. C., Deeley, R. G., and Cole, S. P. (1996). Multidrug resistance protein (MRP)-mediated transport of leukotriene C4 and chemotherapeutic agents in membrane vesicles. Demonstration of glutathione-dependent vincristine transport. *J Biol Chem* **271**, 9675-82.

Loi, C. M., Alvey, C. W., Vassos, A. B., Randinitis, E. J., Sedman, A. J., and Koup, J. R. (1999a). Steady-state pharmacokinetics and dose proportionality of troglitazone and its metabolites. *J Clin Pharmacol* **39**, 920-6.

Loi, C. M., Randinitis, E. J., Vassos, A. B., Kazierad, D. J., Koup, J. R., and Sedman, A. J. (1997). Lack of effect of type II diabetes on the pharmacokinetics of troglitazone in a multiple-dose study. *J Clin Pharmacol* **37**, 1114-20.

Loi, C. M., Young, M., Randinitis, E., Vassos, A., and Koup, J. R. (1999b). Clinical pharmacokinetics of troglitazone. *Clin Pharmacokinet* **37**, 91-104.

Marion, T. L., Leslie, E. M., and Brouwer, K. L. (2007). Use of sandwich-cultured hepatocytes to evaluate impaired bile acid transport as a mechanism of drug-induced hepatotoxicity. *Mol Pharm* **4**, 911-8.

Mennone, A., Soroka, C. J., Cai, S. Y., Harry, K., Adachi, M., Hagey, L., Schuetz, J. D., and Boyer, J. L. (2006). Mrp4<sup>-/-</sup> mice have an impaired cytoprotective response in obstructive cholestasis. *Hepatology* **43**, 1013-21.

Okumura, H., Katoh, M., Minami, K., Nakajima, M., and Yokoi, T. (2007). Change of drug excretory pathway by CCl<sub>4</sub>-induced liver dysfunction in rat. *Biochem Pharmacol* **74**, 488-95.

Parke-Davis. (1998). *Rezulin (troglitazone) package insert*, Morris Plains, NJ.

Rius, M., Nies, A. T., Hummel-Eisenbeiss, J., Jedlitschky, G., and Keppler, D. (2003). Cotransport of reduced glutathione with bile salts by MRP4 (ABCC4) localized to the basolateral hepatocyte membrane. *Hepatology* **38**, 374-84.

Saha, S., New, L. S., Ho, H. K., Chui, W. K., and Chan, E. C. (2010). Direct toxicity effects of sulfo-conjugated troglitazone on human hepatocytes. *Toxicol Lett* **195**, 135-41.

Schuetz, E. G., Strom, S., Yasuda, K., Lecureur, V., Assem, M., Brimer, C., Lamba, J., Kim, R. B., Ramachandran, V., Komoroski, B. J., Venkataramanan, R., Cai, H., Sinal, C. J., Gonzalez, F. J., and Schuetz, J. D. (2001). Disrupted bile acid homeostasis reveals an unexpected interaction among nuclear hormone receptors, transporters, and cytochrome P450. *J Biol Chem* **276**, 39411-8.

van Aubel, R. A., Smeets, P. H., Peters, J. G., Bindels, R. J., and Russel, F. G. (2002). The MRP4/ABCC4 gene encodes a novel apical organic anion transporter in human kidney proximal tubules: putative efflux pump for urinary cAMP and cGMP. *J Am Soc Nephrol* **13**, 595-603.

Watanabe, Y., Nakajima, M., and Yokoi, T. (2002). Troglitazone glucuronidation in human liver and intestine microsomes: high catalytic activity of UGT1A8 and UGT1A10. *Drug Metab Dispos* **30**, 1462-9.

Wielinga, P. R., Reid, G., Challa, E. E., van der Heijden, I., van Deemter, L., de Haas, M., Mol, C., Kuil, A. J., Groeneveld, E., Schuetz, J. D., Brouwer, C., De Abreu, R. A., Wijnholds, J., Beijnen, J. H., and Borst, P. (2002). Thiopurine metabolism and identification of the thiopurine metabolites transported by MRP4 and MRP5 overexpressed in human embryonic kidney cells. *Mol Pharmacol* **62**, 1321-31.

Yamamoto, Y., Nakajima, M., Yamazaki, H., and Yokoi, T. (2001). Cytotoxicity and apoptosis produced by troglitazone in human hepatoma cells. *Life Sci* **70**, 471-82.

Yamazaki, H., Shibata, A., Suzuki, M., Nakajima, M., Shimada, N., Guengerich, F. P., and Yokoi, T. (1999). Oxidation of troglitazone to a quinone-type metabolite

catalyzed by cytochrome P-450 2C8 and P-450 3A4 in human liver microsomes. *Drug Metab Dispos* **27**, 1260-6.

Yoshigae, Y., Konno, K., Takasaki, W., and Ikeda, T. (2000). Characterization of UDP-glucuronosyltransferases (UGTS) involved in the metabolism of troglitazone in rats and humans. *J Toxicol Sci* **25**, 433-41.

Zelcer, N., Reid, G., Wielinga, P., Kuil, A., van der Heijden, I., Schuetz, J. D., and Borst, P. (2003). Steroid and bile acid conjugates are substrates of human multidrug-resistance protein (MRP) 4 (ATP-binding cassette C4). *Biochem J* **371**, 361-7.

Zelcer, N., van de Wetering, K., de Waart, R., Scheffer, G. L., Marschall, H. U., Wielinga, P. R., Kuil, A., Kunne, C., Smith, A., van der Valk, M., Wijnholds, J., Elferink, R. O., and Borst, P. (2006). Mice lacking Mrp3 (Abcc3) have normal bile salt transport, but altered hepatic transport of endogenous glucuronides. *J Hepatol* **44**, 768-75.

Zollner, G., Fickert, P., Silbert, D., Fuchsbichler, A., Marschall, H. U., Zatloukal, K., Denk, H., and Trauner, M. (2003). Adaptive changes in hepatobiliary transporter expression in primary biliary cirrhosis. *J Hepatol* **38**, 717-27.

## **CHAPTER 5**

### **Conclusions and Future Directions**

## Conclusions

Despite over a decade's worth of research following the removal of TRO from the market in 2000, the precise cause of TRO-mediated hepatotoxicity remains unclear. Numerous mechanisms have been proposed, including (i) induction of mitochondrial permeability transition, (ii) induction of apoptosis, (iii) biotransformation to reactive intermediates leading to depletion of GSH, covalent binding to cellular macromolecules, or oxidative stress, and (iv) inhibition of BA transport (reviewed in Yokoi 2010). While there are many potential mechanisms of toxicity, it is not clear why some patients suffered severe hepatotoxicity, while the majority of patients taking TRO did not exhibit impaired liver function. Because numerous drugs and compounds in development inhibit BA transport, the lack of a clear understanding about the relationship between impaired BA transport and drug-induced liver injury, coupled with the lack of predictive models, present a major challenge in the development of drugs with minimal potential for idiosyncratic hepatotoxicity.

Preclinical models were unsuccessful in predicting the hepatotoxic potential of TRO. A key strategy to avoid this pitfall is to develop robust, in vitro, preferably high-throughput methods to identify compounds like TRO early in the development process, and even predict, based on structure-activity relationships, molecular structures that may be transport protein inhibitors before further development. The potential for this type of structure-activity relationship screening to predict inhibitors of BSEP already has been demonstrated (Saito *et al.* 2009). This approach is necessary to prevent development of potentially hepatotoxic compounds until the molecular mechanisms of BA transport inhibition and compensatory BA transport

mechanisms are clarified, and an understanding of individual susceptibility is elucidated. Until it is clear how impaired BA transport by xenobiotics differentially affects individuals based on genotype or phenotype, disease state, concomitant drug use, or other factors, the most conservative approach is to identify and remove these compounds from the development pipeline before they advance into clinical trials.

The goals of this dissertation work were to examine the effect of TRO on the hepatobiliary disposition of individual BAs, to determine the effect of TRO on intracellular BA composition and accumulation, and to elucidate the contribution of the basolateral efflux protein MRP4/Mrp4 to the intracellular accumulation of BAs. A number of model systems were employed to carry out this work, including primary rat and human SCH, suspended rat and human hepatocytes, and inside-out plasma membrane vesicles from MRP4-overexpressing HEK293 cells. In addition, discussion of preliminary experiments utilizing siRNA-mediated knockdown of Mrp4 protein in rat SCH is included in **Future Directions**.

It was initially hypothesized that species differences in hepatic transport protein inhibition following TRO exposure could account for the hepatotoxicity observed in humans but not in rats, such that more potent inhibition of BA transport proteins in human hepatocytes cause intracellular accumulation of BAs that is not observed in rat hepatocytes. While experiments in human SCH and suspended hepatocytes demonstrated that 10  $\mu$ M TRO inhibited both the uptake and biliary efflux of [ $^3$ H]TCA, intracellular accumulation of [ $^3$ H]TCA was not observed in either species (see **Appendix A**). An additional species difference between rats and humans is the composition of the respective BA pools. In rats, TCA is the

predominant BA, comprising nearly 50% of the BA pool; TCA is also the least cytotoxic of the primary BAs. In contrast, TCA makes up <10% of the BA pool in humans, whereas CDCA and its glycine and taurine conjugates are the most abundant BAs, and are also the most cytotoxic of the primary BAs. This led to the hypothesis that more cytotoxic BAs may accumulate within hepatocytes following acute TRO exposure because of differences in the affinity of individual BAs for transport proteins.

**Differential Inhibition of BA Transport by TRO.** The goal of Specific Aim 1 (**Chapter 2**) was to demonstrate that TRO differentially affects the intracellular accumulation of BAs, leading to the accumulation of more cytotoxic BAs, such as CDCA, compared to TCA. In contrast to [<sup>3</sup>H]TCA, TRO significantly increased intracellular accumulation of [<sup>14</sup>C]CDCA species in rat SCH. TRO inhibited the accumulation of [<sup>14</sup>C]CDCA less than [<sup>3</sup>H]TCA because [<sup>14</sup>C]CDCA uptake is primarily Na<sup>+</sup>-independent, while TRO had a greater inhibitory effect on Na<sup>+</sup>-dependent Ntcp function. Studies in suspended rat hepatocytes confirmed that uptake of [<sup>14</sup>C]CDCA was primarily Na<sup>+</sup>-independent, whereas uptake of [<sup>3</sup>H]TCA was primarily Na<sup>+</sup>-dependent, and determined that TRO exhibited a greater inhibitory effect on [<sup>3</sup>H]TCA uptake than [<sup>14</sup>C]CDCA uptake. Therefore, it appears that greater inhibition of [<sup>3</sup>H]TCA uptake precludes its intracellular accumulation.

These results are significant for a number of reasons. First, TCA is the most commonly used BA for transport studies, yet these results clearly indicated that TRO affects individual BAs differently. If screens for inhibitors of BA transport only include one BA substrate (*i.e.*, TCA), then the potential to miss important interactions, such

as the accumulation of CDCA, is obvious. In a comparison of GCA and TCA as model substrates for BA uptake and accumulation in rat and human SCH, Diebert *et al.* reported marked species differences in the accumulation and  $Cl_{bile}$  of GCA and TCA, while the BEIs were very similar; these authors concluded that GCA was the preferable substrate in human whereas TCA was more appropriate for rat SCH (Diebert *et al.* 2010). Second, these results suggest that CDCA and its glycine and taurine conjugates may accumulate in human liver following treatment with TRO. This is supported by the observations that, following extrahepatic biliary obstruction, concentrations of CDCA in human liver increase 20-fold (Greim *et al.* 1973), and that GCDCA is missing from the bile of primary sclerosing cholangitis patients with chronic cholestasis (Ijare *et al.* 2008). Intrahepatic accumulation of CDCA species in humans following TRO treatment would explain the cholestatic-type liver injury in some patients, but since not all patients exhibited cholestasis, then some other mechanism may have been involved, such as impaired compensatory basolateral BA efflux. The concentration of TRO at which significant intracellular accumulation of CDCA was observed (100  $\mu$ M) is higher than the maximum plasma concentrations observed in humans of 3.6-6.3  $\mu$ M (Loi *et al.* 1999); however, the concentration of TRO in the liver has not been determined. Based on estimates by Lee *et al.*, the intracellular concentration in human SCH of TRO and TS following incubation with 10  $\mu$ M TRO reached 49.4-84.7 $\mu$ M and 136-160  $\mu$ M, respectively (Lee *et al.* 2009).

**Effect of TRO on Bile Acid Profiles in Rat and Human SCH.** The experiments in Specific Aim 1 were acute in nature and investigated the disposition of an externally added BA. Hepatocytes continue to synthesize BAs in culture (Dunn

*et al.* 1991), so the goal of Specific Aim 2 (**Chapter 3**) was to characterize the composition and size of the endogenous BA pool in medium, cells, and bile of rat and human SCH following a 24-h exposure to TRO. As detailed in **Chapter 2**, TRO caused the acute accumulation of CDCA and its metabolites, but not of TCA in rat hepatocytes. Based on this finding, it was hypothesized that 24-h exposure to TRO would cause the accumulation of BAs within the hepatocyte, and that CDCA species would accumulate to a greater extent than CA species. Results indicated that in human SCH, TRO had no effect on GCA biliary excretion but decreased the biliary excretion of TCA 43%, TCDCA 67%, and GCDCA 48%; this supported the hypothesis that inhibition of BA transport proteins can differentially affect individual BA species. However, contrary to expectations, there was a trend toward *decreased* accumulation of all the BAs in the cells and bile of human SCH treated with TRO, and the total mass of BAs measured in TRO-treated human SCH was ~19% lower than in control cells. One potential explanation for this finding is that TRO treatment may have decreased BA synthesis in the human hepatocytes, perhaps as an adaptive mechanism, leading to less BA accumulation. Another possible explanation is that BAs and metabolites of TRO [predominantly TS according to (Lee *et al.* 2009)] are excreted back into the culture medium by basolateral efflux transport proteins such as MRP4/Mrp4, and TRO- or TS-mediated inhibition of NTCP/Ntcp and OATPs/Oatps prevented the reuptake of these compounds into the hepatocytes.

Data from **Chapter 2** indicated that unconjugated CDCA, as well as CDCA conjugated to glycine and taurine, accumulated within cells following acute incubation with TRO. Unconjugated CDCA was not added to SCH in experiments

that examined the effect of 24-h TRO exposure on BA disposition, and no endogenous unconjugated CDCA was detected. This finding was expected, because >98% of BAs are conjugated within hepatocytes, and unconjugated BAs returning to hepatocytes from the portal circulation originate from bacteria-mediated deconjugation of BAs in the intestines. It is important to note that in the SCH model, there is no supply of secondary or unconjugated BAs (e.g., DCA, LCA, CDCA) returning to the hepatocytes from the intestines like there is in the in vivo situation, so unless they are added exogenously, the BAs present in the SCH system are primary BAs synthesized from within the hepatocytes. Results from the BA profiling studies suggested that, despite the acute accumulation of CDCA species observed following TRO exposure, all the *endogenous*, synthesized CDCA is conjugated to glycine or taurine (predominantly glycine, in these studies) during longer TRO incubation periods, and can be effluxed back across the basolateral membrane or excreted into bile.

Even though TRO did not cause the intracellular accumulation of BAs over a 24-h incubation, the BA composition in control rat SCH was similar to in vivo reports, while BA composition in human SCH contained a higher proportion of glycine-conjugated BAs. Based on the literature, BAs in rat plasma and bile are ~94-98% conjugated to taurine and the remainder to glycine, while in humans, ~75% of BAs in plasma and bile are conjugated to glycine and ~25% to taurine (Alvaro *et al.* 1986; Byrne *et al.* 2002; Mizuta *et al.* 1999; Tagliacozzi *et al.* 2003). In the present studies, ~90% of BAs in rat SCH were taurine-conjugated, which is consistent with the literature. In human SCH, 99% of BAs were glycine-conjugated, ~24% higher than

what has been reported. One explanation could be depletion of available taurine over time in culture; hepatic taurine concentrations are a major determinant of the proportion of BAs conjugated with taurine versus glycine (Gottfries *et al.* 1966; Hardison and Proffitt 1977). While both rat and human SCH were exposed to the same culture conditions, rat hepatocytes were treated on day 3 and collected on day 4, while human SCH were treated on day 6 and collected on day 7 to allow time for bile canaliculi formation.

The concentrations of total BAs in the medium of rat SCH were comparable to published concentrations in conventionally-cultured hepatocytes (Ellis *et al.* 1998) and SCH (Dunn *et al.* 1991). BA concentrations in the medium of human SCH also were in good agreement with published values for conventionally-cultured human hepatocytes (Ellis *et al.* 1998) and for human plasma (Ahlberg *et al.* 1977; Tagliacozzi *et al.* 2003). The intracellular concentration of total BAs in rat and human SCH were also in agreement with published estimates of hepatocyte concentrations *in vivo* (Blitzer and Boyer 1982; Hofmann 1999). The variability in BA concentrations in hepatocytes from individual human subjects may be due to differing capacities for BA synthesis based on underlying genetic factors, disease states of donor tissue, or liver exposure to drugs/xenobiotics prior to tissue collection.

**TS-Mediated Inhibition of MRP4.** The goal of Specific Aim 3 (**Chapter 4**) was to determine whether TS inhibits BA transport mediated by MRP4, in order to test the hypothesis that TS interferes with compensatory basolateral BA excretion. MRP4 protein is normally expressed at low levels in hepatocytes, but is induced during cholestasis in humans (Gradhand *et al.* 2008), and also in mice (Mennone *et*

*al.* 2006) and rats (Denk *et al.* 2004), presumably as an adaptive response mechanism to compensate for increased intracellular concentrations of BAs. BAs may accumulate within hepatocytes if basolateral and biliary excretion are impaired by TS. Membrane vesicles were prepared from untransfected (CTL) or transfected HEK293 cells overexpressing MRP4 protein. MRP4-mediated uptake of [<sup>3</sup>H]TCA was measured in the presence of increasing concentrations of TS to determine whether they inhibit BA transport. Results suggested that TS inhibited MRP4-mediated [<sup>3</sup>H]TCA transport in a concentration-dependent manner. However, one caveat with these experiments was that the high level of substrate transport by the untransfected control membrane vesicles from HEK293 cells confounded interpretation of the data. An endogenous protein present in HEK293 cells may be capable of transporting TCA. MRP3 protein was not expressed in these parent cells, and past studies have demonstrated that OATP1B1 (Kameyama *et al.* 2005) and OATP2B1 (Sai *et al.* 2006) mRNA were not detected by RT-PCR in HEK293 cells. Transport proteins normally expressed in human kidney (from which the HEK293 cell line is derived), such as MATEs (multidrug and toxic compound extrusion proteins) and OATs (organic anion transporters) may be involved, but the high expression of MRP4 protein in these membrane vesicles implicates MRP4 as the likely protein responsible. As of this writing, further efforts in our laboratory have resulted in the generation of stably-transfected, MRP4-overexpressing HEK293T cells along with mock-transfected control cells that exhibit low background MRP4 transport. Preliminary data (not shown) show robust uptake of the MRP4 substrate E<sub>2</sub>-17βG in membrane vesicles from the stably MRP4-overexpressing cells, while

uptake is minimal in membrane vesicles from the mock-transfected control cells. Use of this more specific model system to confirm that TS inhibits MRP4-mediated transport is the focus of ongoing studies, but is beyond the scope of this dissertation project.

**Consequences of Impaired MRP4 Function.** Data from Specific Aim 3 indicated that TS is a substrate for MRP4; therefore, interindividual differences in MRP4 function may cause intracellular accumulation of TS, which is a potent BSEP inhibitor, and further exacerbate BA accumulation and hepatotoxicity. Furthermore, if TS potentially inhibits MRP4-mediated BA efflux, then the intracellular accumulation of BAs may be even greater than anticipated due to BSEP inhibition alone. Most patients who were administered TRO did not experience idiosyncratic hepatotoxicity, which suggests that even if TS inhibits MRP4-mediated BA transport, there must be a compensatory mechanism by which TS-mediated MRP4 inhibition is overcome, perhaps upregulation of MRP4 mRNA and protein, increased MRP4 protein trafficking to the basolateral membrane, or upregulation of other transport proteins, *i.e.*, MRP3, or OST $\alpha/\beta$ , or increased biliary efflux of TS by BCRP. In the event that an individual could not compensate for impaired MRP4 function, however, accumulation of BAs may occur and contribute to cytotoxicity.

**Key Conclusions.** Overall, this dissertation research has made a number of novel contributions to the field. TRO caused significant intracellular accumulation of [ $^{14}\text{C}$ ]CDCA species in rat SCH. Studies in suspended rat hepatocytes revealed that TRO exhibited a greater inhibitory effect on [ $^3\text{H}$ ]TCA uptake than [ $^{14}\text{C}$ ]CDCA uptake. This differential effect of TRO on the uptake and accumulation of individual BAs

supports the hypothesis that TRO shifts the intracellular BA pool toward more toxic species. The SCH model reflected reasonably well the composition of the in vivo BA pool in rats and humans. Data from plasma membrane vesicles overexpressing MRP4 suggested that TS, the major metabolite of TRO, is an MRP4 substrate and inhibits TCA transport more potently than TRO. Impaired MRP4 function may predispose patients to increased intracellular concentrations of TS, a potent BSEP inhibitor. Furthermore, in humans, accumulation of TS may inhibit compensatory basolateral BA efflux and increase the intrahepatic accumulation of cytotoxic BAs in susceptible patients. On the other hand, inhibition of BSEP and subsequent intracellular accumulation of BAs may not be cytotoxic if cells can upregulate MRP4 to compensate. This may explain, in part, the idiosyncratic nature of TRO hepatotoxicity. This research also has important implications for early drug development, because it suggests that preclinical in vitro screens for drug-induced transport inhibition should include multiple BA substrates, not just TCA, in order to fully characterize the effects of a compound on BA homeostasis.

**Future Directions.** Several issues and intriguing questions were raised during this dissertation research that should be explored further:

**Effects of Transport Protein Inhibitors on Disposition of Primary and Secondary BAs in Rat and Human SCH.** Numerous drugs have been shown to inhibit BA transport proteins, including cyclosporin A, bosentan, glyburide, erythromycin estolate, troleandomycin, glibenclamide, rifampin, ritonavir, saquinavir, and efavirenz (Fattinger *et al.* 2001; Funk *et al.* 2001a; Funk *et al.* 2001b;

Kostrubsky *et al.* 2003; McRae *et al.* 2006; Stieger *et al.* 2000). It is not currently known whether differential inhibition of BA transport is unique to TRO, or if it is characteristic of multiple inhibitors; likewise, the effects of TRO or TS on the disposition of other BA substrates are not known. Therefore, the differential inhibition of TCA versus CDCA uptake and accumulation observed in these studies could be extended to include other inhibitors and the primary BAs GCA, TCDCA, and GCDCA. Furthermore, the secondary BAs lithocholic acid (LCA) and deoxycholic acid (DCA) are even more cytotoxic than CDCA or GCDCA. Even though they make up only a small proportion of total BAs (0.5% and 6.8%, respectively) (Tagliacozzi *et al.* 2003), the effects of TRO and TS on these BAs should be investigated as well. Because the BA pool differs between rats and humans, the use of human SCH could reveal species differences regarding the effects of transport protein inhibitors on individual BAs. In addition, the novel finding from this dissertation work that MK571 inhibits BSEP/Bsep-mediated BA transport warrants further characterization using BSEP/Bsep-expressing membrane vesicles.

**BA Profiling and Optimization of Culture Conditions.** Studies from Specific Aim 2 (**Chapter 3**) suggested that further optimization of the SCH model for the purposes of BA profiling may be necessary. First, because enterohepatic cycling is not present in vitro but represents a major source of BAs presented to the hepatocyte for vectorial transport in vivo, one option is to add BAs to the culture medium to more closely replicate the in vivo situation. In humans, ~95-98% of BAs that are excreted into the bile are taken back up in the intestine and are returned to the liver during enterohepatic cycling; only ~2-5% of BAs per day are newly

synthesized. However, in the SCH model, the culture medium is replaced daily; this removes a substantial mass of BAs from the system that are replaced with newly synthesized BAs. It is not known whether this change in concentration gradient affects the vectorial driving force for BA efflux, increasing efflux from the cells, or how this daily flux in BAs affects expression of enzymes related to BA synthesis such as CYP7A1 or CYP8B1. Additionally, nuclear-receptor mediated feedback regulation of BA synthesis, or factors such as available cholesterol may be impacted. It did appear, based on the BA profiling in human SCH, that depletion of taurine may occur over time in culture, thus shifting the conjugation of newly-synthesized BAs to glycine conjugates more so than taurine conjugates. Optimal addition of taurine may restore the balance between glycine and taurine conjugation to ~75%:25%, similar to that reported in the literature (Alvaro *et al.* 1986; Tagliacozzi *et al.* 2003).

#### **Co-cultures of Hepatocytes with Other Cell Types in Sandwich Culture.**

Another possibility is the exploration of sandwich co-cultures of hepatocytes along with Kupffer cells and stellate cells in order to more accurately recreate the in vivo hepatic environment. This is relevant because Campion *et al.* reported that induction of hepatic Mrp4 in mice in vivo following APAP exposure was dependent on Kupffer cell-derived mediators (Campion *et al.* 2008). Therefore, it is possible that, with appropriate culture conditions, the expression and function of MRP4 may be more inducible by potential hepatotoxins such as TRO, yielding new insights as to the role of MRP4 in compensatory BA transport. Also, cytotoxicity of TRO was increased in the human hepatoma cell line Huh-7 when these cells were co-cultured with the

monocytic cell line THP-1, suggesting that inflammatory mediators released by the THP-1 cells may potentiate toxicity (Edling *et al.* 2009). Thus, even though these two cell lines are immortalized, these data suggest that TRO cytotoxicity in primary hepatocytes also may be modulated by co-culture with other hepatic cell types. In a number of studies by Roth *et al.*, bacteria-derived lipopolysaccharides were added to co-cultures of Kupffer cells and hepatocytes along with toxicants in order to create a model of inflammatory stress-mediated idiosyncratic hepatotoxicity (reviewed in Deng *et al.* 2009). The adaptation of this type of model system to SCH may prove to be a useful in vitro system for identifying idiosyncratic hepatotoxins that also affect the disposition of substrates, including BAs.

**MRP4-Overexpressing Membrane Vesicles from Stably Transfected HEK293T Cells.** As discussed previously, the membrane vesicles studies undertaken in this dissertation research (**Chapter 4**) displayed high background expression of MRP4 protein in the untransfected control HEK293 cells. Recently, a stably-transfected HEK293T cell line was developed in our laboratory with high MRP4 substrate transport capabilities in MRP4-overexpressing cells and very low background transport in mock-transfected cells. Experiments in Specific Aim 3 (**Chapter 4**) may be repeated with membrane vesicles from this stably-transfected MRP4-overexpressing cell line to determine whether (a) TS is an MRP4 substrate, (b) CDCA is an MRP4 substrate, and (c) TS inhibits MRP4-mediated BA transport. Additionally, the effect of BAs on MRP4-mediated TS transport should be explored to determine whether BAs inhibit MRP4-mediated TS efflux. Based on the results of BA profiling experiments performed as part of this dissertation (**Chapter 3**), and data

from Lee *et al.*, BAs and TS may reach similar hepatocellular concentrations [a maximum intracellular concentration of nearly 200  $\mu\text{M}$  was estimated for TS in rat SCH (Lee *et al.* 2009), and the same for total intracellular BAs in human SCH in the BA profiling experiments].

**siRNA-Mediated Transport Protein Knockdown.** RNAi remains a potentially powerful tool to elucidate the role of individual transport proteins in substrate transport or toxic effect. The use of synthetic siRNAs to knock down Mrp2 and Mrp3 protein (Tian *et al.* 2004), and adenoviral-vector mediated RNAi to knock down Bcrp (Yue, *et al.*, 2009) in rat SCH has been performed by our laboratory in order to elucidate the function of these transport proteins. Van Aubel *et al.* used siRNA to knock down MRP4 protein in MRP4-overexpressing HEK293/4.63 cells; using this model, it was then demonstrated that the efflux of the endogenous MRP4 substrate urate decreased, and that the increase in intracellular urate inhibited transport of methotrexate, an exogenous MRP4 substrate (Van Aubel *et al.*, 2005). Pilot experiments (not shown) were designed and conducted to test the hypothesis that impaired Mrp4 function increases hepatocellular accumulation of BAs and increases TRO cytotoxicity. An adenoviral vector expressing an siRNA designed to knock down Mrp4 protein in rat SCH was generated. Accumulation of exogenous [ $^3\text{H}$ ]TCA and [ $^{14}\text{C}$ ]CDCA was measured in rat SCH treated with an adenoviral vector expressing a non-targeting control siRNA or an siRNA targeting Mrp4, with or without exposure to TRO or MK571. Mrp4 protein was successfully knocked down using this approach, and BA transport clearly was affected by siRNA treatment. However, interpretation of the data was confounded by off-target effects, which may

have been caused by adenoviral vector infection of SCH at too high an MOI. To that end, optimization of siRNA-mediated Mrp4 knockdown for more specific knockdown without off-target effects is another logical direction of this research.

These future directions share a common goal of optimizing the available in vitro models to most accurately reflect the in vivo hepatic environment. In this way, continued exploration of the role of endogenous BAs in drug-induced hepatotoxicity, as well as the function of compensatory efflux proteins in the response to hepatotoxicants, may reveal important interactions that could lead to improved screening techniques for new drug candidates.

## REFERENCES

- Ahlberg, J., Angelin, B., Bjorkhem, I., and Einarsson, K. (1977). Individual bile acids in portal venous and systemic blood serum of fasting man. *Gastroenterology* **73**, 1377-82.
- Alvaro, D., Cantafora, A., Attili, A. F., Ginanni Corradini, S., De Luca, C., Minervini, G., Di Biase, A., and Angelico, M. (1986). Relationships between bile salts hydrophilicity and phospholipid composition in bile of various animal species. *Comp Biochem Physiol B* **83**, 551-4.
- Blitzer, B. L., and Boyer, J. L. (1982). Cellular mechanisms of bile formation. *Gastroenterology* **82**, 346-57.
- Byrne, J. A., Strautnieks, S. S., Mieli-Vergani, G., Higgins, C. F., Linton, K. J., and Thompson, R. J. (2002). The human bile salt export pump: characterization of substrate specificity and identification of inhibitors. *Gastroenterology* **123**, 1649-58.
- Campion, S. N., Johnson, R., Aleksunes, L. M., Goedken, M. J., van Rooijen, N., Scheffer, G. L., Cherrington, N. J., and Manautou, J. E. (2008). Hepatic Mrp4 induction following acetaminophen exposure is dependent on Kupffer cell function. *Am J Physiol Gastrointest Liver Physiol* **295**, G294-304.
- Deibert, E., Jackson, J., Mitchell, J., Amaral, K., Witek, R., Ferguson, S., and Sahi, J. (2010). Taurocholate or glycocholate – which is the more appropriate substrate for assessing hepatic bile salt transport? In 9th International ISSX Meeting, Istanbul, Turkey.
- Deng, X., Luyendyk, J. P., Ganey, P. E., and Roth, R. A. (2009). Inflammatory stress and idiosyncratic hepatotoxicity: hints from animal models. *Pharmacol Rev* **61**, 262-82.
- Denk, G. U., Soroka, C. J., Takeyama, Y., Chen, W. S., Schuetz, J. D., and Boyer, J. L. (2004). Multidrug resistance-associated protein 4 is up-regulated in liver but down-regulated in kidney in obstructive cholestasis in the rat. *J Hepatol* **40**, 585-91.
- Dunn, J. C., Tompkins, R. G., and Yarmush, M. L. (1991). Long-term in vitro function of adult hepatocytes in a collagen sandwich configuration. *Biotechnol Prog* **7**, 237-45.

Edling, Y., Sivertsson, L. K., Butura, A., Ingelman-Sundberg, M., and Ek, M. (2009). Increased sensitivity for troglitazone-induced cytotoxicity using a human in vitro co-culture model. *Toxicol In Vitro* **23**, 1387-95.

Ellis, E., Goodwin, B., Abrahamsson, A., Liddle, C., Mode, A., Rudling, M., Bjorkhem, I., and Einarsson, C. (1998). Bile acid synthesis in primary cultures of rat and human hepatocytes. *Hepatology* **27**, 615-20.

Fattinger, K., Funk, C., Pantze, M., Weber, C., Reichen, J., Stieger, B., and Meier, P. J. (2001). The endothelin antagonist bosentan inhibits the canalicular bile salt export pump: a potential mechanism for hepatic adverse reactions. *Clin Pharmacol Ther* **69**, 223-31.

Funk, C., Pantze, M., Jehle, L., Ponelle, C., Scheuermann, G., Lazendic, M., and Gasser, R. (2001a). Troglitazone-induced intrahepatic cholestasis by an interference with the hepatobiliary export of bile acids in male and female rats. Correlation with the gender difference in troglitazone sulfate formation and the inhibition of the canalicular bile salt export pump (Bsep) by troglitazone and troglitazone sulfate. *Toxicology* **167**, 83-98.

Funk, C., Ponelle, C., Scheuermann, G., and Pantze, M. (2001b). Cholestatic potential of troglitazone as a possible factor contributing to troglitazone-induced hepatotoxicity: in vivo and in vitro interaction at the canalicular bile salt export pump (Bsep) in the rat. *Mol Pharmacol* **59**, 627-35.

Gottfries, A., Schersten, T., and Ekdahl, P. H. (1966). The capacity of human liver homogenates to synthesize taurocholic and glycocholic acid in vitro. *Scand J Clin Lab Invest* **18**, 643-53.

Gradhand, U., Lang, T., Schaeffeler, E., Glaeser, H., Tegude, H., Klein, K., Fritz, P., Jedlitschky, G., Kroemer, H. K., Bachmakov, I., Anwald, B., Kerb, R., Zanger, U. M., Eichelbaum, M., Schwab, M., and Fromm, M. F. (2008). Variability in human hepatic MRP4 expression: influence of cholestasis and genotype. *Pharmacogenomics J* **8**, 42-52.

Greim, H., Czygan, P., Schaffner, F., and Popper, H. (1973). Determination of bile acids in needle biopsies of human liver. *Biochem Med* **8**, 280-6.

Hardison, W. G., and Proffitt, J. H. (1977). Influence of hepatic taurine concentration on bile acid conjugation with taurine. *Am J Physiol* **232**, E75-9.

Hofmann, A. F. (1999). Bile acids: the good, the bad, and the ugly. *News Physiol Sci* **14**, 24-29.

Ijare, O. B., Bezabeh, T., Albiin, N., Arnelo, U., Bergquist, A., Lindberg, B., and Smith, I. C. (2008). Absence of glycochenodeoxycholic acid (GCDCA) in human bile is an indication of cholestasis: A (1)H MRS study. *NMR Biomed* **22**, 471-9.

Kameyama, Y., Yamashita, K., Kobayashi, K., Hosokawa, M., and Chiba, K. (2005). Functional characterization of SLCO1B1 (OATP-C) variants, SLCO1B1\*5, SLCO1B1\*15 and SLCO1B1\*15+C1007G, by using transient expression systems of HeLa and HEK293 cells. *Pharmacogenet Genomics* **15**, 513-22.

Kostrubsky, V. E., Strom, S. C., Hanson, J., Urda, E., Rose, K., Burliegh, J., Zocharski, P., Cai, H., Sinclair, J. F., and Sahi, J. (2003). Evaluation of hepatotoxic potential of drugs by inhibition of bile-acid transport in cultured primary human hepatocytes and intact rats. *Toxicol Sci* **76**, 220-8.

Lee, J. K., Marion, T., Abe, K., Lim, C., Pollack, G. M., and Brouwer, K. L. (2009). Hepatobiliary Disposition of Troglitazone and Metabolites in Rat and Human Sandwich-Cultured Hepatocytes: Use of Monte Carlo Simulations to Assess the Impact of Changes in Biliary Excretion on Troglitazone Sulfate Accumulation. *J Pharmacol Exp Ther* **332**, 26-34.

Loi, C. M., Young, M., Randinitis, E., Vassos, A., and Koup, J. R. (1999). Clinical pharmacokinetics of troglitazone. *Clin Pharmacokinet* **37**, 91-104.

McRae, M. P., Lowe, C. M., Tian, X., Bourdet, D. L., Ho, R. H., Leake, B. F., Kim, R. B., Brouwer, K. L. R., and Kashuba, A. D. (2006). Ritonavir, saquinavir, and efavirenz, but not nevirapine, inhibit bile acid transport in human and rat hepatocytes. *J Pharmacol Exp Ther* **318**, 1068-75.

Mennone, A., Soroka, C. J., Cai, S. Y., Harry, K., Adachi, M., Hagey, L., Schuetz, J. D., and Boyer, J. L. (2006). Mrp4<sup>-/-</sup> mice have an impaired cytoprotective response in obstructive cholestasis. *Hepatology* **43**, 1013-21.

Mizuta, K., Kobayashi, E., Uchida, H., Ogino, Y., Fujimura, A., Kawarasaki, H., and Hashizume, K. (1999). Cyclosporine inhibits transport of bile acid in rats: comparison of bile acid composition between liver and bile. *Transplant Proc* **31**, 2755-6.

Sai, Y., Kaneko, Y., Ito, S., Mitsuoka, K., Kato, Y., Tamai, I., Artursson, P., and Tsuji, A. (2006). Predominant contribution of organic anion transporting polypeptide OATP-B (OATP2B1) to apical uptake of estrone-3-sulfate by human intestinal Caco-2 cells. *Drug Metab Dispos* **34**, 1423-31.

Saito, H., Osumi, M., Hirano, H., Shin, W., Nakamura, R., and Ishikawa, T. (2009). Technical pitfalls and improvements for high-speed screening and QSAR analysis to predict inhibitors of the human bile salt export pump (ABCB11/BSEP). *Aaps J* **11**, 581-9.

Stieger, B., Fattinger, K., Madon, J., Kullak-Ublick, G. A., and Meier, P. J. (2000). Drug- and estrogen-induced cholestasis through inhibition of the hepatocellular bile salt export pump (Bsep) of rat liver. *Gastroenterology* **118**, 422-30.

Tagliacozzi, D., Mozzi, A. F., Casetta, B., Bertucci, P., Bernardini, S., Di Ilio, C., Urbani, A., and Federici, G. (2003). Quantitative analysis of bile acids in human plasma by liquid chromatography-electrospray tandem mass spectrometry: a simple and rapid one-step method. *Clin Chem Lab Med* **41**, 1633-41.

Tian, X., Zamek-Gliszczynski, M. J., Zhang, P., and Brouwer, K. L. (2004). Modulation of multidrug resistance-associated protein 2 (Mrp2) and Mrp3 expression and function with small interfering RNA in sandwich-cultured rat hepatocytes. *Mol Pharmacol* **66**, 1004-10.

Van Aubel, R. A., Smeets, P. H., van den Heuvel, J. J., and Russel, F. G. (2005). Human organic anion transporter MRP4 (ABCC4) is an efflux pump for the purine end metabolite urate with multiple allosteric substrate binding sites. *Am J Physiol Renal Physiol* **288**, F327-33.

Yokoi, T. (2010). Troglitazone. *Handb Exp Pharmacol*, 419-35.

Yue, W., Abe, K., and Brouwer, K. L. (2009). Knocking down breast cancer resistance protein (Bcrp) by adenoviral vector-mediated RNA interference (RNAi) in sandwich-cultured rat hepatocytes: a novel tool to assess the contribution of Bcrp to drug biliary excretion. *Mol Pharm* **6**, 134-43.

## **APPENDIX A**

### **Troglitazone-Mediated Inhibition of Taurocholic Acid Transport in Human and Rat Suspended and Sandwich-Cultured Hepatocytes**

Reproduced in part with permission from: Use of Sandwich-Cultured Hepatocytes To Evaluate Impaired Bile Acid Transport as a Mechanism of Drug-Induced Hepatotoxicity. Tracy L. Marion, Elaine M. Leslie, Kim L. R. Brouwer. *Molecular Pharmaceutics* 2007 4 (6), 911-918. Copyright 2007 American Chemical Society.

## Abstract

Drug-induced liver toxicity is a significant problem in drug development and clinical practice, and growing evidence suggests that inhibition of bile acid (BA) transport protein function may be one mechanism of hepatotoxicity. Troglitazone (TRO) is one such drug that caused idiosyncratic hepatotoxicity in humans, but toxicity was not evident in preclinical animal testing. One possible explanation for this is that in humans, but not experimental animal species, TRO causes the intracellular accumulation of BAs in hepatocytes. In vivo and in vitro studies in rats have demonstrated that TRO inhibits BA transport proteins. The goal of this research was to determine how TRO affects in vitro BA transport in human hepatocytes in comparison to rat, in order to test the hypothesis that TRO causes BA accumulation in human, but not rat, hepatocytes. Using sandwich-cultured hepatocytes (SCH) from both species, acute (10-min) intracellular accumulation and biliary excretion of taurocholic acid (TCA) were measured in the presence and absence of TRO. The effects of increasing concentrations of TRO on the basolateral uptake of TCA was examined in suspended human and rat hepatocytes. Results indicated that TRO inhibited both basolateral uptake and canalicular excretion of TCA in a concentration-dependent manner in both human and rat SCH. Uptake of TCA in suspended human hepatocytes was predominantly Na<sup>+</sup>-dependent, whereas uptake in suspended rat hepatocytes involved both Na<sup>+</sup>-dependent and independent mechanisms. Interestingly, TRO inhibited TCA uptake in suspended human hepatocytes more potently (IC<sub>50</sub> = 0.33 μM) than in rat hepatocytes (IC<sub>50</sub> = 1.9 μM). These data suggest that TRO inhibits both BA uptake and excretion in human and

rat hepatocytes. Other factors, such as compensatory basolateral efflux transport protein function or individual BA species, may contribute to TRO-mediated hepatotoxicity in humans.

## Introduction

Drug-induced hepatotoxicity can lead to acute liver failure and even death, and is the most common adverse event leading to the removal of pharmaceuticals from clinical use (Kaplowitz 2001). Idiosyncratic toxicity, or rare hepatotoxic reactions of unknown etiology occurring in a small subset of patients, is a frequent reason for attrition of drug candidates in the development pipeline. Unfortunately, the mechanisms of drug-induced hepatotoxicity are varied and poorly understood, and current models used for safety assessment in drug development do not accurately predict hepatotoxicity in humans. While research into mechanisms of drug-induced hepatotoxicity has focused primarily on the formation of reactive metabolites and cellular damage from stable adduct formation, more recent evidence has led to the hypothesis that inhibition of normal BA transport is another important mechanism of hepatotoxicity (Byrne *et al.* 2002; Fattinger *et al.* 2001; Stieger *et al.* 2000).

Compounds that inhibit one or more of the proteins responsible for BA excretion may cause the intracellular accumulation of BAs in hepatocytes and subsequent toxicity due to detergent effects on cellular membranes, mitochondrial dysfunction, and cellular necrosis (Delzenne *et al.* 1992; Desmet 1995; Gores *et al.* 1998; Pauli-Magnus *et al.* 2005). A number of drugs, including cyclosporin, glibenclamide, rifampin, and troglitazone (TRO), have been shown to inhibit rat Bsep-mediated taurocholic acid (TCA) biliary excretion in vitro (Fattinger *et al.* 2001; Funk *et al.* 2001a; Pauli-Magnus and Meier 2006; Stieger *et al.* 2000). TRO is a peroxisome proliferator-activated receptor gamma (PPAR $\gamma$ ) agonist that was first in a new class of thiazolidinedione antidiabetic agents. TRO was approved by the FDA

in 1997 for the treatment of type II diabetes, but was subsequently withdrawn from the market in 2000 after numerous reports of liver failure. Preclinical toxicological testing of TRO in animals failed to predict this hepatotoxicity, and subsequent research efforts have focused on elucidating the mechanism(s) of TRO-associated hepatotoxicity. While the precise mechanism(s) remain(s) unclear, several hypotheses have been suggested, including metabolism of TRO to electrophilic reactive intermediates, mitochondrial injury and induction of mitochondrial permeability transition, induction of apoptosis, PPAR $\gamma$ -mediated steatosis, and inhibition of BSEP (Masubuchi 2006; Smith 2003).

Recent studies have generated a wealth of data supporting a potential role for altered hepatic transport processes in TRO's hepatotoxicity. TRO decreased bile secretion rates in isolated perfused rat livers (Preininger *et al.* 1999), while both TRO and TRO sulfate (TS), a major metabolite excreted into bile, competitively inhibited rat Bsep in isolated canalicular rat liver plasma membrane vesicles (Funk *et al.* 2001a; Funk *et al.* 2001b). Kostrubsky *et al.* demonstrated that inhibition of TRO sulfation resulted in increased cytotoxicity in human and porcine hepatocyte cultures, presumably due to accumulation of unmetabolized parent compound (Kostrubsky *et al.* 2000). In addition, Kostrubsky *et al.* demonstrated that the biliary excretion of TS and TRO glucuronide (TG) in TR<sup>-</sup> rats was impaired, presumably due to loss of Mrp2 in the case of TG (Kostrubsky *et al.* 2001), and deficient Bcrp in the case of TS (Yue, in press). Kemp *et al.* examined the effect of TRO on BA transport mechanisms in rat SCH (Kemp *et al.* 2005). TRO (10  $\mu$ M) decreased the total accumulation of TCA in cells plus canalicular networks approximately 3-fold;

TRO also significantly decreased the BEI of TCA with an  $IC_{50}$  of  $0.91 \pm 0.12 \mu\text{M}$ . Further investigations in suspensions of freshly isolated rat hepatocytes revealed that  $10 \mu\text{M}$  TRO decreased the initial rate of TCA uptake by ~3-fold.

## Methods

**Chemicals.** TRO was purchased from Biomol (Plymouth Meeting, PA). Taurocholate, dexamethasone, Hanks' balanced salt solution (HBSS), HBSS without calcium chloride, magnesium sulfate, phenol red and sodium bicarbonate, and collagenase (type IV) were purchased from Sigma-Aldrich (St. Louis, MO). Collagenase (type I, class I) was obtained from Worthington Biochemical (Freehold, NJ). [<sup>3</sup>H]TCA (5 ci/mmol; purity > 97%) was purchased from Perkin Elmer (Boston, MA). Dimethyl sulfoxide (DMSO) was purchased from Fisher Scientific (Fairlawn, NJ). Fetal bovine serum (FBS), insulin, and Dulbecco's modified Eagle's medium (DMEM) were purchased from GIBCO (Grand Island, NY). ITS+ Premix (insulin, transferrin, selenium) and BD Matrigel™ Basement Membrane Matrix were purchased from BD Biosciences (Palo Alto, CA). All other chemicals and reagents were of analytical grade and were readily available from commercial sources.

**Hepatocyte Isolation and Culture.** Hepatocytes were isolated from male Wistar rats (220-300 g; Charles River Laboratories, Inc., Raleigh, NC) by a two-step collagenase perfusion method as described previously (Annaert *et al.* 2001; Liu *et al.* 1998). Rats were maintained on a 12-h light/dark cycle with free access to water and rodent chow. Rats were allowed to acclimate for at least 5 days before experimentation. The Institutional Animal Care and Use Committee of the University of North Carolina at Chapel Hill approved all procedures. Human hepatocytes for SCH experiments were isolated by a modification of the above method (Hamilton *et al.* 2001) from freshly resected human liver tissue procured through the Department of Surgery, University of North Carolina at Chapel Hill School of Medicine by

qualified medical staff, with donor consent and with the approval of the UNC Hospitals Ethics Committee. Human hepatocytes used in suspended experiments [Hu274 (48 year-old-female, Caucasian) and Hu299 (43-year-old female, Caucasian)], were obtained from CellzDirect (Pittsboro, NC).

Rat and human hepatocytes were seeded at a density of  $1.5 \times 10^6$  cells per well on 6-well BioCoat™ plates (BD Biosciences, Bedford, MA) in 1.5 ml Dulbecco's modified Eagle's medium containing 5% fetal bovine serum, 10  $\mu$ M insulin, and 1  $\mu$ M dexamethasone. Cells were incubated at 37°C in a humidified incubator and allowed to attach for 2 h (rat) or 3 h (human), at which time the medium was aspirated to remove unattached cells, and medium was replaced. Twenty-four hours later, cells were overlaid with BD Matrigel™ basement membrane matrix at a concentration of 0.25mg/ml in 2 ml ice-cold media containing 1% ITS and 0.1 $\mu$ M dexamethasone. Rat and human hepatocytes were cultured for 3 and 9 more days, respectively, before experimentation to allow maximum formation of canalicular networks between cells; medium was changed daily.

**Transport Studies Using Sandwich-Cultured Primary Rat and Human Hepatocytes.** On day 4 of culture (rat) or day 10 (human), hepatocytes were rinsed 3 times for 20 sec during each rinse with 2 ml per well of warmed Hank's balanced salt solution with or without  $\text{Ca}^{2+}$ . Following the washes, 2 ml of HBSS with or without  $\text{Ca}^{2+}$  was added and cells were incubated at 37°C for 10 min. After incubation, medium was double-aspirated from each well and 1 ml of dosing solution containing HBSS with  $\text{Ca}^{2+}$ , 1  $\mu$ M [ $^3\text{H}$ ]TCA (5  $\mu$ Ci/100 ml), and vehicle (0.1% DMSO) or specified concentrations of TRO was added. Cells were incubated at 37°C for 10

min. After incubation, the dosing solution was aspirated from the cells and uptake was stopped by rinsing cells 3 x with 2 ml ice-cold HBSS with  $\text{Ca}^{2+}$ . After washing, HBSS was aspirated and 1 ml of lysis buffer (Triton X-100 0.5% in phosphate-buffered saline) was added to each well, and plates were shaken for 20 min on a rotary shaker. Aliquots (500  $\mu\text{l}$ ) of sample and 100  $\mu\text{l}$  of dosing solution were collected for quantification of radioactivity, and 500  $\mu\text{l}$  aliquots were reserved for protein quantification. TCA accumulation in collagen-precoated dishes without cells was subtracted to correct for nonspecific binding to the collagen substrate.

### **Transport Studies Using Suspended Primary Rat and Human**

**Hepatocytes.** Isolated hepatocytes were washed twice with ice-cold HBSS modified with 10 mM Tris and 5 mM glucose (+  $\text{Na}^+$  condition) or  $\text{Na}^+$ -free choline buffer (10 mM Tris, 5 mM glucose, 5.4 mM KCl, 1.8 mM  $\text{CaCl}_2$ , 0.9 mM  $\text{MgSO}_4$ , 10 mM HEPES, 137 mM choline). Cells were suspended at  $1 \times 10^6$  cells/ml in the same buffer, placed on ice and used immediately in experiments. Hepatocyte suspensions (4 ml rat; 1 ml human) were pre-incubated at  $37^\circ\text{C}$  for 5 min in bottom-inverted Erlenmeyer flasks (rat) or for 3 min in 16 x 100 mm test tubes (human); vehicle or TRO (0.1-20  $\mu\text{M}$ ) was added followed by [ $^3\text{H}$ ]TCA (1  $\mu\text{M}$ ; 60 nCi/ml). At indicated time points, 200  $\mu\text{l}$  samples were removed, placed in a 0.4 ml polyethylene tube containing a top layer of silicone oil:mineral oil (82:18 v/v) (100  $\mu\text{l}$ ) and a bottom layer of 3 M KOH (50  $\mu\text{l}$ ) and centrifuged. Radioactivity in the cell pellet and supernatant was quantified by liquid scintillation counting. The adherent fluid volume was determined by incubation of cells with [ $^{14}\text{C}$ ]inulin (60 nCi/ml). Protein

concentrations in the incubation mixtures were quantified at the end of each experiment.

**Sample Analysis.** [<sup>3</sup>H]TCA was quantified by liquid scintillation counting using a Packard Minaxi TriCarb scintillation counter (Meriden, CT). Protein concentrations were determined with the BCA (bicinchoninic acid) protein assay kit (Pierce, Rockford, IL) and bovine serum albumin (0.2-2 mg/ml) as a standard using a Bio-Tek FL600 Microplate Fluorescence Reader and KC4 Kineticalc for Windows 2.7 (BioTek Instruments, Inc., Winooski, VT).

**Data Analysis.** The biliary excretion index (BEI), or the fraction of accumulated compound that resides in the bile canaliculi, was calculated using B-CLEAR™ technology (Qualyst, Inc., Research Triangle Park, NC) based on the following equation:

$$\text{BEI} = \left[ \frac{\text{Accumulation}_{\text{cells+bile canaliculi}} - \text{Accumulation}_{\text{cells}}}{\text{Accumulation}_{\text{cells+bile canaliculi}}} \right] \times 100$$

The in vitro biliary clearance ( $Cl_{\text{bile}}$ ) in ml/min/mg protein was calculated using the equation:

$$Cl_{\text{bile}} = \left[ \frac{\text{Accumulation}_{\text{cells+bile canaliculi}} - \text{Accumulation}_{\text{cells}}}{\text{Concentration}_{\text{incubation medium}} \times \text{Incubation time}} \right] \times 100$$

$Cl_{\text{bile}}$  was scaled up to ml/min/kg using 200 mg of protein/g of liver and 40 g of liver/kg of rat body weight (Seglen 1976).

## Results

Results indicated that TRO inhibited TCA uptake and excretion in human SCH, in addition to rat SCH. In agreement with the findings of Kemp *et al.* (2005), in rat SCH, 0.1-10  $\mu\text{M}$  TRO decreased TCA cellular accumulation, and cell + bile accumulation, in a concentration-dependent manner (**Figure A.1**). The BEI of TCA also was reduced from 85.8% to 71.0% at the highest concentration of TRO studied (10  $\mu\text{M}$ ), a reduction of 17.2% compared with the control value, consistent with inhibition of Bsep-mediated TCA excretion into the canalicular lumen. The  $\text{Cl}_{\text{bile}}$  of TCA was reduced in a concentration-dependent manner by TRO, from 38.5 to 33 ml/min/kg at 0.1  $\mu\text{M}$  TRO and to 7.8 ml/min/kg at 10  $\mu\text{M}$  TRO (**Table A.1**). Similar results were observed in human SCH; 1  $\mu\text{M}$  and 10  $\mu\text{M}$  TRO decreased TCA accumulation in cells and cells + bile, as well as the BEI (**Figure A.1**).  $\text{Cl}_{\text{bile}}$  of TCA in human hepatocytes was decreased from 16.8 to 12.6 and 1.9 ml/min/kg, respectively, by 1 and 10  $\mu\text{M}$  TRO (**Table A.1**).

While the SCH model is useful for measuring overall alterations in the hepatobiliary disposition of BAs, and especially for examining alterations in BA excretion, suspended hepatocytes may be preferred for analysis of impaired BA uptake due to the technical ease of determining initial uptake rates. Thus, suspended hepatocytes are a useful tool to further characterize xenobiotic-induced alterations in BA uptake observed in SCH. The effect of TRO on TCA uptake has been assessed previously in rat hepatocytes at a single TRO concentration; TRO significantly inhibited initial TCA uptake (Kemp *et al.* 2005). In the present studies, increasing concentrations of TRO were used to determine concentration-dependent

inhibition of TCA uptake in both rat and human suspended hepatocytes. **Figure A.2** shows the decrease in TCA uptake as a function of TRO concentration in rat and human suspended hepatocytes. The effect of TRO on TCA uptake by rat hepatocytes was assessed in the presence and absence of Na<sup>+</sup> (**Figure A.2A**). Transport in the presence of Na<sup>+</sup> was inhibited more potently (IC<sub>50</sub> = 2.3 μM) than in the absence of Na<sup>+</sup> (IC<sub>50</sub> = 13.3 μM), suggesting that Na<sup>+</sup>-dependent Ntcp is more sensitive to TRO inhibition than the Na<sup>+</sup>-independent Oatps. The overall Na<sup>+</sup>-dependent uptake (*i.e.*, uptake in the presence of Na<sup>+</sup> minus uptake in the absence of Na<sup>+</sup>) of TCA by rat hepatocytes was inhibited potently by TRO (IC<sub>50</sub> = 1.9 μM). Interestingly, TRO was an even more potent inhibitor of Na<sup>+</sup>-dependent TCA uptake in human hepatocytes (IC<sub>50</sub> = 0.33 μM) (**Figure A.2B**). This difference in Ntcp/NTCP inhibition could have implications for species differences in susceptibility to TRO-induced hepatotoxicity (**Figure A.3**).

## Discussion

Inhibition of BA transport protein function, leading to the intracellular accumulation of cytotoxic BAs, has been hypothesized as one mechanism of drug-induced hepatotoxicity (Byrne *et al.* 2002; Fattinger *et al.* 2001; Stieger *et al.* 2000). Inhibition of BA excretion via BSEP may result in BA accumulation within the cell, whereas inhibition of BA uptake would be expected to disrupt BA homeostasis and lead to elevated plasma BA concentrations (**Figure A.3**).

Similar to previous reports in rat SCH (Kemp *et al.* 2005), our results indicated that TRO inhibits both biliary excretion of TCA, as evidenced by decreasing BEI, and basolateral uptake of TCA, as shown by decreased cell accumulation in human SCH;  $Cl_{\text{bile}}$  also was impaired. Overall, the inhibition of both TCA uptake and biliary excretion resulted in a net decrease in intracellular TCA accumulation in both human and rat SCH. This observation is contrary to the original hypothesis that TRO causes the intracellular accumulation of BAs in human hepatocytes but not in rat hepatocytes. However, altered BA homeostasis may play an important role in TRO-mediated hepatotoxicity.

Alterations in bile composition due to decreased intracellular BA content could change the BA:phospholipid ratio of the bile, resulting in supersaturation of bile with cholesterol, the formation of intrahepatic sludge and cholesterol gallstones (Persley and Jain 2000). This may cause a cascade of events that predisposes the liver to cellular injury. In addition, decreased return of BAs from the portal circulation to the hepatocyte leads to increased BA biosynthesis, which is thought to occur because of decreased intracellular BA concentrations; BA synthesis can increase up to 15-fold

under these conditions (Hofmann 1999). TRO-mediated inhibition of NTCP may exacerbate altered BA homeostasis by inducing BA synthesis.

In addition, differences in the BA pool between humans and other animal species may contribute to TRO toxicity. The BA pool in humans is more hydrophobic, with the cytotoxic BA glycochenodeoxycholic acid (GCDCA) comprising 31% of all BAs; in contrast, in rats, more hydrophilic and less cytotoxic TCA constitutes the majority of BAs (Alvaro *et al.* 1986; Tagliacozzi *et al.* 2003). TRO may have a different influence on the hepatic disposition of TCA compared to other BAs such as GCDCA. TRO had a greater effect on Ntcp-mediated TCA uptake in rat SCH; thus, it is possible that BAs that have a high affinity for uptake by the organic anion transporting polypeptides may be less affected by TRO-mediated inhibition of uptake, and may differentially accumulate within cells.

## **Conclusions**

Drug-induced hepatotoxicity is well recognized as a significant but poorly understood issue in drug development. Model systems that can be employed to elucidate factors predisposing patients to drug-induced liver injury, or to determine the hepatotoxic potential of drug candidates, are particularly relevant in current drug development. SCH represent a useful model for examining mechanisms of drug-induced hepatotoxicity. A number of drugs have been shown to impair BA transport using this system. Research from our laboratory demonstrates that TRO, a known hepatotoxin, inhibits BA transport in both human and rat SCH in a concentration-dependent manner. Thus, the SCH model confirms and supplements data from other commonly employed experimental systems such as suspended hepatocytes and membrane vesicles. This model may be an efficient screening tool to identify compounds that alter BA uptake and/or excretion early in drug development. The cellular consequences of such transport modulation may be explored over days in culture in an effort to identify new mechanisms of drug-induced hepatotoxicity.

## **Acknowledgements**

This research was supported by NCI CA106101 and NIH GM41935. EML was the recipient of a postdoctoral fellowship from the Canadian Institutes of Health Research (CIHR). TLM was supported by Curriculum in Toxicology NIH Training Grant T32 ES007126.

TCA Cl <sub>bile</sub> (mL/min/kg)					
TRO	0 μM	0.1 μM	1 μM	5 μM	10 μM
Rat	38.5	33.0	28.1	10.1	7.8
Human	16.8		12.6		1.9

**Table A.1:** Cl<sub>bile</sub> (ml/min/kg) of TCA in sandwich-cultured rat and human hepatocytes with increasing concentrations of TRO.

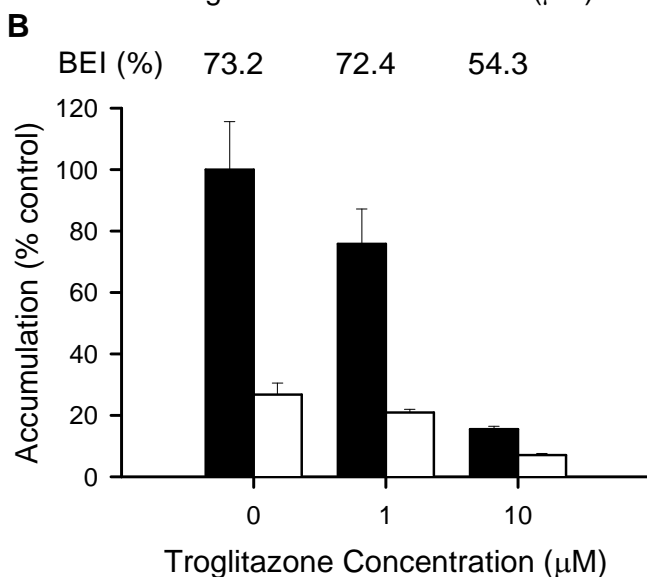
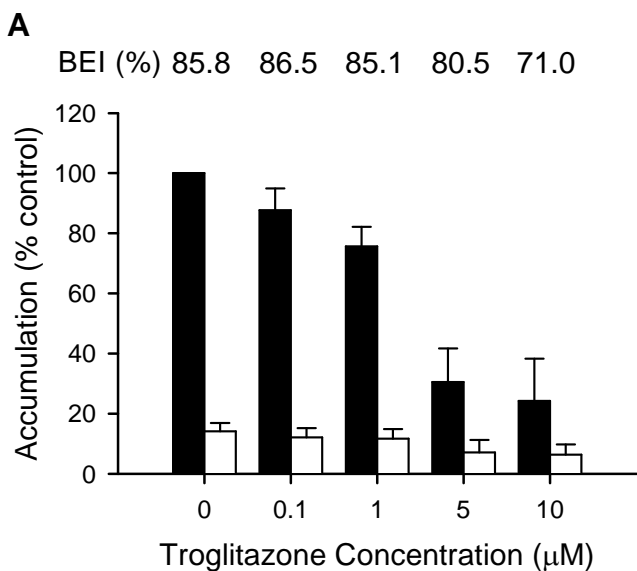


**Figure A.1:** TCA uptake and excretion by sandwich-cultured rat (A) and human (B) hepatocytes in the presence and absence of TRO. On day 4 (rat) or day 10 (human) of culture, hepatocytes were preincubated for 10 min in the presence of  $\text{Ca}^{2+}$  (cells plus bile, solid bars) or absence of  $\text{Ca}^{2+}$  (cells only, white bars), followed by incubation with [ $^3\text{H}$ ]TCA (1  $\mu\text{M}$ ; 60 nCi/ml) in standard buffer at 37°C. [ $^3\text{H}$ ]TCA accumulation by rat hepatocytes and human hepatocytes was measured at 10 min, in the presence of increasing concentrations of TRO. The biliary excretion index (BEI) is defined as the percentage of accumulated substrate residing within the bile

canaliculi. Results in (A) are presented as the mean  $\pm$  SEM of triplicate determinations obtained in 3 independent experiments. Results in (B) are presented as the mean  $\pm$  SD of triplicate determinations in one of two experiments; similar results were observed in the second experiment.

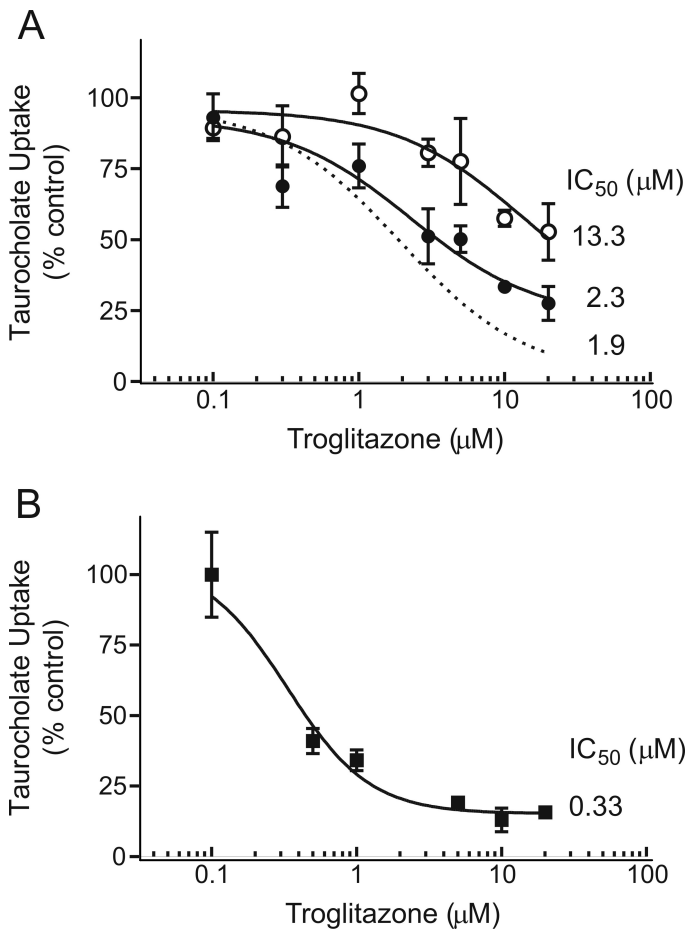


**Figure A.2:** TCA uptake by rat and human primary suspended hepatocytes in the presence and absence of TRO. Freshly isolated hepatocytes were suspended in Na<sup>+</sup>-containing or Na<sup>+</sup>-free/choline-containing HBSS at 1 × 10<sup>6</sup> cells/ml and incubated with [<sup>3</sup>H]TCA (1 μM; 60 nCi/ml) at 37°C. (A) [<sup>3</sup>H]TCA uptake by rat hepatocytes in the presence (●) and absence (○) of Na<sup>+</sup> was measured at 30 s, in the presence of increasing concentrations of TRO. Na<sup>+</sup>-dependent uptake (broken line) was determined by subtracting [<sup>3</sup>H]TCA uptake in the absence of Na<sup>+</sup> from uptake in the presence of Na<sup>+</sup>. Symbols represent mean ± SD obtained in 4 independent experiments, with triplicate determinations in each experiment. (B)

[<sup>3</sup>H]TCA uptake by human hepatocytes was measured at 45 s, in the presence of increasing concentrations of TRO. Na<sup>+</sup>-independent uptake was negligible for these human hepatocyte preparations. Symbols represent mean ± SD of triplicate determinations obtained in one of two experiments (IC<sub>50</sub> for the second experiment was 0.69 μM).

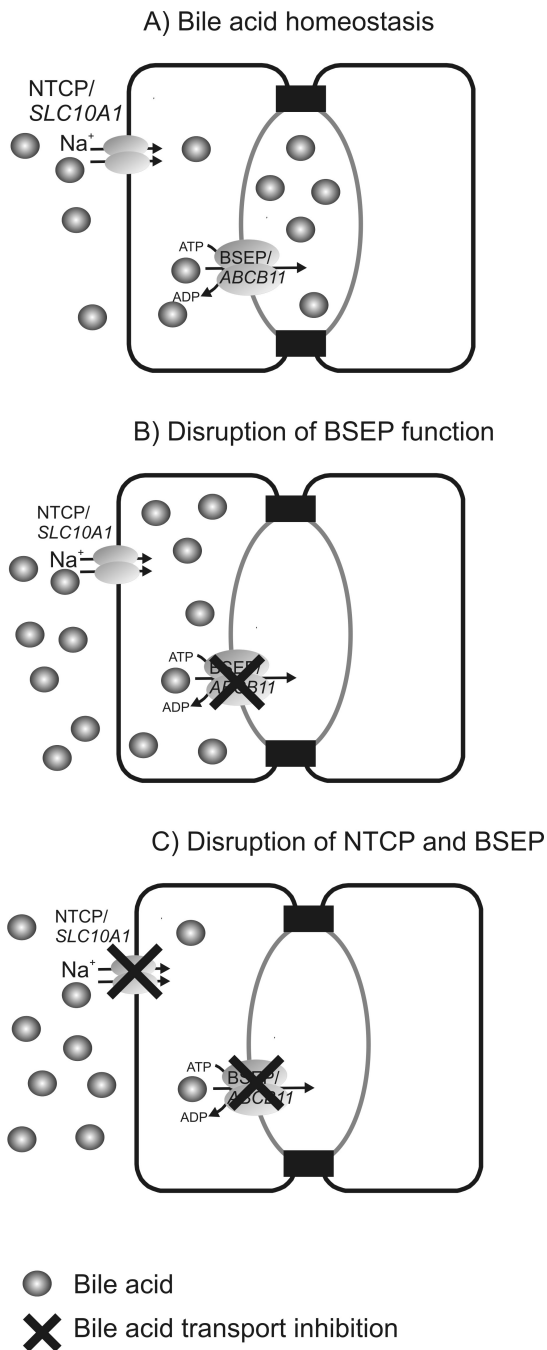


**Figure A.3:** Potential implications of NTCP and BSEP inhibition in plasma, hepatocyte, and bile compartments. (A) NTCP and BSEP-mediated transport of BAs under homeostatic conditions. (B) Disruption of BSEP/Bsep function can result in BA accumulation in the hepatocyte and the plasma. (C) Inhibition of BA basolateral

uptake (NTCP/Ntcp) and canalicular excretion (BSEP/Bsep) may result in less intra-hepatocyte accumulation of BAs. Plasma BA concentrations would increase regardless of whether hepatic BA uptake or excretion is impaired.

## REFERENCES

- Alvaro, D., Cantafora, A., Attili, A. F., Ginanni Corradini, S., De Luca, C., Minervini, G., Di Biase, A., and Angelico, M. (1986). Relationships between bile salts hydrophilicity and phospholipid composition in bile of various animal species. *Comp Biochem Physiol B* **83**, 551-4.
- Annaert, P. P., Turncliff, R. Z., Booth, C. L., Thakker, D. R., and Brouwer, K. L. (2001). P-glycoprotein-mediated in vitro biliary excretion in sandwich-cultured rat hepatocytes. *Drug Metab Dispos* **29**, 1277-83.
- Byrne, J. A., Strautnieks, S. S., Mieli-Vergani, G., Higgins, C. F., Linton, K. J., and Thompson, R. J. (2002). The human bile salt export pump: characterization of substrate specificity and identification of inhibitors. *Gastroenterology* **123**, 1649-58.
- Delzenne, N. M., Calderon, P. B., Taper, H. S., and Roberfroid, M. B. (1992). Comparative hepatotoxicity of cholic acid, deoxycholic acid and lithocholic acid in the rat: in vivo and in vitro studies. *Toxicol Lett* **61**, 291-304.
- Desmet, V. J. (1995). Histopathology of cholestasis. *Verh Dtsch Ges Pathol* **79**, 233-40.
- Fattinger, K., Funk, C., Pantze, M., Weber, C., Reichen, J., Stieger, B., and Meier, P. J. (2001). The endothelin antagonist bosentan inhibits the canalicular bile salt export pump: a potential mechanism for hepatic adverse reactions. *Clin Pharmacol Ther* **69**, 223-31.
- Funk, C., Pantze, M., Jehle, L., Ponelle, C., Scheuermann, G., Lazendic, M., and Gasser, R. (2001a). Troglitazone-induced intrahepatic cholestasis by an interference with the hepatobiliary export of bile acids in male and female rats. Correlation with the gender difference in troglitazone sulfate formation and the inhibition of the canalicular bile salt export pump (Bsep) by troglitazone and troglitazone sulfate. *Toxicology* **167**, 83-98.
- Funk, C., Ponelle, C., Scheuermann, G., and Pantze, M. (2001b). Cholestatic potential of troglitazone as a possible factor contributing to troglitazone-induced hepatotoxicity: in vivo and in vitro interaction at the canalicular bile salt export pump (Bsep) in the rat. *Mol Pharmacol* **59**, 627-35.
- Gores, G. J., Miyoshi, H., Botla, R., Aguilar, H. I., and Bronk, S. F. (1998). Induction of the mitochondrial permeability transition as a mechanism of liver injury during

cholestasis: a potential role for mitochondrial proteases. *Biochim Biophys Acta* **1366**, 167-75.

Hamilton, G. A., Jolley, S. L., Gilbert, D., Coon, D. J., Barros, S., and LeCluyse, E. L. (2001). Regulation of cell morphology and cytochrome P450 expression in human hepatocytes by extracellular matrix and cell-cell interactions. *Cell Tissue Res* **306**, 85-99.

Hofmann, A. F. (1999). Bile Acids: The Good, the Bad, and the Ugly. *News Physiol Sci* **14**, 24-29.

Kaplowitz, N. (2001). Drug-induced liver disorders: implications for drug development and regulation. *Drug Saf* **24**, 483-90.

Kemp, D. C., Zamek-Gliszczynski, M. J., and Brouwer, K. L. (2005). Xenobiotics inhibit hepatic uptake and biliary excretion of taurocholate in rat hepatocytes. *Toxicol Sci* **83**, 207-14.

Kostrubsky, V. E., Sinclair, J. F., Ramachandran, V., Venkataramanan, R., Wen, Y. H., Kindt, E., Galchev, V., Rose, K., Sinz, M., and Strom, S. C. (2000). The role of conjugation in hepatotoxicity of troglitazone in human and porcine hepatocyte cultures. *Drug Metab Dispos* **28**, 1192-7.

Kostrubsky, V. E., Vore, M., Kindt, E., Burliegh, J., Rogers, K., Peter, G., Altrogge, D., and Sinz, M. W. (2001). The effect of troglitazone biliary excretion on metabolite distribution and cholestasis in transporter-deficient rats. *Drug Metab Dispos* **29**, 1561-6.

Liu, X., Brouwer, K. L., Gan, L. S., Brouwer, K. R., Stieger, B., Meier, P. J., Audus, K. L., and LeCluyse, E. L. (1998). Partial maintenance of taurocholate uptake by adult rat hepatocytes cultured in a collagen sandwich configuration. *Pharm Res* **15**, 1533-9.

Masubuchi, Y. (2006). Metabolic and non-metabolic factors determining troglitazone hepatotoxicity: a review. *Drug Metab Pharmacokinet* **21**, 347-56.

Pauli-Magnus, C., and Meier, P. J. (2006). Hepatobiliary transporters and drug-induced cholestasis. *Hepatology* **44**, 778-87.

Pauli-Magnus, C., Stieger, B., Meier, Y., Kullak-Ublick, G. A., and Meier, P. J. (2005). Enterohepatic transport of bile salts and genetics of cholestasis. *J Hepatol* **43**, 342-57.

Persley, K. M., and Jain, R. (2000). Gallstones and Biliary Tract Disease: Gallstone Formation. In 4 Gastroenterology, VI Gallstones and Biliary Tract Disease, ACP Medicine Online (D. Dale and D. Federman, eds.). WebMD Inc., New York.

Preininger, K., Stingl, H., Englisch, R., Furnsinn, C., Graf, J., Waldhausl, W., and Roden, M. (1999). Acute troglitazone action in isolated perfused rat liver. *Br J Pharmacol* **126**, 372-8.

Seglen, P. O. (1976). Preparation of isolated rat liver cells. *Methods Cell Biol* **13**, 29-83.

Smith, M. T. (2003). Mechanisms of troglitazone hepatotoxicity. *Chem Res Toxicol* **16**, 679-87.

Stieger, B., Fattinger, K., Madon, J., Kullak-Ublick, G. A., and Meier, P. J. (2000). Drug- and estrogen-induced cholestasis through inhibition of the hepatocellular bile salt export pump (Bsep) of rat liver. *Gastroenterology* **118**, 422-30.

Tagliacozzi, D., Mozzi, A. F., Casetta, B., Bertucci, P., Bernardini, S., Di Ilio, C., Urbani, A., and Federici, G. (2003). Quantitative analysis of bile acids in human plasma by liquid chromatography-electrospray tandem mass spectrometry: a simple and rapid one-step method. *Clin Chem Lab Med* **41**, 1633-41.

## **APPENDIX B**

### **Data Summary**

pmol/mg protein	cells+bile	cells	SEM cells+bile	SEM cells	BEI (%)	Cl <sub>bile</sub> (ml/min/kg)
CTL	325.0	129.8	8.1	12.4	60.0 ± 9.5	151 ± 26
1 μM TRO	304.7	139.8	23.0	28.0	54.3 ± 12.6	132 ± 33
10 μM TRO	294.7	148.4	12.2	11.5	49.7 ± 6.2	117 ± 16
100 μM TRO	255.7	247.8	25.2	24.2	3.1 ± 0.5	6 ± 2
50 μM MK571	344.9	362.3	17.8	12.7	0.3 ± 0.7	1 ± 2

**Figure 2.1:** Accumulation (mean and SEM; pmol/mg protein), BEI (%), and Cl<sub>bile</sub> (ml/min/kg) of [<sup>14</sup>C]CDCA species in cells + bile and cells in WT rat SCH following a 10-min incubation with 1 μM [<sup>14</sup>C]CDCA and vehicle control (0.1% DMSO; CTL), 1, 10, or 100 μM TRO, or 50 μM MK571.

A	pmol/mg protein	cells+bile	cells	SEM cells+bile	SEM cells	BEI (%)	Cl <sub>bile</sub> (ml/min/kg)
	CTL	325.3	146.0	44.1	24.8	55.7 ± 7.4	140 ± 43
	1 μM TRO	277.6	132.9	27.9	24.9	53.4 ± 8.6	112 ± 5
	10 μM TRO	219.6	118.3	11.9	13.3	46.5 ± 8.8	79 ± 17
	100 μM TRO	230.7	222.2	11.0	13.4	5.9 ± 5.5	11 ± 10
	50 μM MK571	264.0	239.1	16.4	16.0	9.5 ± 1.0	19 ± 0

B	pmol/mg protein	cells+bile	cells	SEM cells+bile	SEM cells	BEI (%)	Cl <sub>bile</sub> (ml/min/kg)
	CTL	38.2	8.1	7.8	2.2	78.8 ± 9.7	24 ± 11
	1 μM TRO	27.8	5.7	5.6	1.7	80.7 ± 4.8	18 ± 6
	10 μM TRO	7.0	2.6	1.8	0.9	65.0 ± 8.4	4 ± 1
	100 μM TRO	5.4	4.1	2.1	1.7	26.1 ± 6.1	1 ± 0
	50 μM MK571	7.5	4.6	2.9	1.6	37.4 ± 6.7	2 ± 2

**Figure 2.2:** Accumulation (mean and SEM; pmol/mg protein), BEI (%), and Cl<sub>bile</sub> (ml/min/kg) of **(A)** [<sup>14</sup>C]CDCA species and **(B)** [<sup>3</sup>H]TCA in cells + bile and cells in TR rat SCH following a 10-min incubation with 1.2 μM [<sup>14</sup>C]CDCA or 1 μM [<sup>3</sup>H]TCA and vehicle control (0.1% DMSO; CTL), 1, 10, or 100 μM TRO, or 50 μM MK571.

pmol/mg protein	cells+bile	cells	SEM cells+bile	SEM cells	BEI (%)	Cl <sub>bile</sub> (ml/min/kg)
CTL	56.5	6.9	10.8	2.1	88.3 ± 2.7	39.6 ± 12.0
10 μM MK571	34.2	11.4	9.1	3.0	66.7 ± 1.7	18.2 ± 8.5
20 μM MK571	23.4	13.3	6.5	3.6	43.1 ± 4.0	8.1 ± 4.1
50 μM MK571	13.4	17.3	3.4	2.0	0.0	0.0

**Figure 2.3:** Accumulation (mean and SEM; pmol/mg protein), BEI (%), and Cl<sub>bile</sub> (ml/min/kg) of [<sup>3</sup>H]TCA in cells + bile and cells in WT rat SCH following a 10-min incubation with 1 μM [<sup>3</sup>H]TCA and vehicle control (0.1% DMSO; CTL), or 10, 20, or 50 μM MK571.

BA Species	Treatment	cells + bile	cells	cells + bile SD	cells SD
CDCA	CTL	0	0	0	0
	Treated	85.6	73.1	7.2	12.8
TCDCA	CTL	34.48	4.40	6.23	1.3
	Treated	185.19	66.77	16.97	6.4
GCDCA	CTL	4.08	1.09	1.43	0.4
	Treated	37.19	15.04	7.13	3.9
TMCA	CTL	310.5	68.9	62.6	22.6
	Treated	353.4	162.3	12.7	47.2
GMCA	CTL	6.1	2.2	1.1	1.0
	Treated	15.1	7.6	3.6	2.5
Total	CTL	355.19	76.65	71.30	25.39
	Treated	676.51	324.77	47.59	72.70

**Figure 2.4:** Parent CDCA and formed CDCA species (taurine- and glycine-conjugated CDCA); TMCA, and GMCA (mean and SD; pmol/mg protein) in cells + bile and cells in WT rat SCH following a 10-min incubation with vehicle CTL (0.1% DMSO; CTL) or 1  $\mu$ M unlabeled CDCA.

CDCA CTL	CTL + Na+	CTL + Na+	CTL + Choline	CTL + Choline	CTL Na+-dep
time	Mean	SEM	Mean	SEM	Mean
15	47.3	1.7	27.7	1.7	19.6
30	81.7	2.1	48.7	3.3	33.0
45	100.0	9.5	64.9	5.2	35.1
CDCA TRO	TRO + Na+	TRO + Na+	TRO + Choline	TRO + Choline	TRO Na+-dep
time	Mean	SEM	Mean	SEM	Mean
15	19.6	5.9	12.1	3.3	7.4
30	32.4	9.7	19.7	5.5	12.8
45	36.9	11.3	23.7	7.5	13.2
CDCA MK571	MK571 + Na+	MK571 + Na+	MK571 + Choline	MK571 + Choline	MK571 Na+-dep
time	Mean	SEM	Mean	SEM	Mean
15	18.9	6.5	13.2	5.0	5.7
30	29.5	10.5	22.3	8.7	7.2
45	37.2	13.3	28.4	11.3	8.9
TCA CTL	CTL + Na+	CTL + Na+	CTL + Choline	CTL + Choline	CTL Na+-dep
time	Mean	SEM	Mean	SEM	Mean
15	41.5	1.8	18.2	6.9	23.4
30	77.2	1.5	26.8	10.4	50.5
45	100.0	9.5	33.6	11.7	66.4
TCA TRO	TRO + Na+	TRO + Na+	TRO + Choline	TRO + Choline	TRO Na+-dep
time	Mean	SEM	Mean	SEM	Mean
15	13.7	6.0	7.5	2.9	6.1
30	16.0	6.0	9.0	3.6	7.1
45	18.3	7.1	9.6	3.5	8.7
TCA MK571	MK571 + Na+	MK571 + Na+	MK571 + Choline	MK571 + Choline	MK571 Na+-dep
time	Mean	SEM	Mean	SEM	Mean
15	10.2	4.6	5.3	2.6	4.9
30	12.9	5.6	7.5	4.2	5.4
45	14.8	6.3	7.7	4.1	7.1

**Figure 2.5:** Accumulation (mean and SEM; % control) of CDCA or TCA at 15, 30, and 45 s in suspended rat hepatocytes in the presence of 1  $\mu\text{M}$  [ $^{14}\text{C}$ ]CDCA or 1  $\mu\text{M}$  [ $^3\text{H}$ ]TCA, and vehicle (0.3% DMSO; CTL), 10  $\mu\text{M}$  TRO, or 50  $\mu\text{M}$  MK571. Total accumulation ( $\text{Na}^+$ -dependent and independent) was measured in  $\text{Na}^+$ -containing buffer (+ $\text{Na}^+$ ).  $\text{Na}^+$ -independent uptake was measured in choline-containing buffer (+Choline).  $\text{Na}^+$ -dependent uptake ( $\text{Na}^+$ -dep) was calculated by subtracting  $\text{Na}^+$ -independent accumulation from total accumulation.

pmol/mg protein		cells + bile	cells	medium	cells + bile range	cells range	medium SD
SUM	day 1	106.8	85.0	468.6	1.4	11.3	66.1
	day 2	27.9	25.7	478.4	0.6	3.1	88.4
	day 3	43.4	20.5	1222.2	24.9	9.7	128.6
	day 4	37.7	16.7	1466.6	21.3	8.2	187.8

**Figure 3.1:** Total accumulation (mean and range or SD; pmol/mg protein) of the sum of all BAs measured in cells + bile, cells, and medium in rat SCH over days 1 through 4 of culture.

TCA	cells + bile	cells	medium	cells + bile SEM	cells SEM	medium range or SD
Rat CTL	16.3	5.5	419.4	5.1	1.0	185.8
Rat 10 $\mu$ M TRO	16.5	5.9	442.1	3.3	0.9	236.2
Human CTL	5.3	3.0	21.6	3.1	1.4	9.6
Human 10 $\mu$ M TRO	2.5	1.4	18.1	1.3	1.1	7.7

**Figure 3.2:** Accumulation (mean and SEM, range, or SD; pmol/mg protein) of TCA in cells + bile, cells, and medium in rat and human SCH following 24-h treatment with vehicle (0.1% DMSO; CTL) or 10  $\mu$ M TRO.

GCA	cells + bile	cells	medium	cells + bile SEM	cells SEM	medium range or SD
Rat CTL	0.6	0.2	48.7	0.3	0.1	36.3
Rat 10 $\mu$ M TRO	0.7	0.4	51.2	0.5	0.1	41.6
Human CTL	1030.2	594.4	3901.0	840.9	482.9	2265.0
Human 10 $\mu$ M TRO	445.1	244.9	3892.5	346.7	202.9	2495.9

**Figure 3.3:** Accumulation (mean and SEM, range, or SD; pmol/mg protein) of GCA in cells + bile, cells, and medium in rat and human SCH following 24-h treatment with vehicle (0.1% DMSO; CTL) or 10  $\mu$ M TRO.

TCDCA	cells + bile	cells	medium	cells + bile SEM	cells SEM	medium range or SD
Rat CTL	17.0	12.3	90.1	7.9	7.6	81.4
Rat 10 $\mu$ M TRO	12.5	9.6	83.9	5.0	5.1	73.4
Human CTL	6.6	5.0	5.1	1.9	1.2	2.9
Human 10 $\mu$ M TRO	3.5	3.3	6.6	0.2	0.5	1.1

**Figure 3.4:** Accumulation (mean and SEM, range, or SD; pmol/mg protein) of TCDCA in cells + bile, cells, and medium in rat and human SCH following 24-h treatment with vehicle (0.1% DMSO; CTL) or 10  $\mu$ M TRO.

GCDCA	cells + bile	cells	medium	cells + bile SEM	cells SEM	medium range or SD
Rat CTL	2.8	1.7	50.2	0.5	0.8	16.8
Rat 10 $\mu$ M TRO	2.2	1.6	40.2	0.3	0.4	7.0
Human CTL	1075.6	781.8	1485.8	980.9	685.7	1022.8
Human 10 $\mu$ M TRO	556.9	478.6	1177.0	528.5	470.4	653.1

**Figure 3.5:** Accumulation (mean and SEM, range, or SD; pmol/mg protein) of GCDCA in cells + bile, cells, and medium in rat and human SCH following 24-h treatment with vehicle (0.1% DMSO; CTL) or 10  $\mu$ M TRO.

SUM OF ALL	cells + bile	cells	medium	cells + bile SEM	cells SEM	medium range or SD
Rat CTL	33.3	18.0	547.5	12.5	8.6	288.2
Rat 10 $\mu$ M TRO	29.0	15.9	555.6	8.1	5.8	322.4
Human CTL	1906.0	1245.7	4874.4	1644.1	1054.1	2970.1
Human 10 $\mu$ M TRO	907.3	655.8	4584.8	789.0	606.9	2842.1

**Figure 3.6:** Accumulation (mean and SEM, range, or SD; pmol/mg protein) of total BAs measured in cells + bile, cells, and medium in rat and human SCH following 24-h treatment with vehicle (0.1% DMSO; CTL) or 10  $\mu$ M TRO.

		TCA	GCA	TCDCA	GCDCA
Rat CTL	cells + bile	44.1	2.5	45.9	7.5
	cells	27.5	2.3	61.5	8.7
	bile	63.8	2.7	27.4	6.1
	medium	68.9	8.0	14.8	8.3
RAT TRO	cells + bile	51.3	3.0	38.7	7.0
	cells	33.3	3.1	54.4	9.2
	bile	73.1	3.0	19.8	4.2
	medium	71.6	8.3	13.6	6.5
Human CTL	cells + bile	0.3	48.6	0.3	50.8
	cells	0.2	42.9	0.4	56.5
	bile	0.3	59.4	0.2	40.1
	medium	0.4	72.0	0.1	27.4
Human TRO	cells + bile	0.3	44.2	0.4	55.2
	cells	0.3	33.6	0.4	65.7
	bile	0.2	71.6	0.1	28.0
	medium	0.4	76.4	0.1	23.1

**Figure 3.7:** Accumulation of individual BA species (% total) in cells + bile, cells, bile, and medium in rat and human SCH following 24-h treatment with vehicle (0.1% DMSO; CTL) or 10  $\mu$ M TRO.

time (min)	TS uptake (nM)	SD
1	9.4	0.9
5	22.4	5.6

**Figure 4.1:** ATP-dependent uptake (mean and SD; nM) at 1 and 5 min of TS into MRP4-expressing membrane vesicles incubated with 10  $\mu$ M TS.

treatment	uptake rate (pmol/mg protein/90 s)	SD
CTL	114.4	7.5
1 $\mu$ M TS	91.1	1.7
10 $\mu$ M TS	45.2	8.3
18 $\mu$ M MK571	10.9	11.3

**Figure 4.2:** Uptake of [ $^3$ H]MTX (mean and SD; pmol/mg protein/90 s) into MRP4-expressing membrane vesicles in the presence of vehicle (0.1% DMSO; CTL), 1 or 10  $\mu$ M TS, or 18  $\mu$ M MK571.

treatment	uptake clearance ( $\mu\text{l}/\text{min}/\text{mg}$ protein)	SD
CTL	57.5	1.0
50 $\mu\text{M}$ TS	3.0	0.6
50 $\mu\text{M}$ MK571	4.0	0.5

**Figure 4.3:** Uptake clearance (mean and SD;  $\mu\text{l}/\text{min}/\text{mg}$  protein) of [ $^3\text{H}$ ]DHEAS into MRP4-expressing membrane vesicles in the presence of vehicle (0.1% DMSO; CTL), 50  $\mu\text{M}$  TS, or 50  $\mu\text{M}$  MK571.

	time (min)	ATP-dependent uptake (pmol/mg protein)	range
MRP4	1	48.8	8.7
MRP4	2	111.8	0.5
MRP4	5	179.8	15.4
MRP4	10	210.9	13.6
MRP4	20	237.6	6.9
CTL	1	10.6	0.1
CTL	2	57.6	5.0
CTL	5	85.2	8.7
CTL	10	80.7	10.1
CTL	20	72.1	3.0

**Figure 4.4:** ATP-dependent uptake (mean and range; pmol/mg protein) at 1, 2, 5, and 10 min of [<sup>3</sup>H]TCA in CTL and MRP4-expressing membrane vesicles.

	TS ( $\mu\text{M}$ )	ATP-dependent uptake rate pmol/mg protein/min	SEM
MRP4	0	49.4	6.8
MRP4	0.1	49.1	6.0
MRP4	0.3	42.4	3.7
MRP4	1	40.9	2.2
MRP4	3	29.0	2.0
MRP4	10	27.3	3.7
MRP4	30	20.1	2.4
MRP4	100	14.2	1.4
CTL	0	37.7	1.3
CTL	0.1	37.6	2.2
CTL	0.3	34.2	0.8
CTL	1	33.3	5.9
CTL	3	20.6	1.5
CTL	10	16.1	1.0
CTL	30	16.8	4.8
CTL	100	11.4	0.8

**Figure 4.5:** ATP-dependent uptake rate (mean and SEM; pmol/mg protein/min) of [ $^3\text{H}$ ]TCA in CTL membrane vesicles and MRP4-expressing membrane vesicles in the presence of increasing concentrations of TS (0-100  $\mu\text{M}$ ).

rat	cells + bile	cells	cells + bile SEM	cells SEM
CTL	100.00	14.20	0.00	2.77
0.1 $\mu$ M TRO	87.74	12.19	7.20	3.00
1 $\mu$ M TRO	75.64	11.72	6.49	3.22
5 $\mu$ M TRO	30.54	7.11	11.23	4.18
10 $\mu$ M TRO	24.26	6.43	14.02	3.37

human	cells + bile	cells	cells + bile SD	cells SD
CTL	100.00	26.83	15.64	3.77
1 $\mu$ M TRO	75.84	20.93	11.32	1.05
10 $\mu$ M TRO	15.58	7.12	0.90	0.50

**Figure A.1:** Accumulation (mean and SEM or SD; % control) of TCA in cells + bile and cells in rat and human SCH following a 10-min incubation with 1  $\mu$ M [ $^3$ H]TCA and vehicle (0.1% DMSO; CTL), 1, or 10  $\mu$ M TRO.

[TRO] ( $\mu\text{M}$ )	+ Na <sup>+</sup>	+ Na <sup>+</sup> SEM	- Na <sup>+</sup>	- Na <sup>+</sup> SEM	Na <sup>+</sup> -dependent
0	100.00	6.78	100.00	11.20	100.00
0.1	93.19	8.27	89.42	3.69	92.35
0.3	68.90	7.48	86.41	10.81	83.40
1	76.01	7.70	101.56	7.11	53.74
3	51.26	9.67	80.61	4.80	51.70
5	50.23	4.72	77.61	15.15	25.99
10	33.49	1.44	57.58	2.88	18.22
20	27.60	5.95	52.81	9.91	6.04

**Figure A.2.A:** TCA uptake (% control; mean and SEM) by rat primary suspended hepatocytes in the presence of increasing concentrations of TRO (0-20  $\mu\text{M}$ ).

[<sup>3</sup>H]TCA uptake in the presence and absence of Na<sup>+</sup> was measured at 30 s, in the presence of increasing concentrations of TRO. Na<sup>+</sup>-dependent uptake was determined by subtracting [<sup>3</sup>H]TCA uptake in the absence of Na<sup>+</sup> from uptake in the presence of Na<sup>+</sup>.